SMITHSONIAN INSTITUTION
ASTROPHYSICAL OBSERVATORY

Research in Space Science

SPECIAL REPORT

Number 199

ATMOSPHERIC DENSITIES AND TEMPERATURES FROM PRECISELY REDUCED OBSERVATIONS OF THE EXPLORER IX SATELLITE

by

Max Roemer

February 3, 1966

CAMBRIDGE, MASSACHUSETTS 02138

SAO Special Report No. 199

ATMOSPHERIC DENSITIES AND TEMPERATURES FROM PRECISELY REDUCED OBSERVATIONS OF THE EXPLORER IX SATELLITE

by

Max Roemer

Smithsonian Institution
Astrophysical Observatory
Cambridge, Massachusetts 02138

ATMOSPHERIC DENSITIES AND TEMPERATURES FROM PRECISELY REDUCED OBSERVATIONS OF THE EXPLORER IX SATELLITE[1]

By Max Roemer[2]

1964 ½

Abstract. --The atmospheric drag of the Explorer IX satellite through May 1963 was derived using precisely reduced photographs taken with the Baker-Nunn cameras. The accuracy of an individual acceleration was determined to be ±5%. Analysis of the atmospheric density data revealed a latitude-dependent seasonal density variation of ±25% at a latitude of 39° and an average height of 690 km. The atmospheric density at a given height is higher in winter than in summer. The statistics of 100 atmospheric variations related to geomagnetic storms give 5.2 ± 0.4 hours as the average time lag between the maximum of a geomagnetic storm and the peak in atmospheric density. The influence of the variation of the drag coefficient with atmospheric composition on the absolute density values is discussed.

[1] This work was supported by grant NsG 87-60 from the National Aeronautics and Space Administration.

[2] Astrophysicist, Smithsonian Astrophysical Observatory; on leave from Astronomische Institute der Universität Bonn, Germany.

Introduction

Following the first paper on the atmospheric drag of the Explorer IX Satellite (1961 δ1) based on precisely reduced Baker-Nunn photographic observations (Jacchia and Slowey, 1964a), we present an analysis of the precisely reduced observational material in the time interval October 12, 1961, to June 9, 1963. The observations prior to January 1, 1963 are published in the Smithsonian Astrophysical Observatory (SAO), Catalogs of Precisely Reduced Observations P-9, P-10, and P-11; Special Reports No. 137, 138, and 147, respectively (Stern, 1963a, b; 1964). Orbits from precisely reduced observations were computed without a major gap through June 9, 1963; i.e., some 300 days before the demise of the Explorer IX Satellite. After that date computation of orbits from photoreduced observations became more and more tedious though not impossible, and gaps of considerable length occurred frequently. Partly because of the rapidly decreasing perigee height and the accompanying increase in the atmospheric drag, predictions were from time to time not accurate enough for a high number of observations per day. In addition, poor distribution of observations along the orbit made orbit computation often more difficult. Less accurate field-reduced observations, on the other hand, yielded orbits from June 1963 through the end of the lifetime of Satellite 1961 δ1 with a time resolution of the accelerations comparable to an analysis based on precisely reduced observations (Jacchia and Slowey, 1965). Thus we decided to use precisely reduced observations only through June 9, 1963.

The first section deals with the computation of precision orbits and the accuracy of accelerations derived from photoreduced Baker-Nunn observations. Atmospheric densities and temperatures computed from these accelerations are the basic results of this analysis and are discussed in Section 2 and collected in Table 3. These values are compared with the static diffusion models of the upper atmosphere by Jacchia (1964) in Section 3. In Section 3.1 the influence of variable drag coefficients on the

absolute density values is discussed. In Section 3.2 we show that even a satellite probing the atmosphere between latitudes ±39° only can establish the seasonal variation in atmospheric density found independently by using high-inclination satellites (Jacchia and Slowey, 1966). Finally, in Section 4, the time delay in the geomagnetic activity effect is studied, based on 71 additional atmospheric perturbations related to increased geomagnetic activity, bringing the total of delay times published (Jacchia and Slowey, 1964a; Priester, 1965) to some 120.

1. Computation of precision orbits and accelerations

Orbital elements from the precisely reduced observations were computed at 1-day intervals, using observations within a 4-day interval centered on the epoch. We used DOI-3.4, an advanced version of the Differential Orbit Improvement Program documented by Gaposchkin (1964). Luni-solar perturbations and the perturbations due to the tesseral harmonics of the earth's gravitational field are incorporated in this program. We were not, therefore, bothered by fluctuations resulting from these perturbations as in the first analysis of the drag acting on the Explorer IX Satellite based on photoreduced observations (Jacchia and Slowey, 1964a).

Least-squares fittings of the orbital elements were made over periods of 26 days with a 6-day overlap between sections. The length in time covered by a section and the overlap are identical with those of the first analysis by Jacchia and Slowey (1964a). Since we also have an overlap of sections with this analysis, we continued the numbering of the sections beginning with No. 13. The fitted elements are given in Table 1. Contrary to SAO Special Report No. 125 (Jacchia and Slowey, 1964a), the sine terms are not physically meaningful although they pick up residuals of the lunar perturbation effects from time to time. Generally they were introduced only to improve the fit. Sine terms with periods of about 12 hours caused by the "ellipticity of the equator" do not occur in the least-squares fittings since they are accounted for in the DOI program. The long-period perturbations due to the zonal harmonics of the form $\sin \omega$ and $\sin 2\omega$ contribute to the high-order polynomials needed to represent the influence of solar radiation pressure on the orbit. The mean anomaly is represented by a fit without sine terms because the DOI program uses the first derivative of the polynomial part only for the computation of mean motion n and semimajor axis a. Furthermore, systematic residuals less than 10^{-3} revolutions can be tolerated in the mean anomaly (Jacchia, 1963). A comparison of the least-squares fit of the

inclination with the values computed for the individual epochs within the 600-day interval yields the r.m.s. error of an individual determination of the inclination: $\sigma_i = 0.58 \pm 0.25$ second of arc. To characterize the precision of the photoreduced Baker-Nunn observations in a different way, we computed the standard deviation of an individual observation from the scatter in the mean anomaly for section 27: $\sigma_M = 3.0$ seconds of arc.

Taking the least-squares fit of the orbital elements as given in Table 1 and the individual observations, we derived the acceleration of the satellite by the method fully described by Jacchia (1963) and by Jacchia and Slowey (1963). The contribution of solar radiation pressure to the acceleration was evaluated using Kozai's (1961) formulation of the effect and assuming specular reflection. A value of 2.00 cal/cm^2 min for the solar constant and an area-to-mass ratio of 15.84 cm^2/g for the Explorer IX Satellite were used in the computations.

The overlap of our first two sections with the earlier analysis by Jacchia and Slowey (1964a) provided an opportunity to estimate the overall accuracy of the determination of accelerations with the method established at SAO. If we assume that the mean $\dot{P}_{i,av}$ of the accelerations at a specific epoch as determined by Jacchia and Slowey and as derived in this analysis, is the "true" value of the acceleration, we compute the relative deviation $(\dot{P}_i - \dot{P}_{i,av})/\dot{P}_{i,av}$ of the accelerations $\dot{P}_i$ given in column 3 of Table 3 within the time interval Modified Julian Day (MJD) 37598 - 37635. In Figure 1 a histogram of these 110 data points is shown. The systematic error of -0.7% (indicating that our individual accelerations $\dot{P}_i$ are in the average slightly smaller than ones given in SAO Special Report No. 125) is small compared to the standard deviation of a single acceleration value, $\sigma_{\dot{P}} = 5.0\%$. This value, calculated by comparing results obtained from the same observational material by two different investigators using independent solutions for the orbital elements and the derivation of accelerations, is a sound estimate of the absolute accuracy of accelerations deduced from precisely reduced Baker-Nunn observations.

2. Atmospheric densities and temperatures

Atmospheric densities at perigee were computed by numerical integration of the drag acting on the satellite along its orbit, taking into account the rotation and oblateness of the atmosphere as well as the diurnal bulge. The only change from the procedure described in detail by Jacchia and Slowey (1963) was the use of Jacchia's latest (1964) atmospheric model for computing the relative change in density along the orbit. A constant drag coefficient of $C_D = 2.2$ was adopted for the computation.

Densities at perigee were reduced to a standard height close to the perigee height. In the case of Explorer IX, we had to use more than one standard height because of the large variation in the perigee height. For the reduction of the density ρ at perigee height z to a density ρ_0 at a standard height z_0, an expression of the form

$$\rho_0 = \rho \cdot \exp\left\{-\frac{h_0 - h}{H_\rho}\right\} \tag{1}$$

is used, where H_ρ is the density scale height determined from a suitable model. Any uncertainty ΔH_ρ in the scale height produces an error $\Delta \rho_0$ in the density at standard height (Roemer, 1963):

$$\frac{\Delta \rho_0}{\rho_0} = \frac{\Delta H_\rho}{H_\rho} \cdot \frac{h_0 - h}{H_\rho} \quad . \tag{2}$$

Therefore the ratio $(h_0 - h/H_\rho)$ should be kept as small as feasible. The standard heights used for Explorer IX and the intervals to which they apply are given in Table 2.

The temperature at perigee was computed from the atmospheric density with the help of Jacchia's 1964 atmospheric model. Also minimum nighttime temperatures were calculated by applying the formula for the distribution around the globe of the temperature above the thermopause as given by that atmospheric model. Table 3 contains the numerical results. The time in Modified Julian Days (MJD = JD - 2,400,000.5) is listed in the first column. The observed rate of change of the anomalistic period (acceleration) is given in the second column. The acceleration due to solar radiation pressure is in the third column. The difference between columns two and three, the acceleration ascribed entirely to atmospheric drag, appears in column four. The common logarithms of the gas density, in g/cm^3, at the actual perigee height and at the standard height are given in columns five and six. In column seven the exospheric temperature at perigee is listed. The following three columns present information on the location of the perigee with respect to the earth and the sun, the height of perigee above the geoid (column eight), the difference in right ascension between perigee and the sun (column nine), and the declination of the perigee minus the declination of the sun (column ten). The last column gives the nighttime exospheric temperature.

The information given by columns five and seven of Table 3, the logarithm of the atmospheric density at the actual perigee height, and the exospheric temperature at perigee, are plotted in Figures 2a-2d. Plots of the solar flux at 10.7-cm wavelength and of means of the 3-hourly geomagnetic index a_p adapted to the time resolution of the density determination are shown for comparison. Furthermore, normalized curves of the diurnal and semi-annual variations, according to Jacchia's 1964 model, and the plot of the perigee height, are given. The systematic variation of the perigee density with perigee height can be seen easily if we compare the plots at the top and the bottom of Figures 2a-2d. This slow variation in density was preferred to a plot with sudden changes of the density reduced to standard height, which occur every time a new standard height is used. The dominant feature in

the density and temperature plot is variations connected with geomagnetic variations. Oscillations of density and temperature in phase with the 27-day variation of the solar decimetric flux are important through June 1962. With the sun in near minimum condition, the amplitude of the variations in the solar 10.7-cm flux is small for the remaining part of this analysis. Thus the atmospheric variations correlated with the solar decimetric radio flux are no longer an important feature of the density and temperature plot. The diurnal effect, although with a relatively slow variation in the case of the Explorer IX Satellite, can be seen more easily in the temperature plot after July 1962. Due to the slow motion of the satellite's perigee with respect to the sun, this satellite is specifically suited for a study of the semiannual variation. But the semiannual variation of temperature and density is not easily recognizable in the density and temperature plot because the amplitude in the years 1961-1963 is relatively small and the time interval covered by each diagram is smaller than one cycle of the variation. According to the formula for the semiannual temperature variation given by Jacchia (1964), the total amplitude is smaller than 100° K and often masked by the other atmospheric variations.

From the early statistics of the geomagnetic activity effect that were based on fluctuations in atmospheric densities and temperatures during pronounced geomagnetic storms, Jacchia and Slowey (1963) found that temperature variations were linearly related to the geomagnetic planetary index a_p. From this result we would expect fewer fluctuations in the temperature plot in Figure 2 than are obviously present. In accordance with recent results by Jacchia and Slowey (1964b) and by Newton, Horowitz, and Priester (1964), oscillations in atmospheric density and temperature occur even during small-scale perturbations of the geomagnetic field. Figure 3 shows an example of the temperature variations during a relatively quiet interval in February and March 1963. With the exception of the geomagnetic perturbation beginning on March 8, the average of the daily planetary index A_p is 5. If the relation between temperature and A_p deduced from storm-type perturbations (Jacchia and Slowey, 1964a) were applicable, we would hardly recognize any temperature

variations. Instead we see lively fluctuations of the nighttime temperature with an approximately linear relation to the K_p index. The solar activity effect, both the erratic and the long-term components, and the semiannual variation have been removed from the nighttime temperature data by use of an atmospheric model (Jacchia, 1964) in order to make the temperatures intercomparable for the entire 45-day period. From the data of Figure 3 it appears that the temperature increase, corresponding to an increase of 1 K_p unit, is 20° for an average K_p value of 1.2. Jacchia and Slowey (1964b) determined $\Delta T/\Delta K_p = 30$ for $\overline{K}_p = 1$ from the Explorer XVII and Injun III Satellites with perigee heights near 250 km. Their diagram of the temperature variations derived from Explorer VIII at 426-km altitude seems to indicate a value $\Delta T/\Delta K_p$, which is a little smaller than 30. For a comparison we have to bear in mind that the data in Figure 3 cover a time interval that is much smaller than that analyzed by Jacchia and Slowey (1964b). There is also the problem of resolution. We relate drag data with a nominal resolution of 0.5-day to 1.0-day means of K_p compared to 1.0 day and 2.0 days, respectively, in Jacchia and Slowey's analysis. The actual time resolution of the drag data is probably less than the nominal resolution during relatively quiet periods due to a smoothing effect in the drag determination. Therefore, we do not see rapid small-scale variations of the 0.5-day means of K_p and especially not the lively fluctuations of the 3-hourly K_p in the temperature data. Taking all this into account, the difference between the result deduced from the Explorer IX Satellite and the result obtained by Jacchia and Slowey (1964b) does not seem to be alarming.

3. Comparison with the atmospheric model by Jacchia (1964)

Comparison of results obtained from drag analysis with atmospheric models is a powerful tool for deducing variations in the atmosphere not accounted for in the model and for improving relations given by the model (e. g., Roemer, 1963, 1964). In this paper "observed" quantities at a given epoch, i. e., atmospheric density and temperature at perigee derived from the drag data, were compared with "computed" values derived from Jacchia's 1964 atmospheric model. For a given date, altitude, and location with respect to the sun-earth-direction, a computer program developed by Slowey generates atmospheric density and temperature taking into account the variation within the solar cycle, within one solar rotation, the semiannual variation, diurnal variation, and the variation correlated with geomagnetic activity in accordance with the atmospheric model by Jacchia (1964). Residuals in exospheric temperature and the logarithm of density at perigee in the sense of "observed" minus "computed" are plotted in Figure 4. Rather than plotting all individual residuals with a time resolution of up to 0.2 day, 5-day means are given in the figure. Densities and temperatures derived from the accelerations based on photoreduced observations of the Explorer IX Satellite for the first 300 days (Jacchia and Slowey, 1964a) are included in the comparison. Thus, residuals of temperature and density with respect to the atmospheric model covering three quarters of the satellite's lifetime are shown in Figure 4. Apart from systematic deviations that are obvious from the 5-day means, an individual temperature value given by the model has a r. m. s. error of ±25° K indicating the consistency of recent atmospheric models.

3.1 Influence of the drag coefficient on absolute density values.

Apart from variations with a fairly regular quasi-periodic pattern the residuals in the logarithm of density are on the average above the zero line prior to May 1963. A check with the density data derived from field-reduced observations by Jacchia and Slowey (1965) until the demise of

the satellite proved that the behavior of the residuals after MJD 38100 is not isolated but that the average of the residuals is near the zero level. A comparison with the curve of the perigee height shows that the density deduced from drag data seems to be higher than the value given by the atmospheric model for altitudes above some 600 km. There is no systematic difference for altitudes around 500 km indicating a higher number density of a light constituent of the gas mixture. These conclusions are based on the residuals taken at face value and are justified only if we can be sure that our assumption of a constant drag coefficient of $C_D = 2.2$ was correct. This value was adopted to assure consistency of the densities and temperatures with those given by Jacchia and Slowey (1964a), and it is the value commonly used in the analysis of satellite drag above 200 km.

Coulomb drag and induction drag contribute only up to 3.5% of the neutral drag to the total drag experienced by the Explorer IX Satellite according to a study by Hohl and Wood (1963). Generation of Alfvén waves as a drag mechanism proposed by Drell, Foley, and Ruderman (1965) is not effective for a satellite of only 3.6-m diameter. Therefore additional drag due to the movement of the Explorer IX Satellite through a plasma cannot resolve the systematic difference in the density residuals above 600 km.

In a recent critical review of experimental and theoretical determinations of the energy accommodation coefficient, Cook (1965) studied the choice of drag coefficients for satellites. According to his conclusions an accommodation coefficient near unity is unlikely to be correct in the case of the Explorer IX Satellite above 500 km. But this had been implicitly assumed in our adoption of a drag coefficient $C_D = 2.2$. The effect of a smaller accommodation coefficient is to increase the drag coefficient if diffuse reemission of the gas molecules is the dominant interaction process. Diffuse reemission is very likely in the case of a technical surface that is not

smooth down to atomic dimensions. The standard formula for the drag coefficient of a sphere with diffuse reemission and a constant reemission speed over the entire surface is

$$C_D = 2\left(1 + \frac{1}{s^2} - \frac{1}{4s^4}\right) \cdot \operatorname{erf}(s) + \frac{2s^2 + 1}{\sqrt{\pi}\, s^3} \cdot \exp(-s^2) + \frac{2\sqrt{\pi}}{3s_r} \quad , \qquad (3)$$

where s is the molecular speed ratio, i.e., the speed of the satellite divided by the most probable molecular speed of the gas. The ratio of the speed of an incoming molecule to that of a reemitted molecule, is given by

$$s_r = \left\{1 + \alpha\left(\frac{E_s}{E_i} - 1\right)\right\}^{1/2} \quad , \qquad (4)$$

where α is the energy accommodation coefficient, E_i the average kinetic energy of an incident molecule, and E_s the average kinetic energy of a molecule reemitted with a velocity corresponding to the surface temperature of the satellite.

For a test of the influence of the variation of the drag coefficient along the satellite's orbit we used the orbital parameters and acceleration given in Tables 1 and 3 for the epoch MJD 37650. The numerical integration of the drag acting on the satellite along its orbit was done with Simpson's rule and a spacing of 10° in eccentric anomaly. The drag coefficient was treated as a dependent variable of the eccentric anomaly in two out of four model calculations. For the variation in density and mean molecular weight along the orbit, we used a model atmosphere with a nighttime temperature of 813° K, which was the result for MJD 37650 (see Table 3). Tabular values below 1000 km were found by interpolation of the atmospheric models given by Jacchia (1964). Above 1000 km, tabular values were generated by computing the number densities $n_i(z)$ of the atmospheric constituents at altitude z

$$n_i(z) = n_{i,0} \cdot \exp\left\{-\frac{n_i\, g_0}{kT} \cdot \frac{R_0 \cdot (z - z_0)}{R_0 + z}\right\} \quad , \qquad (5)$$

where $n_{i,0}$ is the number density of the i-th constituent given by Jacchia's model at z_0 = 1000 km, g_0 the acceleration of gravity at the geocentric distance R_0 corresponding to z_0, m_i the molecular mass, k Boltzmann's constant, and T the exospheric temperature as given by the formula for the diurnal variation (Jacchia, 1964).

A description of the assumptions and results of the four model calculations follows.

a) The drag coefficient $C_D = 2.2$ was kept constant along the orbit. This value had been used in the entire analysis, and it corresponds to an energy accommodation coefficient $\alpha \simeq 1$, if we assume the surface temperature to be 273° K. The principal purpose of this model calculation was to check whether the spacing of 10° in eccentric anomaly in the numerical integration is narrow enough. The resultant density at perigee of $\rho_a = 1.210 \times 10^{-17}$ g/cm^3 deviates by only 2% from the result obtained with 150 tabular values around the orbit $\rho_0 = 1.186 \times 10^{-17}$ g/cm^3 (see Table 3).

b) In this case the simplest model of the variability of the drag coefficient was applied. The degree of energy transfer was kept constant for all heights and the drag coefficient along the orbit changed due to varying molecular speed ratios s and s_r only (Izakov, 1965). With a value $C_D = 2.2$ for the drag coefficient at perigee the resultant density at perigee $\rho_b = 1.197 \times 10^{-17}$ g/cm^3 is only slightly different from the result in case a.

c) From Cook's study of the rate of energy transfer between satellite and gas (Cook, 1965) we took the following expression for the accommodation coefficient α :

$$\alpha = \frac{3.6\,\mu}{(1+\mu)^2} \quad , \tag{6}$$

where μ is the ratio of the mass of an incident gas atom to the mass of a surface atom. According to Cook's (1965) discussion we assumed that the outermost layer of the satellite's surface is formed by oxygen atoms. For the "observed" temperature at perigee of 961° K at MJD 37650 (see Table 3), Jacchia's (1965) atmospheric model gives a mean molecular weight of 6.2 at 760 km altitude. With these values equation (6) yields $\alpha = 0.73$ and the drag coefficient at perigee is $C_D = 2.65$, according to equation (3). Using this drag coefficient for the entire orbit the density at perigee is $\rho_c = 1.005 \times 10^{-17}$ g/cm^3; i.e., 17% lower than in case a.

d) In this calculation we took account of the variation in the drag coefficient along the orbit due to a varying accommodation coefficient according to equation (6) and due to the changing molecular speed ratio s. With a drag coefficient at perigee as given in case c, the density at perigee is $\rho_d = 9.764 \times 10^{-18}$ g/cm^3.

These calculations are summarized in Table 4. A comparison of the results shows that the choice of the drag coefficient at perigee is the dominating factor. The relative difference between cases c and d of only 3% illustrates the fact that the density at perigee derived from satellite accelerations does not depend critically on the variation of the drag coefficient along the orbit, at least in the case of the Explorer IX Satellite. This small difference is due to the high-lapse rate of atmospheric density as compared to the increase of the drag coefficient with altitude. If we use a drag coefficient at perigee $C_{D,P}$ determined by equation (6), which is presumably better adapted to the conditions above the thermopause than the value 2.2, simple multiplication of the density values in Table 3 by the ratio $(2.2/C_{D,P})$ yields "corrected" densities with an error of less than +5%.

The result of these model calculations shows that a more sophisticated value of the drag coefficient than $C_D = 2.2$ can explain 20 to 25% of the average positive density residuals at altitudes above 600 km. If we assume that nonneutral drag contributes up to 3.5% of the neutral drag (Hohl and Wood, 1963), we are still left with "observed" density values 10 to 20% higher than those computed from Jacchia's 1964 atmospheric model. To explain this discrepancy we may take a less conservative value for the drag coefficient around $C_D = 3.0$ above 600 km but one which would still yield values near 2.2 in the 400 to 500-km altitude region. A different approach would be postulating a 10 to 20% higher number density of helium above 600 km. The increase in the He concentration at the height z_0, where diffusive separation begins, would be only two-thirds of the above-mentioned 10 to 20% since thermal diffusion enhances the concentration at the escape level z_c by $[T(z_0)/T(z_c)]^{-\alpha}$, where T is the atmospheric temperature and α the thermal diffusion coefficient (MacDonald, 1963). The difficulty with this explanation is the fact that the He concentration at 120 km in Jacchia's 1964 model is already 40% higher than that adopted in the COSPAR reference atmosphere (CIRA, 1965).

3.2 Latitude-dependent seasonal variation of atmospheric density.

Variations with a fairly regular pattern are superposed on the systematic deviations in the residuals of log ρ and of the temperature from the zero-line. The computed values take into account the variations in atmospheric temperature and density which are included in the atmospheric model (Jacchia, 1964), i.e., diurnal variation, variations with solar activity, geomagnetic activity effect, and semiannual variation. Of these, only the curve of the diurnal variation has a resemblance to the variation of the residuals (see Figure 4), where the geocentric angle between the satellite's perigee and the center of the diurnal bulge is plotted below the density residuals.

The density residuals seem to increase with the angular distance from the bulge, although in several cases this relation is reversed, e. g., from September through November 1961. One might explain this by an overestimated amplitude of the diurnal density variation as given by the atmospheric model. An increased concentration of helium would decrease the amplitude of the day-to-night variation. But high-inclination satellites with perigee heights up to 615 km have again confirmed the density and temperature distribution around the globe (Jacchia, 1965).

A comparison of the residuals with the plot of the latitude of perigee and the time of the year shows that the observed density reaches relative maxima when the satellite's perigee is nearest to the winter pole, as in June 1961, August 1961, December 1961, June 1962, and December 1962; the density is lowest in the summer hemisphere, as in July 1961, January 1962, and July 1962. A seasonal variation in that sense, i. e., with high densities above the winter pole and low densities near the summer pole, has recently been found by Jacchia and Slowey (1966) from the drag of high-inclination satellites. Jacchia (1965) has given a simple model for this seasonal variation in the residuals

$$\Delta \log \rho \propto \pm \sin^2 \phi \cdot \cos \frac{2\pi}{T} (\text{d - Jan. 20}) , \qquad (7)$$

where ϕ is the latitude of perigee, T the tropical year in days, and d the day of the year. The plus sign is used for positive ϕ and the minus sign for negative latitudes. Expression (7) is plotted at the bottom of Figure 4 and seems to be well correlated with the density residuals.

In order to decide whether the variations of the residuals in log ρ represent a seasonal variation or whether they are caused by a smaller amplitude of the diurnal effect, we computed the correlation coefficient between the residuals and these two curves. Because of the systematic displacement of the residuals from the zero-line (see Section 3. 1), the data

were divided into three sections and individual correlation coefficients for each section were calculated. Applying Fisher's z -transformation (e. g., Tippett, 1952), we obtained correlation coefficients for the entire interval. The correlation coefficient between the residuals in log ρ and expression (7) for the seasonal variation is $r_1 = 0.47$ and is significantly greater than the correlation coefficient between Δ log ρ and the angular distance from the bulge $r_2 = 0.22$. If the seasonal variations in the upper atmosphere are in part an extension of those in the homosphere, irregularities and deviations from the simple model should be expected. Furthermore, in the corresponding seasons there might be some systematic differences in the two hemispheres. If we take this into account, a correlation coefficient of $r = 0.47$ deduced from a moderate inclination satellite ($i \approx 39°$) seems to be encouraging.

If we designate the right-hand side of expression (7) by A and if we compare the maxima and minima in the Δ log ρ plot with the Δ log ρ values at epochs when A equals zero, we find the average density variation, corresponding to a change in A between 0 and 0.34, to be $\overline{\Delta \log \rho} = 0.10$. This value corresponds to a seasonal variation in density at 39° latitude of ±25%. If we extrapolate this result to a variation in A between 0 and 1.0, i.e., to the poles, the semiamplitude of the seasonal variation at a mean height of 690 km is a factor 2 in density. This result is in good agreement with the value 1.8 determined by Jacchia and Slowey (1966) at 614 km.

4. Time delay of the geomagnetic activity effect

Jacchia and Slowey (1964a) were the first to study the delay time between the atmospheric reaction and the maxima of geomagnetic storms with data derived from precisely reduced observations of the Explorer IX Satellite. The high area-to-mass ratio and precise acceleration data with high time resolution make this satellite a sensitive probe for atmospheric variations with a short time-scale. The time delay of 51 atmospheric density increases related to geomagnetic perturbations was examined based on the data in Table 3 for intervals when the time-resolution of the drag data was 0.2 day. In addition, 20 events during the last 300 days of the lifetime of the Explorer IX were analyzed using drag data with 0.2-day time resolution as given by Jacchia and Slowey (1965 and unpublished data).

The phase shifts were determined by comparing the peak in the plot of the atmospheric temperature with the maximum of the geomagnetic activity variation. For that the 3-hourly planetary geomagnetic indices a_p were adjusted to the time resolution of the satellite data. Only the time lag between the corresponding maxima in the temperature and geomagnetic activity plot was examined. The mean value of the time lag based on these 71 events and the scatter of the individual determinations was practically the same as in the results reported by Jacchia and Slowey (1964a). Therefore, the 30 values of the delay time based on the first 300 days of the satellite's lifetime were included in this analysis. The grand mean of all delay times based on the Satellite 1961 δ1 is $\overline{\Delta t} = 0.216 \pm 0.015$ day or $\overline{\Delta t} = 5.2 \pm 0.4$ hours. The data cover the altitude range from 770 to 300 km, and no conspicuous dependence of the time lag on altitude could be discovered. The delay-time data from Explorer IX are distributed between 8 and 23 hours local time with a mean data density of 7 values per hour. Combined with the results from the Injun III and Explorer XVII Satellites obtained by Priester (1965), these

data practically rule out any dependence of the time delay on local time, as can be seen in Figure 5. Thus the atmospheric reaction related to major geomagnetic perturbations occurs apparently worldwide at the same time on the day- and the night-side of the earth.

The events analyzed are atmospheric variations correlated with geomagnetic storms in the range from 4 to 9 of the 3-hourly K_p indices. There is no indication of a dependence of the delay time on the intensity of the geomagnetic storm within that range (Figure 6). Due to the limited resolution of $\pm$ 0.05 day of the present data the statistics are poor. But at least one might conclude that a possible dependence cannot be linear with K_p for the entire range.

Due to the scatter of the individual values and the relatively low inclination of 39°, an investigation of a dependence on latitude is not possible. Results from satellites with perigee heights below 215 km obtained by Jacobs (1965) indicate a dependence of the delay time on latitude. Four of the satellites treated have latitudes of perigee below 40°, i.e., in the latitude region sampled by the Explorer IX Satellite, and yield delay times between 0.4 and 0.8 day. In a recent analysis of the drag of the San Marco Satellite, another low-altitude satellite with a mean perigee height of 200 km, Jacchia and Verniani (1965) also find a higher value of the delay time $\Delta t = 9$ hours, but the number of geomagnetic storms in the interval covered by this analysis is far smaller than in the case of the Explorer IX Satellite.

In Table 5 the individual values of the delay time are collected together with several parameters. The first two columns give the number and the MJD Day, followed by the maximum 3-hourly geomagnetic a_p index during the storm in column three, and the time lag Δt in days between the maximum of the geomagnetic variation and the peak of the atmospheric reaction in the fourth column. In the last three columns parameters indicating the location of the perigee are listed, namely the local time ℓt of the perigee, the latitude of perigee ϕ, and the perigee height z_p.

Acknowledgments

I am very grateful to Dr. Luigi G. Jacchia for his suggestion of this analysis and for continuing interest. I thank him and Mr. Jack W. Slowey for stimulating discussions. The assistance of Mrs. Maya Broman, Mrs. Helene Cornelius, Mrs. Mary M. Thorndike, and Mr. Donald Singley is gratefully acknowledged.

References

CIRA

1965. Cospar International Reference Atmosphere. Compiled by the members of Cospar Working Group IV. North-Holland Publ. Co., Amsterdam.

COOK, G. E.

1965. Satellite drag coefficients. Royal Aircraft Establishment, Technical Rept. No. 65005, 34 pp.

DRELL, S. D., FOLEY, H. M., AND RUDERMAN, M. A.

1965. Drag and propulsion of large satellites in the ionosphere: An Alfvén propulsion engine in space. Journ. Geophys. Res., vol. 70, pp. 3131-3145.

GAPOSCHKIN, E. M.

1964. Differential orbit improvement (DØI-3). Smithsonian Astrophys. Obs. Spec. Rep. No. 161, 70 pp.

HOHL, F., AND WOOD, G. P.

1963. The electrostatic and electromagnetic drag forces on a spherical satellite in a rarefied partially ionized atmosphere. In Rarefied Gas Dynamics, vol. II, ed. by J. A. Laurmann, Academic Press, New York, pp. 45-64.

IZAKOV, M. N.

1965. Some problems of investigating the structure of the upper atmosphere and constructing its model. In Space Research V, ed. by D. G. King-Hele, P. Muller, and G. Righini, North-Holland Publ. Co., Amsterdam, pp. 1191-1213.

JACCHIA, L. G.

1963. The determination of atmospheric drag on artificial satellites. In Dynamics of Satellites, ed. by M. Roy, Springer-Verlag, Berlin, pp. 136-142.

1964. Static diffusion models of the upper atmosphere with empirical temperature profiles. Smithsonian Astrophys. Obs. Spec. Rep. No. 170, 53 pp.

1965. Density variations in the heterosphere. Smithsonian Astrophys. Obs. Spec. Rep. No. 184, 24 pp.

JACCHIA, L. G., AND SLOWEY, J. W.

1963. Accurate drag determinations for eight artificial satellites; atmospheric densities and temperatures. Smithsonian Contr. Astrophys., vol. 8, no. 1, 99 pp.

1964a. An analysis of the atmospheric drag of the Explorer IX satellite from precisely reduced observations. In Space Research IV, ed. by P. Muller, North-Holland Publ. Co., Amsterdam, pp. 257-270. See also Smithsonian Astrophys. Obs. Spec. Rep. No. 125, 57 pp.

1964b. Temperature variations in the upper atmosphere during geomagnetically quiet intervals. Journ., Geophys. Res., vol. 69, pp. 4145-4148.

1965. Densities and temperatures from the atmospheric drag on six satellites. Smithsonian Astrophys. Obs. Spec. Rep. No. 171, 111 pp.

1966. Seasonal variations in the heterosphere. Smithsonian Astrophys. Obs. Spec. Rep. (to be published).

JACCHIA, L. G., AND VERNIANI, F.

1965. Atmospheric densities and temperatures from the drag analysis of the San Marco satellite. Smithsonian Astrophys. Obs. Spec. Rep. No. 193, 10 pp.

JACOBS, R. L.

1965. Atmospheric heating between 80 and 115 nautical miles as determined from satellite drag analysis. LMSC Tracking Note No. 68.

KOZAI, Y.

1961. Effects of solar radiation pressure on the motion of an artificial satellite. Smithsonian Astrophys. Obs. Spec. Rep. No. 56, pp. 25-33.

MACDONALD, G. J. F.

1963. The escape of helium from the earth's atmosphere. Revs. Geophys., vol. 1, pp. 305-349.

NEWTON, G. P., HOROWITZ, R., AND PRIESTER, W.

1964. Atmospheric densities from Explorer XVII density gages and a comparison with satellite drag data. Journ. Geophys. Res., vol. 69, pp. 4690-4692.

PRIESTER, W.

1965. On the variations of the thermospheric structure. Goddard Space Flight Center, NASA, 25 pp.

ROEMER, M.

1963. Die Dichte der Hochatmosphäre und ihre variationen während der phase abklingerder sonnenatctivität 1958-1962. Veröff. Univ. Sternwarte Bonn, No. 68, 146 pp.

1964. Exospheric densities deduced from satellite drag data. In Space Research IV, ed. by P. Muller, North-Holland Publ. Co., Amsterdam, pp. 244-256.

STERN, P.

1963a. Catalog of precisely reduced observations P-9. Smithsonian Astrophys. Obs. Spec. Rep. No. 137, 93 pp.

1963b. Catalog of precisely reduced observations P-10. Smithsonian Astrophys. Obs. Spec. Rep. No. 138, 202 pp.

1964. Catalog of precisely reduced observations P-11. Smithsonian Astrophys. Obs. Spec. Rep. No. 147, 293 pp.

TIPPETT, L. H. C.

1952. The Methods of Statistics. Dover Publications, New York, 395 pp.

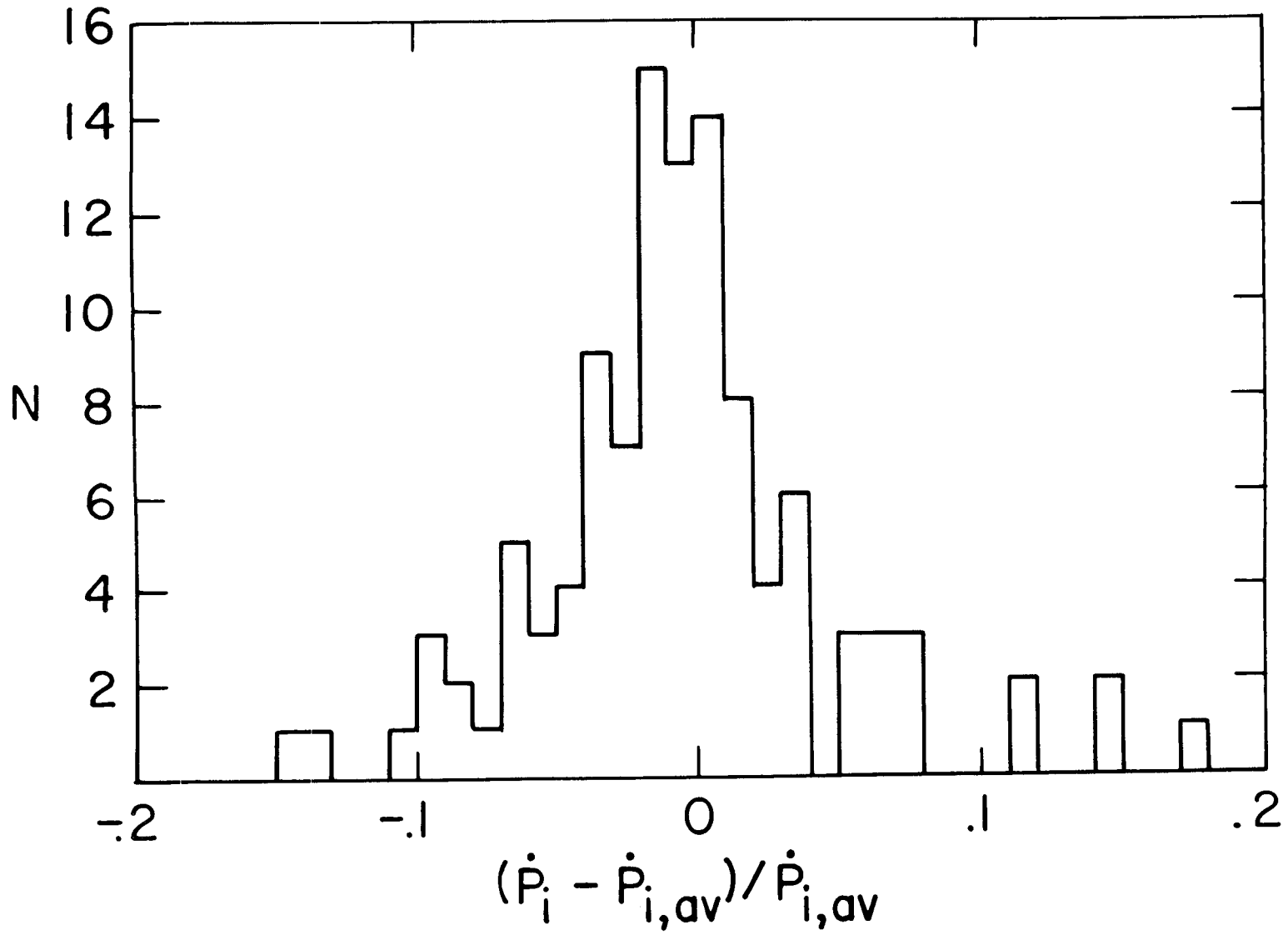

Figure 1.--Histogram of the relative deviation $(\dot{P}_i - \dot{P}_{i,av})/\dot{P}_{i,av}$ of 110 accelerations P_i given in Table 3, yielding an r.m.s. error of an individual acceleration of ± 5%.

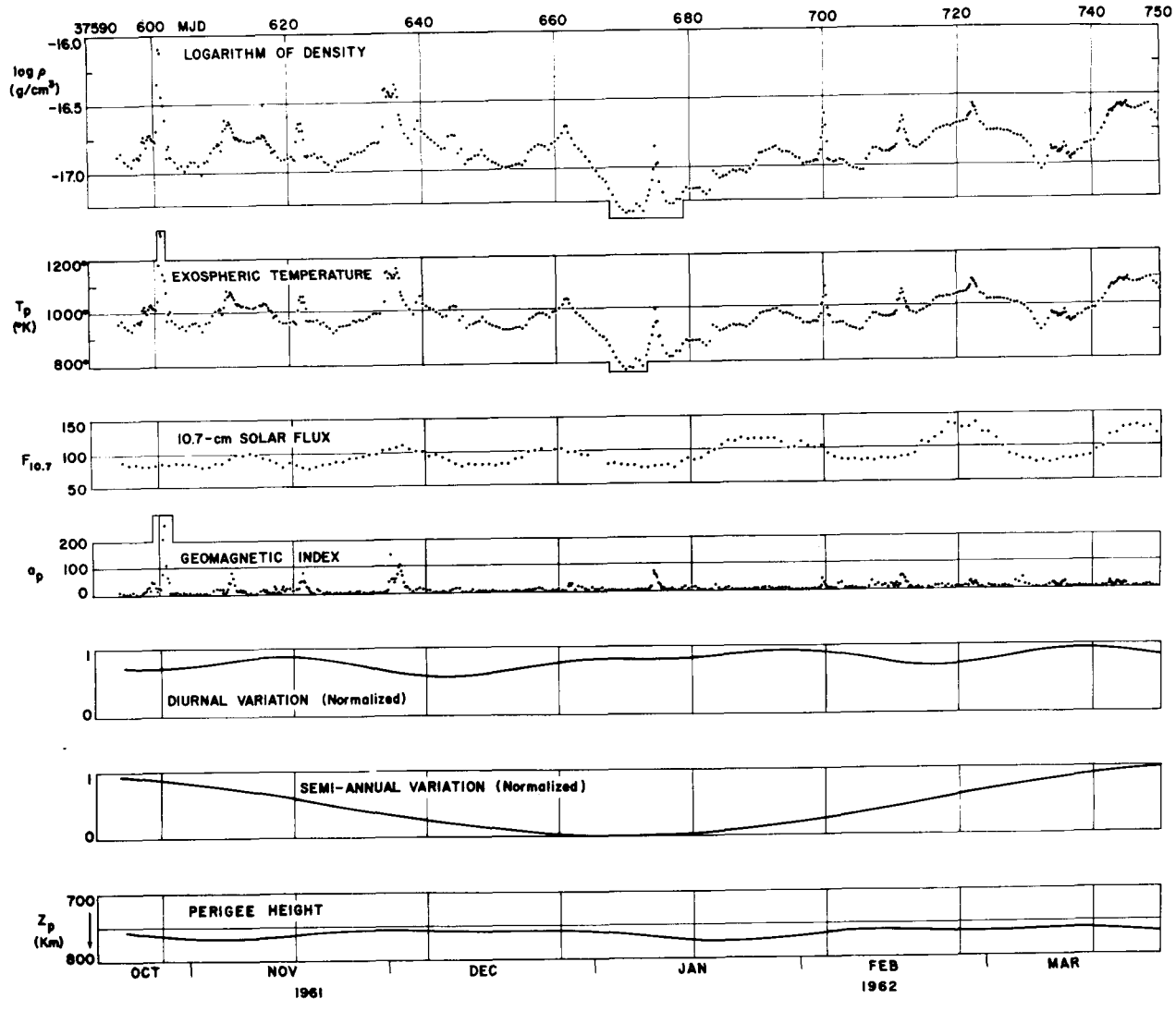

(2a)

Figures 2a-2d. --Atmospheric densities at perigee and exospheric temperatures compared with the 10.7-cm solar flux, the planetary geomagnetic index A_p, the normalized diurnal and semiannual variations, and the perigee height.

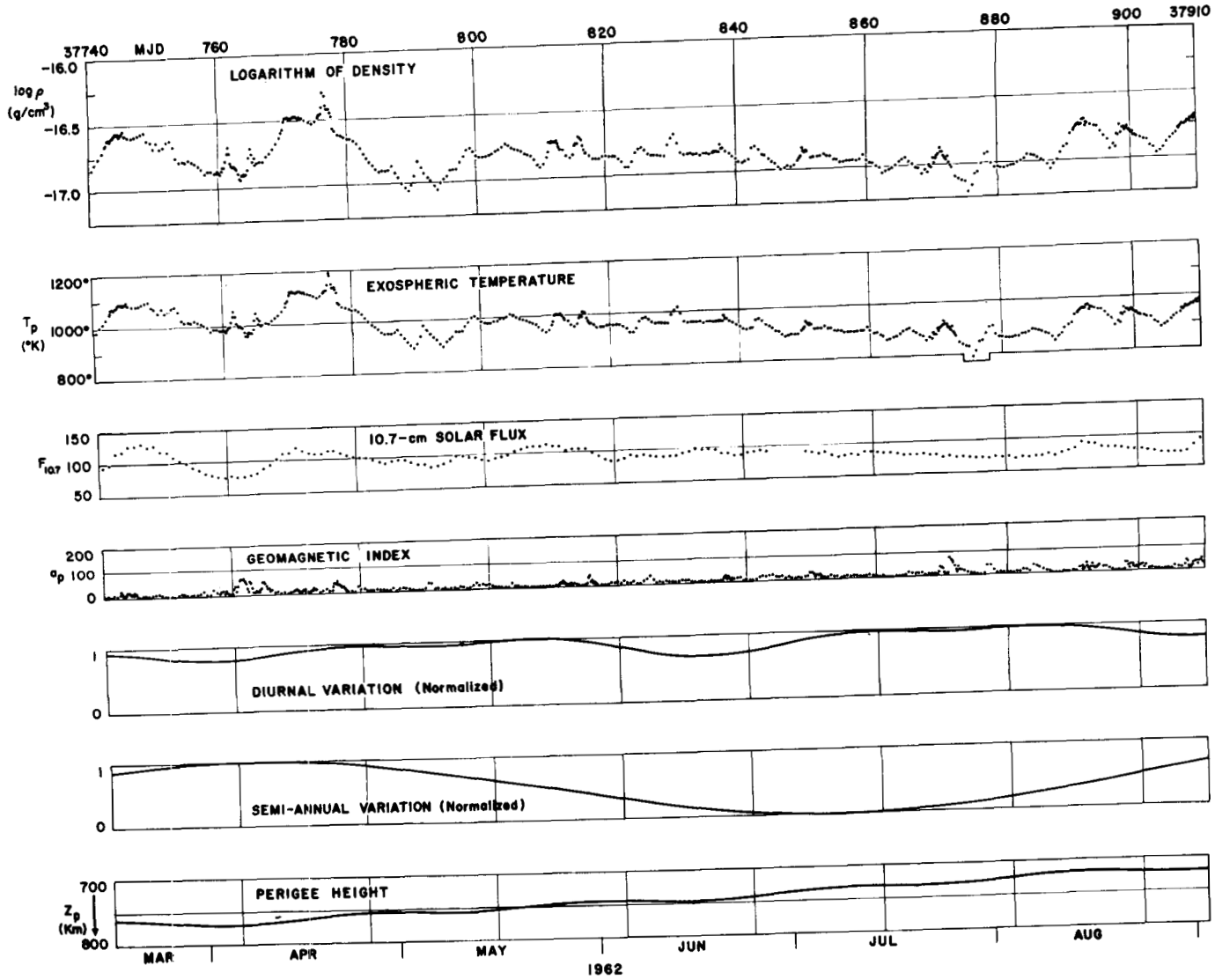
37740 MJD 760 780 800 820 840 860 880 900 37910
LOGARITHM OF DENSITY
log ρ (g/cm³)
-16.0
-16.5
-17.0
EXOSPHERIC TEMPERATURE
T_p (°K)
1200°
1000°
800°
10.7-cm SOLAR FLUX
F10.7
150
100
50
GEOMAGNETIC INDEX
a_p
200
100
0
DIURNAL VARIATION (Normalized)
1
0
SEMI-ANNUAL VARIATION (Normalized)
1
0
PERIGEE HEIGHT
Z_p (Km)
700
800
MAR
APR
MAY
JUN
JUL
AUG
1962

(2b)

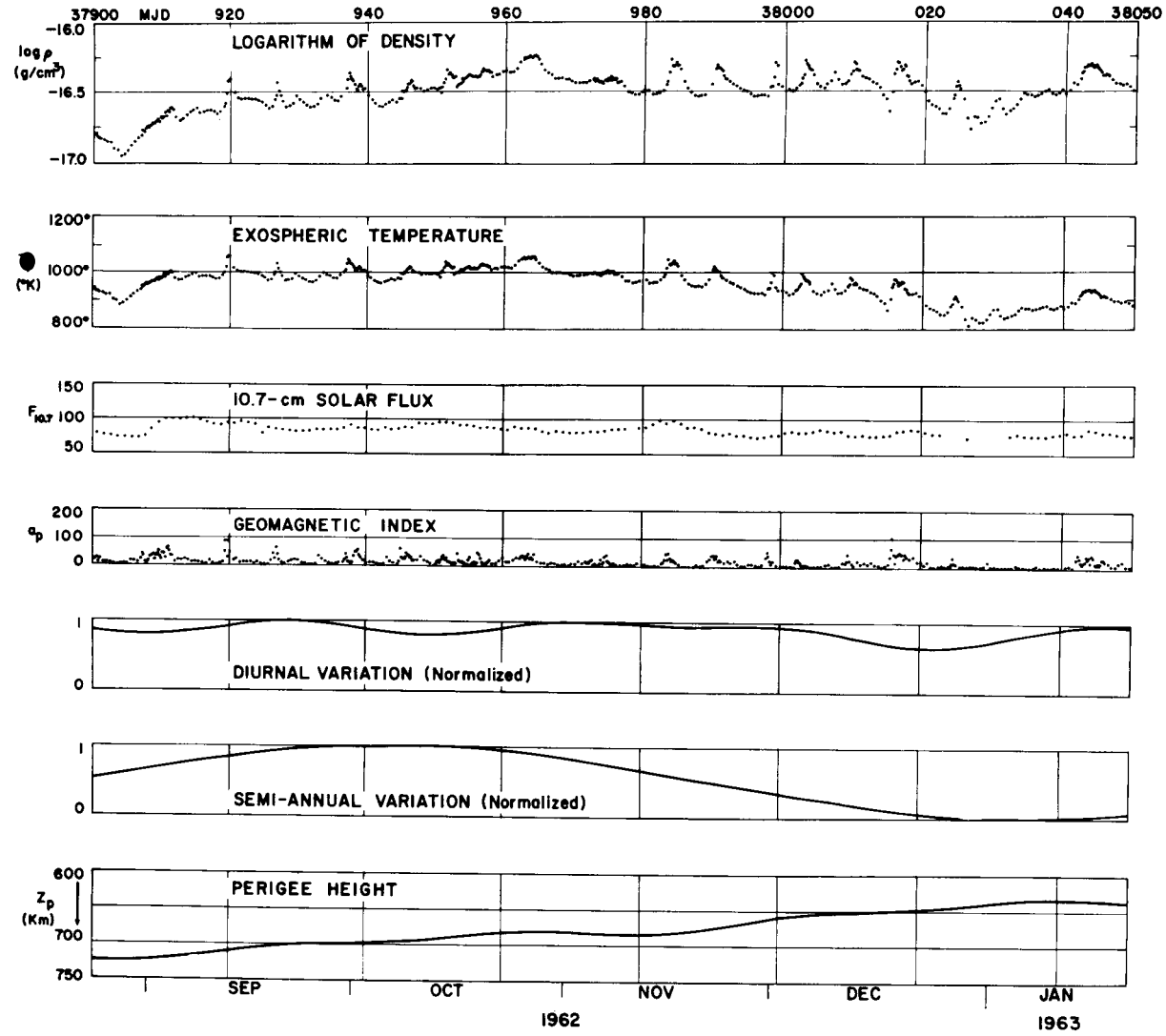
37900 MJD 920 940 960 980 38000 020 040 38050
LOGARITHM OF DENSITY
log ρ (g/cm³)
-16.0
-16.5
-17.0
EXOSPHERIC TEMPERATURE
(°K)
1200°
1000°
800°
10.7-cm SOLAR FLUX
F10.7
150
100
50
GEOMAGNETIC INDEX
ap
200
100
0
DIURNAL VARIATION (Normalized)
1
0
SEMI-ANNUAL VARIATION (Normalized)
1
0
PERIGEE HEIGHT
Zp (Km)
600
700
750
SEP
OCT
NOV
DEC
JAN
1962
1963

(2c)

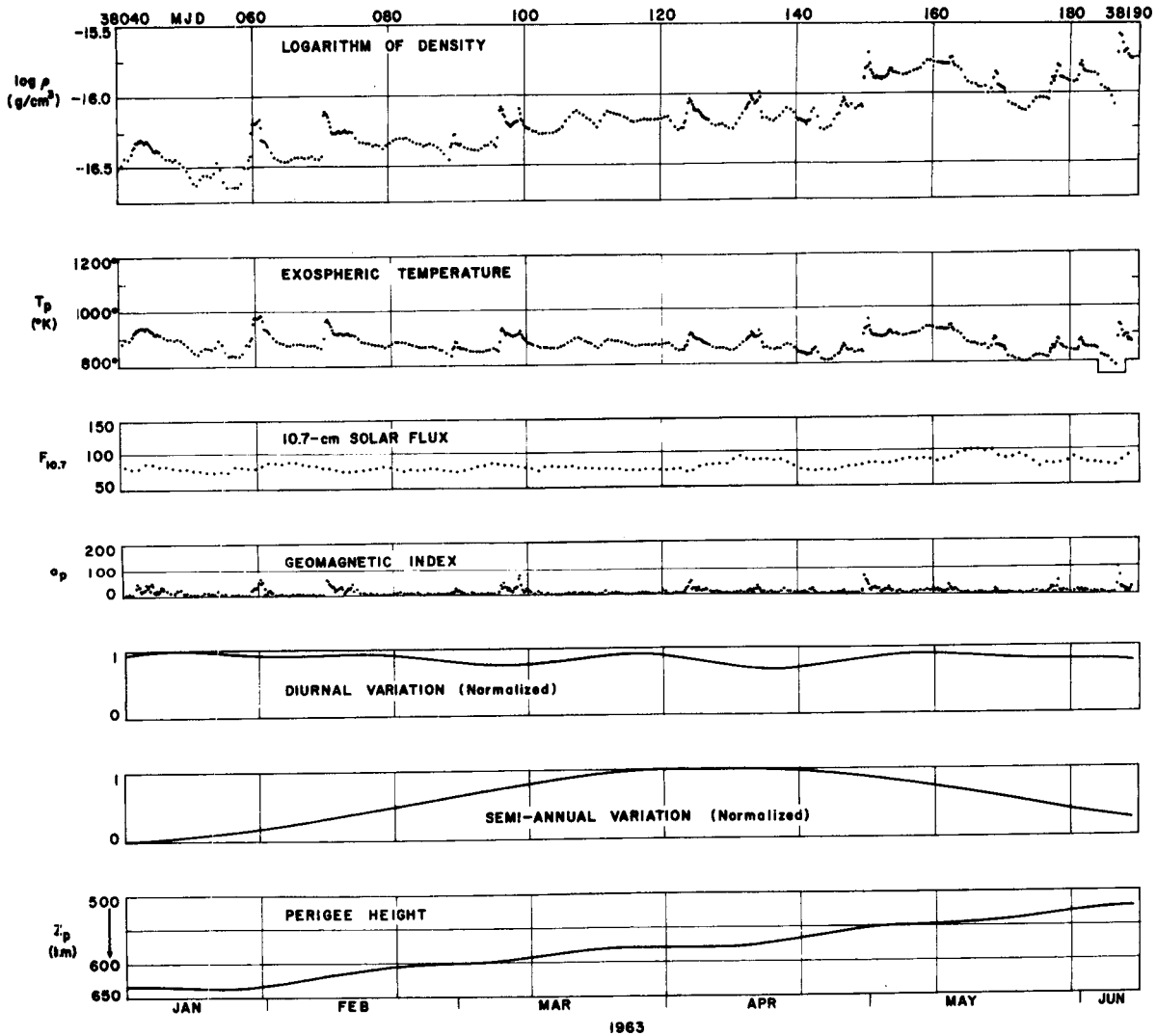
38040 MJD 060 080 100 120 140 160 180 38190
LOGARITHM OF DENSITY
log ρ (g/cm³)
-15.5
-16.0
-16.5
EXOSPHERIC TEMPERATURE
Tp (°K)
1200°
1000°
800°
10.7-cm SOLAR FLUX
F10.7
150
100
50
GEOMAGNETIC INDEX
ap
200
100
0
DIURNAL VARIATION (Normalized)
1
0
SEMI-ANNUAL VARIATION (Normalized)
1
0
PERIGEE HEIGHT
Zp (km)
500
600
650
JAN
FEB
MAR
APR
MAY
JUN
1963

(2d)

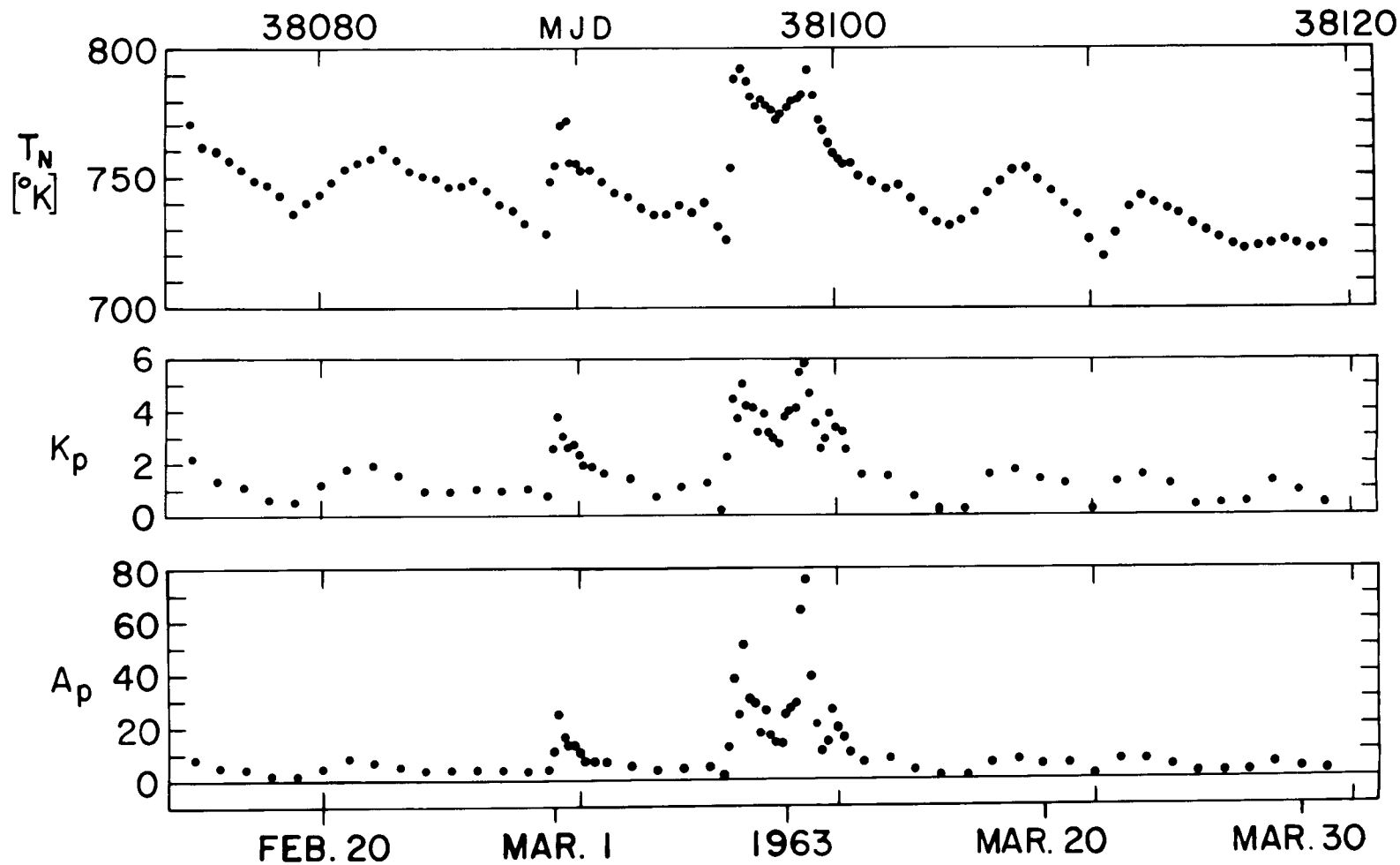

Figure 3. --Variations of the nighttime temperature during the geomagnetically quiet period of February and March 1963.

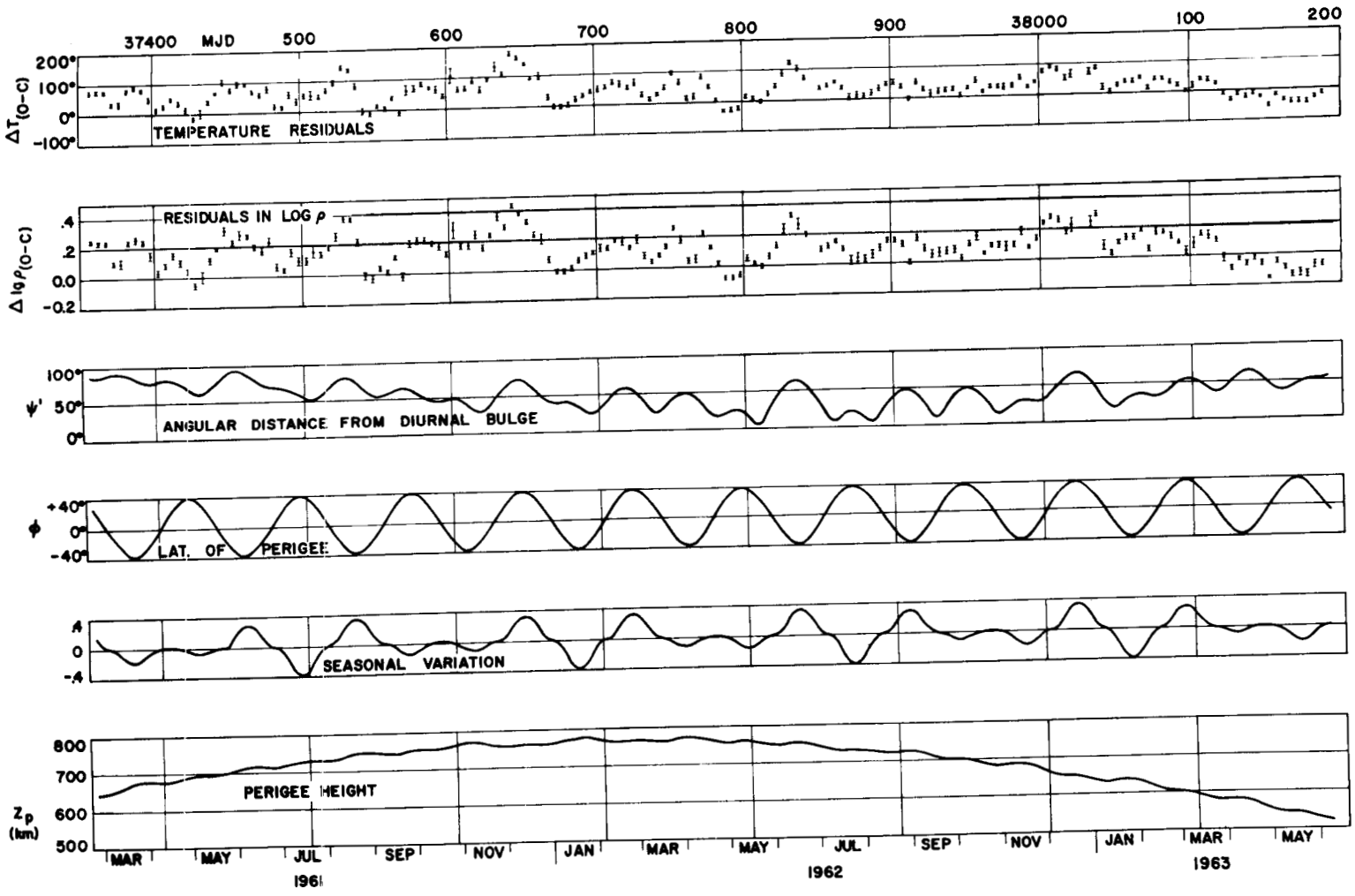

Figure 4. --Comparison of density and temperature data derived from the Explorer IX Satellite with Jacchia's (1964) atmospheric model.

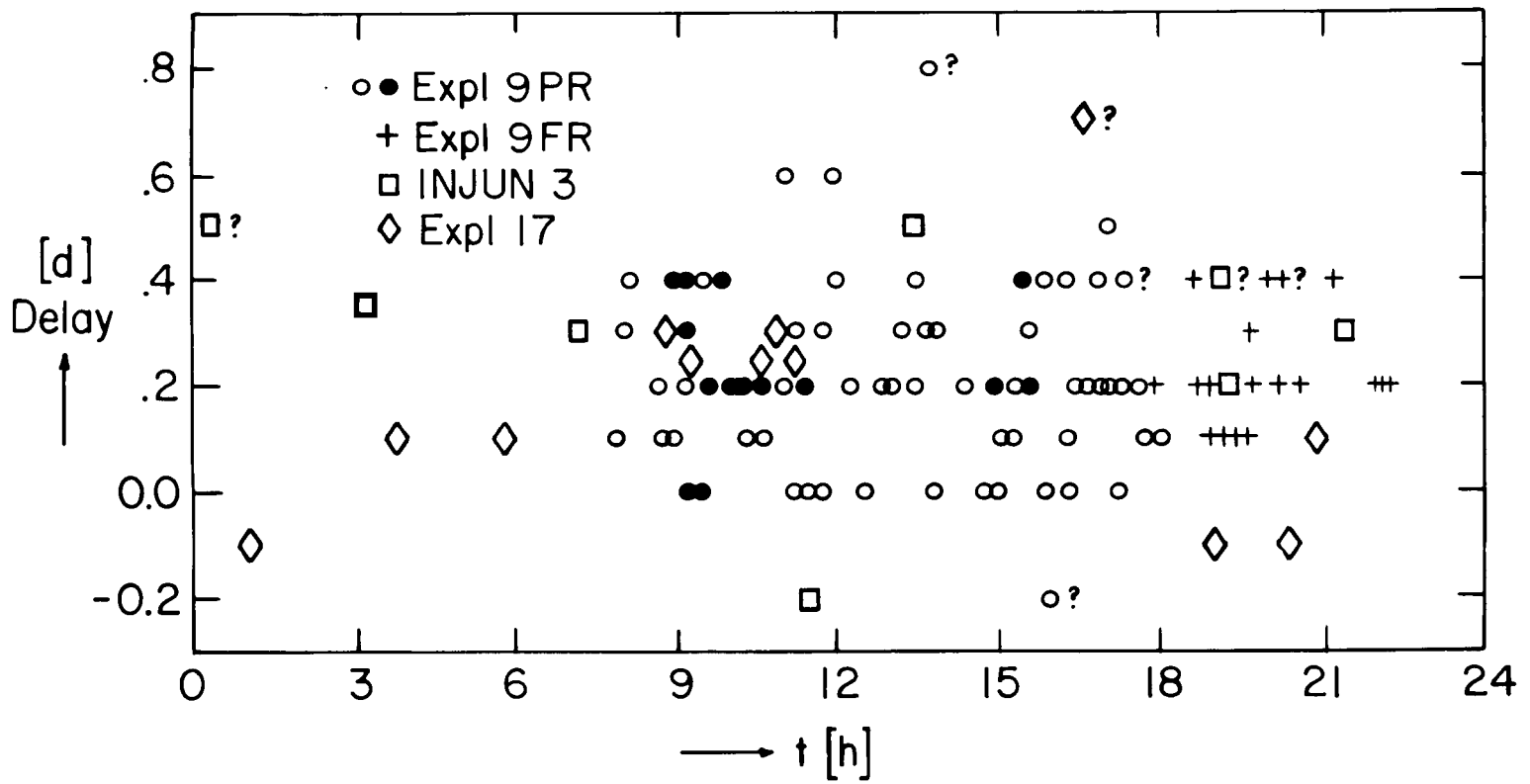

Figure 5.--Time lag between geomagnetic storm peaks and the related density increases versus local time of perigee.

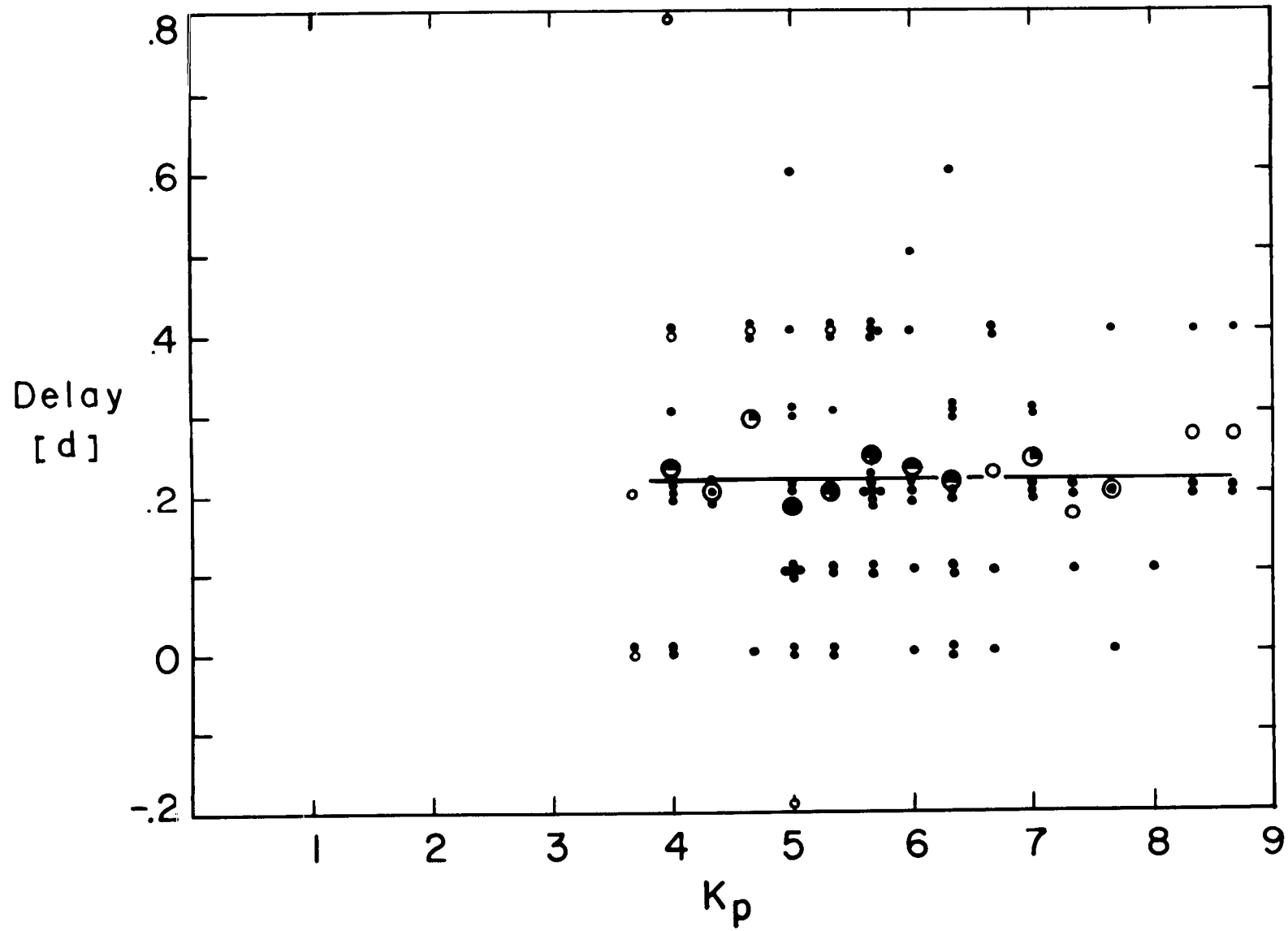

Figure 6.--Time delay in the geomagnetic activity effect versus intensity of the geomagnetic storm.

Table 1. --Least-squares fitting of orbital elements determined from precisely reduced observations

The orbital elements $Y_i(T)$ are represented by a polynomial and a sine term in the form:

$$Y_i(T) = a_0 + a_1 t + a_2 t^2 + a_3 t^3 + a_4 t^4 + a_5 t^5 + a_6 t^6$$
$$+ A \cdot \sin (B + C \cdot t)$$

where $t = T - T_0$ is the time in days elapsed from the TIME ORIGIN T_0. In the printout the t^n are omitted and also the "sin," brackets, and "t" in the sine term. Printed are only the a_i of the polynomial part in one line followed by a line giving the amplitude A, phase angle B, and frequency C of the sine term in the following format:

line 1 : a_0 a_1 a_2 a_3 a_4 a_5 a_6

line 2 : A B C

If there is no sine term in the fit of the elements ω (PERIGEE), Ω (NODE), i (INCLINATION), and e (ECCENTRICITY) this is indicated by asterisks. The MEAN ANOMALY M never has a sine term; therefore, there are no asterisks following the polynomial part. The elements ω, Ω, i are expressed in degrees and the mean anomaly in revolutions.

Table 1 (Continued)

SECTION 13 MJD 37594.0 TO 37620.0 (OCT 22,1961 TO NOV 17,1961)

TIME ORIGIN = 37594.00

PERIGEE						
199.9506	4.779782	0.0082870	-0.00112360	0.697152E-04	-0.1983094E-05	0.210444E-07
0.0106	74.35	24.00				
NODE						
352.47280	-3.629383	0.00081829	-0.110442E-03	0.694753E-05	-0.208404E-06	0.239573E-08
0.00033	213.279	34.06				
INCLINATION						
38.82808	-0.000444	0.00028553	-0.48794E-04	0.356397E-05	-0.119012E-06	0.14833E-08
0.00063	285.283	34.06				
ECCENTRICITY						
0.1059238	-0.64693E-04	0.40182E-05	-0.697596E-06	0.62580E-07	-0.233904E-08	0.314077E-10
0.0000127	180.29439	24.00				
MEAN ANOMALY						
0.077757	12.177313	0.62779E-04	-0.11513E-05	0.2031E-07	0.333E-10	

SECTION 14 MJD 37614.0 TO 37640.0 (NOV 11,1961 TO DEC 7,1961)

TIME ORIGIN = 37614.00

PERIGEE						
296.0603	4.800157	-0.010860	0.00278683	-0.2449778E-03	0.888747E-05	-0.115213E-06
0.0553	317.89	24.00				
NODE						
279.92756	-3.6289172	0.00047628	-0.81561E-04	0.582039E-05	-0.192043E-06	0.23451E-08
0.00013	83.244	34.06				
INCLINATION						
38.82680	-0.000652	0.0002330	-0.420790E-04	0.327635E-05	-0.115215E-06	0.149337E-08
0.00019	104.160	34.06				
ECCENTRICITY						
0.1052041	-0.00001343	-0.48429E-05	0.182053E-05	-0.1506255E-06	0.516901E-08	-0.64510E-10
0.0000356	328.01507	24.00				
MEAN ANOMALY						
0.643277	12.179121	0.48259E-04	-0.5488E-07	-0.4450E-08	0.6178E-09	

Table 1 (Continued)

SECTION 15 MJD 37634.0 TO 37660.0 (DEC 1,1961 TO DEC 27,1961)

TIME ORIGIN = 37634.00

PERIGEE						
31.9393	4.762171	0.0026167	-0.593668E-03	0.420690E-04	-0.1279593E-05	0.147848E-07
0.0088	359.47	24.00				
NODE						
207.35413	-3.6303265	-0.00011178	-0.132992E-04	0.118228E-05	-0.29315E-07	0.2230E-09
0.00024	38.495	34.06				
INCLINATION						
38.82175	-0.0007168	-0.00003596	0.4415E-05	0.12162E-06	-0.14414E-07	0.25858E-09
0.000038	342.842	34.06				
ECCENTRICITY						
0.1058937	0.56672E-04	0.17075E-05	-0.431380E-06	0.70732E-08	0.27427E-09	-0.6823E-11
0.0000136	97.93785	24.00				
MEAN ANOMALY						
0.245725	12.181346	0.113924E-03	-0.34220E-05	0.95727E-07	-0.13738E-08	

SECTION 16 MJD 37654.0 TO 37680.0 (DEC 21,1961 TO JAN 16,1962)

TIME ORIGIN = 37654.00

PERIGEE						
127.0594	4.76571	0.0061948	-0.1480368E-02	0.1391869E-03	-0.531673E-05	0.71472E-07
0.0355	159.26	24.00				
NODE						
134.70591	-3.631063	-0.00026736	0.529058E-04	-0.410359E-05	0.147651E-06	-0.199161E-08
0.00041	163.903	34.06				
INCLINATION						
38.818253	0.00030198	0.00011360	-0.2802885E-04	0.2529990E-05	-0.979353E-07	0.1370200E-08
0.000137	139.4168	34.06				
ECCENTRICITY						
0.1058180	-0.00009481	0.60651E-05	-0.99375E-06	0.632696E-07	-0.159788E-08	0.13543E-10
0.0000095	43.47565	24.00				
MEAN ANOMALY						
0.901757	12.183806	0.1281E-05	0.25381E-05	-0.148255E-06	0.25967E-08	

Table 1 (Continued)

SECTION 17 MJD 37674.0 TO 37700.0 (JAN 10,1962 TO FEB 5,1962)

TIME ORIGIN = 37674.00

PERIGEE						
222.8159	4.812759	-0.0019439	0.00034931	-0.22522E-04	0.61035E-06	-0.59961E-08
0.0135	255.49	24.00				
NODE						
62.08948	-3.6339261	0.00052836	-0.84423E-04	0.616323E-05	-0.209563E-06	0.266778E-08
0.00082	17.547	34.06				
INCLINATION						
38.82439	0.000243	0.00002122	-0.2895E-05	-0.6690E-07	0.11754E-07	-0.26161E-09
0.00059	137.499	34.06				
ECCENTRICITY						
0.1042557	-0.00005050	0.103120E-04	-0.154223E-05	0.107061E-06	-0.326046E-08	0.36553E-10
0.0000232	79.41678	24.00				
MEAN ANOMALY						
0.583223	12.184242	0.16178E-04	-0.2252E-06	0.3191E-07	-0.4457E-09	

SECTION 18 MJD 37694.0 TO 37720.0 (JAN 30,1962 TO FEB 25,1962)

TIME ORIGIN = 37694.00

PERIGEE						
319.0526	4.81501	-0.0003986	-0.00029533	0.322230E-04	-0.1374595E-05	0.204085E-07
0.0120	148.28	24.00				
NODE						
349.49528	-3.629881	-0.00017948	0.152376E-04	-0.101568E-05	0.34367E-07	-0.4812E-09
0.00028	276.543	34.06				
INCLINATION						
38.82524	-0.000610	0.00001681	0.21758E-05	-0.26693E-06	0.10607E-07	-0.14773E-09
0.00047	26.292	34.06				
ECCENTRICITY						
0.1040389	0.23142E-04	0.93693E-05	-0.156813E-05	0.1232827E-06	-0.430735E-08	0.539751E-10
0.0000292	129.95377	24.00				
MEAN ANOMALY						
0.276404	12.185261	0.54797E-04	-0.11382E-05	0.82136E-07	-0.14480E-08	

Table 1 (Continued)

SECTION 19 MJD 37714.0 TO 37740.0 (FEB 19,1962 TO MAR 17,1962)

TIME ORIGIN = 37714.00

PERIGEE						
54.8791	4.756564	0.001331	0.00023770	-0.419785E-04	0.205146E-05	-0.31520E-07
0.0189	8.50	24.00				
NODE						
276.86451	-3.632880	-0.0002181	-0.12192E-05	0.143475E-05	-0.73255E-07	0.112145E-08
0.00035	296.990	34.06				
INCLINATION						
38.81879	0.0004870	-0.00029876	0.43070E-04	-0.261372E-05	0.71926E-07	-0.73650E-09
0.00018	332.265	34.06				
ECCENTRICITY						
0.1050931	0.61856E-04	-0.108134E-04	0.1186274E-05	-0.854147E-07	0.285752E-08	-0.346251E-10
0.0000251	268.07246	24.00				
MEAN ANOMALY						
0.002953	12.187617	0.33215E-04	0.45253E-05	-0.227945E-06	0.33875E-08	

SECTION 20 MJD 37734.0 TO 37760.0 (MAR 11,1962 TO APR 6,1962)

TIME ORIGIN = 37734.00

PERIGEE						
150.3022	4.77683	0.0001424	0.00065952	-0.690487E-04	0.266048E-05	-0.354859E-07
0.0236	323.50	24.00				
NODE						
204.17649	-3.6337146	-0.00013556	0.256297E-04	-0.241633E-05	0.94150E-07	-0.132668E-08
0.00054	197.575	34.06				
INCLINATION						
38.818110	0.00002840	0.56987E-04	-0.716962E-05	0.541250E-06	-0.191183E-07	0.241740E-09
0.000070	53.2966	34.06				
ECCENTRICITY						
0.1047702	-0.47682E-04	-0.44138E-05	0.886362E-06	-0.57292E-07	0.173446E-08	-0.201165E-10
0.0000144	339.21403	24.00				
MEAN ANOMALY						
0.779118	12.189890	-0.9747E-05	0.47982E-05	-0.7590E-07	-0.1555E-09	

Table 1 (Continued)

SECTION 21 MJD 37754.0 TO 37780.0 (MAR 31,1962 TO APR 26,1962)

TIME ORIGIN = 37754.00

PERIGEE						
246.3786	4.811279	0.0022274	-0.369864E-03	0.249080E-04	-0.747086E-06	0.79997E-08
0.0097	89.20	24.00				
NODE						
131.48328	-3.635623	-0.00026996	0.176859E-04	-0.28475E-06	-0.13381E-07	0.36236E-09
0.00040	206.476	34.06				
INCLINATION						
38.825168	0.00033271	-0.101797E-03	0.198475E-04	-0.1572833E-05	0.528875E-07	-0.644873E-09
0.000284	323.1991	34.06				
ECCENTRICITY						
0.1042555	0.7385E-05	-0.38135E-05	0.128792E-05	-0.1195971E-06	0.451072E-08	-0.599673E-10
0.0000107	339.54513	24.00				
MEAN ANOMALY						
0.598810	12.192612	0.112318E-03	-0.620385E-05	0.267985E-06	-0.348193E-08	

SECTION 22 MJD 37774.0 TO 37800.0 (APR 20,1962 TO MAY 16,1962)

TIME ORIGIN = 37774.00

PERIGEE						
342.6283	4.810556	0.0000136	-0.00022001	0.170934E-04	-0.561498E-06	0.6852E-08
0.0088	127.74	24.00				
NODE						
58.73946	-3.639571	0.00055633	-0.90236E-04	0.575546E-05	-0.169015E-06	0.18702E-08
0.00016	98.363	34.06				
INCLINATION						
38.82645	-0.0000569	-0.0001251	0.130591E-04	-0.48567E-06	0.4946E-08	0.4636E-10
0.00055	248.639	34.06				
ECCENTRICITY						
0.1046493	0.22355E-04	0.61047E-05	-0.51215E-06	0.19181E-07	-0.25286E-09	-0.1081E-11
0.0000084	39.97123	24.00				
MEAN ANOMALY						
0.478095	12.195400	0.137999E-03	-0.440589E-05	0.12110E-06	-0.12426E-08	

Table 1 (Continued)

SECTION 23 MJD 37794.0 TO 37820.0 (MAY 10,1962 TO JUN 5,1962)

TIME ORIGIN = 37794.00

PERIGEE					
78.4551	4.780185	-0.0019949	0.00022092	-0.74342E-05	0.8992E-07
0.0061	237.43	24.00			
NODE					
345.94850	-3.640761	-0.00011652	0.34500E-05	-0.5993E-07	-0.651E-09
0.00020	113.022	34.00			
INCLINATION					
38.82030	-0.0000194	0.00008576	-0.115684E-04	0.5872E-06	-0.9861E-08
0.00052	171.480	34.00			
ECCENTRICITY					
0.1056232	0.46149E-04	-0.35172E-05	0.5213E-07	0.1962E-08	-0.40195E-10
0.0000077	86.88062	24.00			
MEAN ANOMALY					
0.421481	12.198493	0.62899E-04	0.14223E-05	-0.63366E-07	0.113496E-08

SECTION 24 MJD 37814.0 TO 37840.0 (MAY 30,1962 TO JUN 25,1962)

TIME ORIGIN = 37814.00

PERIGEE					
174.1293	4.798189	0.0009928	-0.00002213	-0.9491E-06	0.3268E-07
0.0040	22.45	24.00			
NODE					
273.10293	-3.6438883	-0.00013516	0.4973E-05	-0.3281E-06	0.6341E-08
0.00037	1.437	34.00			
INCLINATION					
38.82416	0.000101	0.0000301	0.6877E-06	-0.19659E-06	0.5036E-08
0.00022	22.061	34.00			
ECCENTRICITY					
0.1057453	-0.00000711	0.18941E-05	0.56187E-07	-0.48363E-08	0.76298E-10
0.0000031	240.16805	24.00			
MEAN ANOMALY					
0.421302	12.201690	0.62582E-04	0.368076E-05	-0.158528E-06	0.18746E-08

SECTION 25 MJD 37834.0 TO 37860.0 (JUN 19,1962 TO JUL 15,1962)

TIME ORIGIN = 37834.00

PERIGEE					
270.26310	4.805001	0.0012091	-0.89125E-04	0.38621E-05	-0.73342E-07
0.00651	115.960	24.00			
NODE					
200.17844	-3.648221	-0.00028299	0.25384E-04	-0.87698E-06	0.10102E-07
0.000042	192.314	34.00			
INCLINATION					
38.82831	-0.000053	0.00001094	0.4122E-05	-0.3332E-06	0.6203E-08
0.00017	303.924	34.00			
ECCENTRICITY					
0.1062905	0.38392E-04	0.8492E-06	-0.230073E-06	0.139426E-07	-0.235991E-09
0.0000081	284.20223	24.00			
MEAN ANOMALY					
0.490236	12.204996	0.57854E-04	-0.112690E-05	0.28954E-07	-0.1263E-09

SECTION 26 MJD 37854.0 TO 37880.0 (JUL 9,1962 TO AUG 4,1962)

TIME ORIGIN = 37854.00

PERIGEE					
6.5088	4.80783	0.0009664	-0.294188E-03	0.152360E-04	-0.24171E-06
0.0036	79.50	24.00			
NODE					
127.19570	-3.649001	-0.00005660	-0.3314E-05	0.14241E-06	-0.1563E-08
0.00037	89.113	34.00			
INCLINATION					
38.83037	-0.0004750	0.0000311	-0.2173E-05	0.1222E-06	-0.2172E-08
0.00023	74.309	34.00			
ECCENTRICITY					
0.1070284	0.00005332	0.23678E-05	-0.250893E-06	0.104722E-07	-0.17947E-09
0.0000123	59.04415	24.00			
MEAN ANOMALY					
0.608503	12.206797	0.46981E-04	0.8781E-06	-0.7135E-08	-0.1381E-09

Table 1 (Continued)

SECTION 27 MJD 37874.0 TO 37900.0 (JUL 29,1962 TO AUG 24,1962)

TIME ORIGIN = 37874.00

PERIGEE					
102.3561	4.786555	0.000150	0.00002164	0.840E-06	-0.3307E-07
0.0076	29.66	24.00			
NODE					
54.18501	-3.6515193	-0.00024045	0.19433E-04	-0.81690E-06	0.109390E-07
0.00069	233.345	34.00			
INCLINATION					
38.82906	0.0001068	0.00008275	-0.78274E-05	0.2921E-06	-0.3848E-08
0.00046	9.123	34.00			
ECCENTRICITY					
0.1081398	0.00004501	-0.66417E-05	0.50492E-06	-0.17840E-07	0.25145E-09
0.0000094	201.47192	24.00			
MEAN ANOMALY					
0.768732	12.209306	0.00009500	-0.276695E-05	0.12200E-06	-0.14841E-08

SECTION 28 MJD 37894.0 TO 37920.0 (AUG 18,1962 TO SEP 13,1962)

TIME ORIGIN = 37894.00

PERIGEE					
198.3534	4.82154	-0.0005826	0.88178E-04	-0.41589E-05	0.6628E-07
0.0074	191.94	24.00			
NODE					
341.11821	-3.6555658	-0.00005782	-0.7414E-05	0.3260E-06	-0.4503E-08
0.00034	176.532	34.00			
INCLINATION					
38.836353	0.0004802	-0.96895E-04	0.109501E-04	-0.44860E-06	0.59958E-08
0.000548	287.2457	34.00			
ECCENTRICITY					
0.1083780	0.28567E-04	-0.29432E-05	0.56981E-06	-0.270979E-07	0.42025E-09
0.0000168	229.37679	24.00			
MEAN ANOMALY					
0.985474	12.212501	0.114224E-03	-0.12100E-05	0.59363E-07	-0.100099E-08

Table 1 (Continued)

SECTION 29 MJD 37914.0 TO 37940.0 (SEP 7,1962 TO OCT 3,1962)

TIME ORIGIN = 37914.00

PERIGEE					
294.8088	4.827545	-0.0016061	0.00025243	-0.142424E-04	0.24257E-06
0.0113	269.36	24.00			
NODE					
267.96193	-3.6596499	-0.00016394	0.87592E-05	-0.43636E-06	0.5800E-08
0.00031	128.512	34.00			
INCLINATION					
38.84190	0.0000989	0.00003392	-0.5985E-05	0.22991E-06	-0.2514E-08
0.00017	214.353	34.00			
ECCENTRICITY					
0.1093341	0.00005292	0.51036E-05	-0.478384E-06	0.22301E-07	-0.36484E-09
0.0000211	16.74426	24.00			
MEAN ANOMALY					
0.277824	12.216735	0.84152E-04	0.27532E-05	-0.111640E-06	0.20214E-08

SECTION 30 MJD 37934.0 TO 37960.0 (SEP 27,1962 TO OCT 23,1962)

TIME ORIGIN = 37934.00

PERIGEE					
31.2332	4.804888	-0.0003588	-0.00007083	0.31388E-05	-0.1672E-07
0.0091	38.13	24.00			
NODE					
194.72289	-3.665542	-0.00017599	0.4453E-05	-0.32644E-06	0.6876E-08
***	***	***			
INCLINATION					
38.83891	-0.0009867	0.00017441	-0.13160E-04	0.55246E-06	-0.8591E-08
0.00043	274.943	34.00			
ECCENTRICITY					
0.1110080	0.105171E-03	-0.10392E-05	0.7283E-07	-0.74849E-08	0.14453E-09
0.0000116	128.59328	24.00			
MEAN ANOMALY					
0.656820	12.221375	0.183123E-03	-0.298393E-05	0.15142E-06	-0.28183E-08

Table 1 (Continued)

SECTION 31 MJD 37954.0 TO 37980.0 (OCT 17,1962 TO NOV 12,1962)

TIME ORIGIN = 37954.00

PERIGEE					
127.0807	4.78894	0.0021293	0.00003951	-0.46274E-05	0.8835E-07
0.0088	205.77	24.00			
NODE					
121.34640	-3.6710658	-0.0004710	0.484069E-04	-0.22041E-05	0.32905E-07
0.00047	84.634	34.00			
INCLINATION					
38.84461	0.0011266	-0.00002381	0.1362E-05	-0.1270E-06	0.2857E-08
0.00059	207.040	34.00			
ECCENTRICITY					
0.1125555	0.20857E-04	-0.30990E-05	0.22091E-06	-0.80150E-08	0.14666E-09
0.0000213	274.11712	24.00			
MEAN ANOMALY					
0.148859	12.227902	0.53893E-04	0.80771E-05	-0.294530E-06	0.39873E-08

SECTION 32 MJD 37974.0 TO 38000.0 (NOV 6,1962 TO DEC 2,1962)

TIME ORIGIN = 37974.00

PERIGEE					
223.5778	4.852765	-0.0023359	0.313670E-03	-0.15271E-04	0.24166E-06
0.0150	245.28	24.00			
NODE					
47.87827	-3.6772377	-0.00002296	-0.63385E-05	0.1252E-06	-0.1438E-08
0.00140	302.509	34.00			
INCLINATION					
38.85670	-0.0000853	0.00014046	-0.21422E-04	0.118237E-05	-0.21885E-07
0.00069	113.689	34.00			
ECCENTRICITY					
0.1126917	0.00000910	0.96663E-05	-0.836176E-06	0.359943E-07	-0.54211E-09
0.0000218	32.07656	24.00			
MEAN ANOMALY					
0.758602	12.233622	0.125397E-03	0.30033E-05	-0.81636E-07	0.7205E-09

Table 1 (Continued)

SECTION 33 MJD 37994.0 TO 38020.0 (NOV 26,1962 TO DEC 22,1962)

TIME ORIGIN = 37994.00

PERIGEE						
320.5405	4.848499	-0.0023076	0.00023324	-0.12612E-04	0.21666E-06	
0.0025	221.37	24.00				
NODE						
334.28773	-3.6826796	-0.00014734	-0.8262E-05	0.2870E-06	-0.3591E-08	
0.00036	17.232	34.00				
INCLINATION						
38.85842	0.0013282	-0.0006791	0.106044E-03	-0.769195E-05	0.258417E-06	-0.32340E-08
0.00087	97.735	34.00				
ECCENTRICITY						
0.1140697	0.00010462	0.37077E-05	-0.38753E-06	0.189699E-07	-0.34395E-09	
0.0000127	96.37549	24.00				
MEAN ANOMALY						
0.494461	12.240245	0.147665E-03	0.168965E-05	-0.17724E-07	-0.1722E-09	

SECTION 34 MJD 38014.0 TO 38040.0 (DEC 16,1962 TO JAN 11,1963)

TIME ORIGIN = 38014.00

PERIGEE						
57.1187	4.800339	0.0037351	-0.00061641	0.33781E-04	-0.56010E-06	
0.0107	99.08	24.00				
NODE						
260.54375	-3.6925358	-0.00014687	-0.94696E-05	0.61847E-06	-0.97197E-08	
0.00066	339.118	34.00				
INCLINATION						
38.85148	-0.000092	0.00017225	-0.28685E-04	0.23301E-05	-0.85085E-07	0.11472E-08
0.00031	53.161	34.00				
ECCENTRICITY						
0.1164693	0.131197E-03	-0.67938E-05	0.430072E-06	-0.207986E-07	0.36044E-09	
0.0000068	181.39261	24.00				
MEAN ANOMALY						
0.368665	12.247309	0.235920E-03	-0.295399E-05	-0.126954E-06	0.38512E-08	

Table 1 (Continued)

SECTION 35 MJD 38034.0 TO 38060.0 (JAN 5,1963 TO JAN 31,1963)

TIME ORIGIN = 38034.00

PERIGEE						
153.2953	4.853269	-0.0018193	0.254188E-03	-0.8722E-05	0.8666E-07	
***	***	***				
NODE						
186.62418	-3.6960774	-0.00042746	0.552096E-04	-0.299051E-05	0.51153E-07	
0.00089	87.963	34.00				
INCLINATION						
38.86277	-0.0003993	0.00060420	-0.776671E-04	0.411362E-05	-0.97276E-07	0.8251E-09
***	***	***				
ECCENTRICITY						
0.1176229	-0.32540E-04	0.104174E-04	-0.118313E-05	0.579775E-07	-0.93744E-09	
0.0000340	34.16649	24.00				
MEAN ANOMALY						
0.377504	12.252342	0.33892E-04	0.528999E-05	-0.88523E-07		

SECTION 36 MJD 38054.0 TO 38080.0 (JAN 25,1963 TO FEB 20,1963)

TIME ORIGIN = 38054.00

PERIGEE						
250.5442	4.38222	-0.0031158	0.00029371	-0.11620E-04	0.154389E-06	
0.0066	136.70	24.00				
NODE						
112.65904	-3.7018690	0.00005915	-0.327475E-04	0.223263E-05	-0.73903E-07	0.9311E-09
***	***	***				
INCLINATION						
38.87451	0.001231	-0.00051472	0.81880E-04	-0.569034E-05	0.180985E-06	-0.21700E-08
***	***	***				
ECCENTRICITY						
0.1179662	0.00006461	-0.3691E-05	0.121940E-05	-0.1023034E-06	0.364575E-08	-0.47352E-10
***	***	***				
MEAN ANOMALY						
0.46614	12.256948	0.00018667	-0.4566E-06	0.210E-07		

Table 1 (Continued)

SECTION 37 MJD 38074.0 TO 38100.0 (FEB 14,1963 TO MAR 12,1963)

TIME ORIGIN = 38074.00

PERIGEE						
347.9223	4.860385	-0.0012321	0.266772E-03	-0.29080E-04	0.121336E-05	-0.173968E-07
***	***	***				
NODE						
38.56371	-3.7094153	0.0002150	-0.675188E-04	0.421650E-05	-0.118782E-06	0.123134E-08
***	***	***				
INCLINATION						
38.87785	0.0008739	-0.00027626	0.23041E-04	-0.82483E-06	0.11427E-07	
0.00035	226.723	34.00				
ECCENTRICITY						
0.119762	0.00010970	0.9821E-05	-0.13485E-05	0.66580E-07	-0.11317E-08	
0.000044	86.8142	24.00				
MEAN ANOMALY						
0.679370	12.264768	0.00015271	0.57752E-05	-0.273069E-06	0.46273E-08	

SECTION 38 MJD 38094.0 TO 38120.0 (MAR 6,1963 TO APR 1,1963)

TIME ORIGIN = 38094.00

PERIGEE						
84.8871	4.84061	-0.0007090	-0.97691E-04	0.220185E-04	-0.99306E-06	0.140751E-07
***	***	***				
NODE						
324.29477	-3.718581	-0.00032566	0.154697E-04	-0.6251E-06	0.8906E-08	
***	***	***				
INCLINATION						
38.87373	0.0003499	0.00003328	-0.132E-06	-0.380E-08	-0.8588E-09	
0.00064	217.353	34.00				
ECCENTRICITY						
0.122095	0.00013644	-0.19968E-04	0.22825E-05	-0.139336E-06	0.40512E-08	-0.43874E-10
***	***	***				
MEAN ANOMALY						
0.053244	12.272484	0.321782E-03	-0.829563E-05	0.314287E-06	-0.41865E-08	

Table 1 (Continued)

SECTION 39 MJD 38114.0 TO 38140.0 (MAR 26,1963 TO APR 21,1963)

TIME ORIGIN = 38114.00

PERIGEE						
181.8713	4.880794	-0.0002587	0.116165E-03	-0.65096E-05	0.105092E-06	
0.0073	129.77	24.00				
NODE						
249.84538	-3.7265661	0.00018451	-0.683994E-04	0.50400E-05	-0.1797192E-06	0.243682E-08
***	***	***				
INCLINATION						
38.88970	0.000071	0.00010547	-0.17593E-04	0.125041E-05	-0.41101E-07	0.52240E-09
***	***	***				
ECCENTRICITY						
0.1229659	-0.2294E-05	0.112258E-04	-0.1318667E-05	0.851773E-07	-0.2609600E-08	0.304144E-10
***	***	***				
MEAN ANOMALY						
0.602174	12.282128	0.229194E-03	0.11290E-05	-0.911E-08		

SECTION 40 MJD 38134.0 TO 38160.0 (APR 15,1963 TO MAY 11,1963)

TIME ORIGIN = 38134.00

PERIGEE						
279.6070	4.88731	-0.0008922	0.102495E-03	-0.41397E-05	0.5652E-07	
0.0081	219.17	24.00				
NODE						
175.22874	-3.7381589	0.00006666	-0.29566E-04	0.14160E-05	-0.23768E-07	
0.00023	272.292	34.00				
INCLINATION						
38.89453	-0.0000976	0.00027893	-0.42325E-04	0.308864E-05	-0.106862E-06	0.13782E-08
***	***	***				
ECCENTRICITY						
0.1240794	0.00006242	0.98393E-05	-0.1085192E-05	0.484948E-07	-0.755592E-09	
0.0000191	32.55118	24.00				
MEAN ANOMALY						
0.34403	12.292086	0.00039643	-0.14965E-04	0.49681E-06	-0.4216E-08	

Table 1 (Continued)

SECTION 41 MJD 38154.0 TO 38180.0 (MAY 5,1963 TO MAY 31,1963)

TIME ORIGIN = 38154.00

PERIGEE						
	17.3291	4.88633	0.0016120	-0.260877E-03	0.127563E-04	-0.19801E-06
	0.0063	49.97	24.00			
NODE						
	100.40549	-3.744181	-0.00024839	-0.23905E-04	0.120279E-05	-0.18178E-07
	0.00072	100.168	34.00			
INCLINATION						
	38.90555	0.0002369	-0.00009398	0.45087E-05	-0.161E-08	-0.1794E-08
	0.00042	114.125	34.00			
ECCENTRICITY						
	0.125925	0.0001171	-0.00000911	0.89291E-06	-0.38376E-07	0.56397E-09
	***	***	***			
MEAN ANOMALY						
	0.290551	12.302615	0.308396E-03	0.180305E-04	-0.949831E-06	0.148107E-07

SECTION 42 MJD 38170.0 TO 38189.0 (MAY 21,1963 TO JUN 9,1963)

TIME ORIGIN = 38170.00

PERIGEE							
	95.4426	4.93843	0.0111145	-0.00436251	0.3485493E-03	-0.81303E-05	
	0.1571	162.27	24.00				
NODE							
	40.39697	-3.7633257	0.00261587	-0.408332E-03	0.2318082E-04	-0.460045E-06	
	0.00339	9.726	34.00				
INCLINATION							
	38.90152	0.001692	-0.0005642	0.77587E-04	-0.43026E-05	0.8461E-07	
	0.00085	211.266	34.00				
ECCENTRICITY							
	0.127180	0.00011195	-0.25377E-04	0.46576E-05	-0.43931E-06	0.196496E-07	-0.33293E-09
	***	***	***				
MEAN ANOMALY							
	0.23823	12.316132	0.00011194	0.24357E-04	-0.111985E-05	0.2081E-07	

Table 2. --Standard heights

Time interval MJD	Standard height (km)
37594. 0-37635. 0	750
37635. 2-37777. 0	760
37777. 2-37816. 8	750
37817. 0-37836. 5	740
37836. 6-37837. 8	750
37838. 0-37849. 5	740
37849. 8-37856. 0	750
37856. 5-37869. 0	740
37869. 4-37876. 0	750
37876. 5-37917. 0	720
37917. 5-37957. 8	700
37958. 0-38017. 6	670
38017. 8-38057. 0	640
38057. 5-38076. 5	630
38077. 0-38117. 5	600
38118. 0-38137. 0	575
38137. 5-38189. 0	550

Table 3.--Acceleration, drag, atmospheric densities, temperatures, and geometric parameters from precisely reduced observations

MJD	$-10^7\dot{P}$	$10^7\dot{P}_R$	$-10^7\dot{P}_A$	$\log \rho_\pi$ (g/cm^3)	$\log \rho_s$ (g/cm^3)	T_π (°K)	z (km)	$\alpha_\pi - \alpha_\odot$ (deg.)	$\delta_\pi - \delta_\odot$ (deg.)	T_N
37594.5	3.91	2.42	6.3	-16.88	-16.85	962	757.4	341.6	-2.7	800
95.0	4.38	2.34	6.7	.85	.81	974	757.9	341.3	-4.0	811
95.5	3.68	2.27	5.9	.91	.87	951	758.4	341.0	-5.2	793
96.0	3.46	2.20	5.7	.94	.90	942	758.9	340.8	-6.4	785
96.5	3.33	2.14	5.5	.95	.91	936	759.4	340.6	-7.6	781
97.0	4.12	2.10	6.2	.89	.85	962	759.9	340.4	-8.8	802
97.5	4.32	2.04	6.4	.88	.83	966	760.5	340.3	-9.9	806
37597.6	4.26	2.03	6.3	-16.88	-16.84	964	760.6	340.3	-10.1	805
97.8	4.15	2.01	6.2	.90	.85	961	760.8	340.2	-10.6	802
98.0	4.56	2.00	6.6	.86	.82	973	761.0	340.2	-11.0	812
98.2	5.98	2.00	8.0	.77	.72	1010	761.2	340.2	-11.5	843
98.4	6.57	1.98	8.5	.73	.68	1023	761.4	340.1	-11.9	854
98.6	5.98	1.96	7.9	.77	.72	1010	761.6	340.1	-12.3	843
98.8	5.40	1.93	7.3	.81	.76	995	761.8	340.1	-12.7	830
99.0	6.34	1.92	8.3	.75	.70	1017	762.1	340.1	-13.2	849
99.2	6.78	1.92	8.7	.72	.67	1027	762.3	340.1	-13.6	858
99.4	6.88	1.91	8.8	.72	.66	1030	762.5	340.2	-14.0	859
99.6	6.49	1.91	8.4	.74	.68	1021	762.7	340.2	-14.4	853
99.8	6.27	1.90	8.2	.76	.70	1016	762.9	340.2	-14.8	848
37600.0	6.22	1.90	8.1	.76	.70	1016	763.1	340.3	-15.2	848
00.2	6.01	1.90	7.9	.77	.71	1011	763.3	340.3	-15.5	844
00.4	7.48	1.90	9.4	.69	.63	1043	763.5	340.4	-15.9	870
00.6	17.22	1.89	19.1	.35	.28	1180	763.7	340.4	-16.3	985
00.8	31.51	1.88	33.4	.09	.02	1298	763.9	340.5	-16.6	1083
01.0	29.79	1.88	31.7	.11	.05	1286	764.1	340.6	-17.0	1073
01.2	13.74	1.88	15.6	.44	.37	1141	764.3	340.7	-17.3	952
01.4	12.02	1.88	13.9	.50	.43	1119	764.5	340.8	-17.7	933
01.6	9.12	1.88	11.0	.61	.54	1075	764.7	340.9	-18.0	896
01.8	4.37	1.88	6.2	.89	.83	968	764.9	341.0	-18.3	807
02.0	5.36	1.88	7.2	.82	.75	997	765.1	341.1	-18.6	831
02.2	5.67	1.88	7.5	.80	.73	1005	765.3	341.2	-18.9	837
02.4	4.46	1.88	6.3	.89	.82	972	765.5	341.4	-19.2	810
37602.5	4.45	1.88	6.3	-16.89	-16.82	972	765.6	341.4	-19.4	809
03.0	4.03	1.89	5.9	.92	.85	960	766.0	341.8	-20.1	799
03.5	3.57	1.89	5.5	.96	.89	945	766.4	342.3	-20.7	785
04.0	3.78	1.90	5.7	.94	.87	953	766.8	342.8	-21.2	792
04.5	3.30	1.90	5.2	.99	.91	936	767.2	343.3	-21.7	777
05.0	3.73	1.91	5.6	.94	.87	953	767.5	343.9	-22.2	790
05.5	4.00	1.94	5.9	.92	.84	963	767.9	344.6	-22.5	798
06.0	3.98	1.96	5.9	.92	.84	964	768.1	345.2	-22.8	797
06.5	3.62	1.97	5.6	.95	.87	953	768.4	345.9	-23.0	787
07.0	2.97	1.98	4.9	-17.01	.93	929	768.6	346.7	-23.2	766
07.5	3.84	2.00	5.8	-16.93	.85	962	768.8	347.4	-23.2	792
08.0	3.94	2.02	6.0	.92	.83	966	769.0	348.2	-23.2	795
08.5	4.69	2.02	6.7	.86	.77	990	769.1	349.0	-23.1	813
09.0	5.27	2.01	7.3	.81	.73	1005	769.1	349.7	-23.0	824
09.5	5.49	2.00	7.5	.80	.71	1011	769.2	350.5	-22.7	828
37609.6	5.70	2.00	7.7	-16.79	-16.70	1016	769.2	350.7	-22.6	832
09.8	5.55	2.00	7.5	.80	.71	1013	769.2	351.0	-22.5	828
10.0	4.89	2.00	6.9	.84	.75	996	769.2	351.3	-22.4	814
10.2	5.92	2.00	7.9	.77	.68	1022	769.2	351.5	-22.2	835
10.4	7.29	2.00	9.3	.69	.60	1052	769.2	351.8	-22.0	859
10.6	8.84	2.00	10.8	.62	.53	1081	769.1	352.1	-21.9	882
10.8	7.68	2.00	9.7	.67	.58	1060	769.1	352.4	-21.7	864
11.0	8.05	2.00	10.0	.65	.56	1067	769.1	352.7	-21.5	870
11.2	8.59	1.99	10.6	.63	.54	1077	769.0	353.0	-21.2	877
11.4	8.28	1.98	10.3	.64	.55	1071	769.0	353.2	-21.0	872

Table 3 (Continued)

MJD	$-10^7\dot{P}$	$10^7\dot{P}_R$	$-10^7\dot{P}_A$	$\log \rho_\pi$ (g/cm^3)	$\log \rho_s$ (g/cm^3)	T_π (°K)	z (km)	$\alpha_\pi - \alpha_\odot$ (deg.)	$\delta_\pi - \delta_\odot$ (deg.)	T_N
37611.6	7.65	1.97	9.6	-16.67	-16.58	1059	768.9	353.5	-20.8	862
11.8	7.18	1.95	9.1	.70	.61	1049	768.9	353.8	-20.5	853
12.0	6.54	1.94	8.5	.73	.65	1035	768.8	354.0	-20.2	841
12.2	6.25	1.92	8.2	.75	.67	1028	768.8	354.2	-20.0	835
12.4	6.46	1.91	8.4	.74	.65	1033	768.7	354.5	-19.7	838
12.6	6.33	1.90	8.2	.75	.66	1030	768.6	354.7	-19.4	835
12.8	6.04	1.89	7.9	.77	.68	1023	768.5	354.9	-19.1	829
37613.0	6.08	1.88	8.0	-16.76	-16.68	1023	768.4	355.1	-18.7	829
13.5	5.99	1.84	7.8	.77	.69	1020	768.2	355.7	-17.9	826
14.0	5.90	1.80	7.7	.78	.70	1017	767.9	356.1	-17.0	822
14.5	5.92	1.74	7.7	.78	.70	1016	767.6	356.5	-16.0	821
15.0	6.13	1.68	7.8	.77	.69	1019	767.3	356.8	-15.0	823
15.5	6.51	1.59	8.1	.75	.67	1026	767.0	357.1	-13.9	827
37615.6	6.60	1.56	8.2	-16.75	-16.67	1027	766.9	357.2	-13.7	828
15.8	6.48	1.52	8.0	.76	.68	1023	766.8	357.3	-13.2	825
16.0	6.54	1.50	8.0	.75	.68	1024	766.6	357.4	-12.8	825
16.2	6.93	1.45	8.4	.73	.66	1032	766.5	357.4	-12.3	831
16.4	6.82	1.42	8.2	.74	.67	1029	766.3	357.5	-11.8	828
16.6	6.71	1.39	8.1	.75	.67	1025	766.2	357.6	-11.4	825
16.8	6.34	1.35	7.7	.77	.70	1015	766.0	357.6	-10.9	817
17.0	6.01	1.30	7.3	.80	.73	1006	765.9	357.7	-10.4	809
17.2	6.00	1.27	7.3	.80	.73	1004	765.7	357.7	-9.9	808
17.4	5.81	1.22	7.0	.82	.75	998	765.6	357.7	-9.4	803
17.6	5.27	1.18	6.4	.86	.79	982	765.4	357.7	-8.9	790
17.8	5.40	1.13	6.5	.85	.79	984	765.3	357.8	-8.3	791
18.0	5.52	1.10	6.6	.85	.78	986	765.1	357.8	-7.8	793
37618.5	5.00	0.98	6.0	-16.90	-16.83	966	764.7	357.7	-6.5	777
19.0	4.90	0.86	5.8	.91	.85	959	764.3	357.7	-5.1	771
19.5	5.04	0.74	5.8	.91	.85	959	763.8	357.5	-3.7	771
20.0	5.27	0.61	5.9	.90	.85	962	763.4	357.4	-2.3	774
20.5	5.54	0.48	6.0	.89	.83	966	763.0	357.2	-0.8	777
37620.8	5.38	0.40	5.8	-16.91	-16.86	958	762.7	357.1	0.1	771
21.0	5.36	0.34	5.7	.92	.86	955	762.5	357.0	0.7	769
21.2	7.21	0.28	7.5	.78	.72	1007	762.4	356.9	1.3	811
21.4	8.90	0.21	9.1	.68	.63	1043	762.2	356.7	1.9	840
21.6	9.58	0.16	9.7	.65	.59	1055	762.0	356.6	2.5	850
21.8	8.58	0.10	8.7	.71	.65	1034	761.9	356.5	3.1	833
22.0	9.78	0.03	9.8	.65	.59	1056	761.7	356.4	3.7	852
22.2	8.80	-0.02	8.8	.70	.65	1035	761.5	356.3	4.3	835
22.4	7.82	-0.09	7.7	.76	.71	1011	761.4	356.1	4.9	816
22.6	6.17	-0.14	6.0	.89	.84	964	761.2	356.0	5.5	779
22.8	6.22	-0.20	6.0	.89	.84	964	761.1	355.8	6.1	779
37623.0	6.34	-0.27	6.1	-16.88	-16.84	965	760.9	355.7	6.8	780
23.5	6.54	-0.40	6.1	.88	.83	967	760.5	355.3	8.3	782
24.0	6.73	-0.52	6.2	.87	.83	969	760.2	354.9	9.9	785
24.5	6.53	-0.68	5.8	.90	.86	957	759.8	354.5	11.5	776
25.0	6.80	-0.82	6.0	.89	.85	960	759.5	354.0	13.1	780
25.5	6.51	-0.98	5.5	.93	.89	945	759.1	353.6	14.7	769
26.0	6.45	-1.12	5.3	.95	.91	937	758.8	353.1	16.3	765
26.5	6.17	-1.28	4.9	.99	.96	920	758.5	352.7	17.9	752
27.0	6.55	-1.40	5.1	.97	.93	930	758.2	352.2	19.5	761
27.5	7.07	-1.51	5.6	.93	.89	944	758.0	351.7	21.1	775
28.0	7.24	-1.62	5.6	.92	.89	945	757.7	351.2	22.7	778
28.5	7.42	-1.72	5.7	.92	.88	948	757.5	350.8	24.3	781
29.0	7.63	-1.82	5.8	.91	.88	951	757.3	350.3	25.9	785

Table 3 (Continued)

MJD	$-10^7\dot{P}$	$10^7\dot{P}_R$	$-10^7\dot{P}_A$	$\log \rho_\pi$ (g/cm^3)	$\log \rho_s$ (g/cm^3)	T_π (°K)	z (km)	$\alpha_\pi - \alpha_\odot$ (deg.)	$\delta_\pi - \delta_\odot$ (deg.)	T_N
37629.5	8.22	-1.93	6.3	-16.87	-16.84	965	757.2	349.8	27.5	799
30.0	8.17	-2.00	6.2	.88	.85	961	757.0	349.4	29.0	798
30.5	8.47	-2.05	6.4	.86	.83	968	756.9	348.9	30.6	806
31.0	8.44	-2.07	6.4	.86	.83	966	756.8	348.5	32.2	806
31.5	8.64	-2.05	6.6	.85	.82	972	756.7	348.1	33.7	813
32.0	8.99	-2.01	7.0	.82	.79	983	756.7	347.7	35.2	824
32.5	9.20	-1.97	7.2	.80	.77	989	756.7	347.4	36.7	831
33.0	9.19	-1.89	7.3	.80	.77	990	756.7	347.0	38.2	834
33.5	9.07	-1.78	7.3	.80	.77	990	756.7	346.7	39.7	836
37633.6	9.17	-1.75	7.4	-16.79	-16.76	993	756.7	346.6	40.3	839
33.8	8.34	-1.68	6.7	.85	.82	972	756.8	346.5	40.5	822
34.0	6.68	-1.65	5.0	.99	.96	919	756.8	346.4	41.1	778
34.2	10.92	-1.60	9.3	.68	.65	1035	756.8	346.3	41.7	877
34.4	17.70	-1.48	16.2	.41	.38	1140	756.9	346.2	42.2	967
34.6	17.91	-1.40	16.5	.40	.37	1143	756.9	346.1	42.8	970
34.8	15.94	-1.30	14.6	.46	.43	1120	756.9	346.0	43.3	951
35.0	17.00	-1.20	15.8	.42	.39	1134	757.0	346.0	43.9	965
35.2	16.47	-1.10	15.4	.44	.45	1129	757.0	345.9	44.4	961
35.4	15.80	-1.00	14.8	.45	.47	1122	757.0	345.8	45.0	956
35.6	15.49	-0.88	14.6	.46	.48	1120	757.0	345.8	45.5	954
35.8	16.19	-0.79	15.4	.44	.45	1130	757.1	345.7	46.0	964
36.0	17.08	-0.67	16.4	.41	.42	1142	757.1	345.7	46.6	976
36.2	16.97	-0.56	16.4	.41	.42	1142	757.2	345.6	47.1	976
36.4	15.01	-0.50	14.5	.47	.48	1118	757.2	345.6	47.6	956
36.6	11.55	-0.42	11.1	.60	.61	1068	757.2	345.6	48.1	914
36.8	10.79	-0.42	10.4	.63	.64	1055	757.3	345.5	48.6	903
37637.0	10.10	-0.42	9.7	-16.67	-16.68	1042	757.3	345.5	49.1	893
37.5	8.98	-0.41	8.6	.73	.74	1019	757.4	345.5	50.3	874
38.0	8.34	-0.40	7.9	.77	.78	1004	757.6	345.6	51.5	863
38.5	7.68	-0.39	7.3	.81	.82	988	757.7	345.7	52.6	851
39.0	9.48	-0.37	9.1	.70	.71	1029	757.8	345.8	53.7	888
39.5	10.72	-0.35	10.4	.64	.65	1054	758.0	346.0	54.7	910
40.0	9.24	-0.32	8.9	.71	.72	1025	758.1	346.3	55.6	886
40.5	8.82	-0.30	8.5	.74	.74	1016	758.2	346.6	56.5	879
41.0	8.45	-0.29	8.2	.76	.77	1008	758.3	346.9	57.4	873
41.5	8.12	-0.25	7.9	.78	.78	1001	758.5	347.3	58.2	867
42.0	7.73	-0.22	7.5	.80	.81	993	758.6	347.8	58.9	860
42.5	7.36	-0.19	7.2	.83	.83	984	758.7	348.3	59.5	853
43.0	7.06	-0.17	6.9	.85	.85	976	758.8	348.8	60.1	846
43.5	7.09	-0.13	7.0	.84	.85	978	758.9	349.4	60.6	848
44.0	8.39	-0.10	8.3	.75	.76	1011	759.0	350.0	61.0	876
44.5	8.51	-0.08	8.4	.75	.75	1014	759.1	350.6	61.4	878
45.0	8.41	-0.04	8.4	.75	.75	1012	759.1	351.2	61.6	877
45.5	6.45	-0.01	6.4	.88	.89	963	759.2	351.9	61.8	833
46.0	6.89	0.00	6.9	.85	.85	976	759.3	352.6	61.9	844
46.5	5.51	0.02	5.5	.96	.96	933	759.3	353.3	62.0	806
47.0	5.77	0.08	5.8	.93	.93	944	759.4	353.9	61.9	815
47.5	5.88	0.09	6.0	.92	.92	948	759.4	354.6	61.8	817
48.0	6.10	0.11	6.2	.90	.90	956	759.5	355.3	61.6	823
48.5	6.17	0.13	6.3	.90	.90	959	759.5	355.9	61.3	824
49.0	6.61	0.18	6.8	.86	.86	973	759.5	356.5	60.9	835
49.5	6.05	0.20	6.2	.90	.90	957	759.5	357.0	60.4	821
50.0	5.70	0.22	5.9	.93	.93	947	759.6	357.6	59.9	810
50.5	5.47	0.23	5.7	.94	.95	940	759.6	358.0	59.3	803
51.0	5.30	0.28	5.6	.96	.96	936	759.6	358.5	58.7	798
51.5	5.15	0.30	5.4	.97	.97	931	759.6	358.9	58.0	793
52.0	4.94	0.32	5.3	.98	.99	925	759.6	359.2	57.2	786
52.5	4.90	0.35	5.2	.99	.99	924	759.6	359.5	56.3	784

Table 3 (Continued)

MJD	$-10^7\dot{P}$	$10^7\dot{P}_R$	$-10^7\dot{P}_A$	$\log \rho_\pi$ (g/cm^3)	$\log \rho_s$ (g/cm^3)	T_π (°K)	z (km)	$\alpha_\pi - \alpha_\odot$ (deg.)	$\delta_\pi - \delta_\odot$ (deg.)	T_N
37653.0	4.71	0.56	5.3	-16.98	-16.98	925	759.6	359.7	55.4	783
53.5	4.34	0.98	5.3	.98	.98	927	759.6	359.9	54.5	784
54.0	3.85	1.57	5.4	.97	.97	931	759.6	0.0	53.5	785
54.5	3.06	2.40	5.5	.96	.96	933	759.5	0.1	52.4	785
55.0	2.50	2.82	5.3	.98	.98	928	759.5	0.1	51.3	780
55.5	2.40	3.23	5.6	.95	.95	939	759.5	0.1	50.1	788
56.0	2.79	3.57	6.4	.88	.89	963	759.5	0.0	49.0	806
56.5	2.80	3.83	6.6	.86	.86	971	759.4	359.9	47.7	811
57.0	2.84	4.07	6.9	.84	.84	979	759.4	359.8	46.5	817
57.5	2.88	4.25	7.1	.82	.83	985	759.4	359.6	45.2	820
58.0	2.68	4.40	7.1	.83	.83	984	759.4	359.3	43.9	818
58.5	2.45	4.44	6.9	.84	.84	979	759.4	359.1	42.5	813
59.0	2.04	4.48	6.5	.87	.87	969	759.4	358.8	41.1	803
59.5	2.69	4.49	7.2	.82	.82	988	759.5	358.4	39.7	817
60.0	2.84	4.50	7.3	.81	.81	992	759.5	358.1	38.3	820
60.5	3.23	4.49	7.7	.78	.78	1002	759.6	357.7	36.9	827
61.0	3.83	4.45	8.3	.74	.75	1016	759.7	357.3	35.4	837
37661.4	4.74	4.41	9.1	-16.69	-16.70	1035	759.9	356.9	34.2	852
61.6	4.85	4.39	9.2	.69	.69	1037	759.9	356.7	33.6	853
61.8	4.79	4.37	9.2	.69	.69	1035	760.0	356.6	33.0	852
62.0	4.05	4.33	8.4	.74	.74	1019	760.1	356.4	32.5	838
37662.5	3.36	4.27	7.6	-16.78	-16.78	1002	760.3	355.9	30.9	823
63.0	2.75	4.18	6.9	.83	.83	984	760.5	355.4	29.4	808
63.5	2.47	4.05	6.5	.86	.86	973	760.7	355.0	27.9	799
64.0	2.36	3.92	6.3	.88	.88	967	761.0	354.5	26.4	793
64.5	2.00	3.80	5.8	.92	.91	952	761.3	354.0	24.8	780
65.0	1.75	3.68	5.4	.95	.95	940	761.6	353.5	23.3	770
65.5	1.47	3.54	5.0	.99	.99	925	762.0	353.0	21.8	757
66.0	1.37	3.41	4.8	-17.02	-17.01	916	762.3	352.5	20.2	750
66.5	1.12	3.28	4.4	.06	.05	900	762.7	352.0	18.7	736
67.0	1.07	3.17	4.2	.08	.07	893	763.1	351.5	17.1	731
67.5	0.98	3.03	4.0	.11	.09	882	763.6	351.0	15.6	722
68.0	0.73	2.90	3.6	.16	.14	862	764.0	350.6	14.1	705
68.5	0.48	2.80	3.3	.21	.19	840	764.5	350.1	12.6	687
69.0	0.27	2.68	2.9	.26	.25	816	765.0	349.7	11.0	668
69.5	0.17	2.56	2.7	.30	.29	798	765.5	349.3	9.5	653
70.0	0.15	2.43	2.6	.33	.31	784	766.0	348.9	8.1	642
70.5	0.15	2.32	2.5	.35	.34	773	766.5	348.5	6.6	633
71.0	0.34	2.21	2.5	.34	.32	783	767.0	348.2	5.1	640
71.5	0.39	2.11	2.5	.35	.33	778	767.6	347.9	3.7	637
72.0	0.86	2.00	2.9	.28	.25	813	768.1	347.7	2.3	665
72.5	0.87	1.90	2.8	.30	.27	806	768.6	347.4	0.9	659
73.0	0.75	1.80	2.5	.34	.31	785	769.2	347.3	-0.5	643
73.5	1.29	1.71	3.0	.26	.22	826	769.7	347.1	-1.8	676
37673.8	1.61	1.66	3.3	-17.21	-17.18	846	770.0	347.1	-2.6	693
74.0	1.98	1.61	3.6	.17	.13	867	770.2	347.0	-3.2	710
74.2	1.19	1.58	2.8	.30	.26	808	770.4	347.0	-3.7	661
74.4	2.58	1.55	4.1	.10	.06	897	770.6	347.0	-4.2	734
74.6	3.32	1.51	4.8	.02	-16.97	929	770.8	347.0	-4.7	761
74.8	5.23	1.48	6.7	-16.85	.80	994	771.0	347.0	-5.2	813
75.0	3.79	1.44	5.2	.98	.93	946	771.2	347.0	-5.7	774
75.2	3.88	1.41	5.3	.97	.93	948	771.4	347.0	-6.2	776
75.4	2.63	1.38	4.0	-17.11	-17.07	892	771.6	347.0	-6.6	730
37675.5	2.66	1.37	4.0	-17.11	-17.07	893	771.7	347.0	-6.9	731
76.0	2.17	1.29	3.5	.19	.14	861	772.2	347.2	-8.0	705
76.5	1.80	1.21	3.0	.26	.21	830	772.7	347.3	-9.2	679

Table 3 (Continued)

MJD	$-10^7\dot{P}$	$10^7\dot{P}_R$	$-10^7\dot{P}_A$	$\log \rho_\pi$ (g/cm^3)	$\log \rho_s$ (g/cm^3)	T_π (°K)	z (km)	$\alpha_\pi - \alpha_\odot$ (deg.)	$\delta_\pi - \delta_\odot$ (deg.)	T_N
37677.0	1.72	1.16	2.9	-17.28	-17.24	821	773.1	347.5	-10.2	671
77.5	1.78	1.11	2.9	.28	.23	822	773.5	347.8	-11.2	672
78.0	2.02	1.07	3.1	.24	.20	838	773.9	348.1	-12.2	685
78.5	2.06	1.02	3.1	.25	.20	838	774.3	348.5	-13.1	684
79.0	2.46	1.00	3.5	.19	.13	865	774.7	348.9	-14.0	706
79.5	2.73	0.98	3.7	.15	.10	880	775.0	349.4	-14.7	718
80.0	2.68	0.96	3.6	.16	.11	877	775.4	349.9	-15.5	715
80.5	2.69	0.95	3.6	.16	.10	877	775.7	350.5	-16.1	714
81.0	2.71	0.93	3.6	.16	.10	878	775.9	351.1	-16.7	714
81.5	2.72	0.92	3.6	.16	.10	878	776.2	351.8	-17.2	714
82.0	2.57	0.90	3.5	.18	.13	868	776.4	352.5	-17.6	705
82.5	2.42	0.90	3.3	.21	.15	859	776.5	353.2	-18.0	697
83.0	2.66	0.89	3.5	.17	.11	874	776.7	353.9	-18.2	709
83.5	3.83	0.88	4.7	.03	-16.96	933	776.7	354.6	-18.4	756
84.0	3.61	0.87	4.5	.05	.99	923	776.8	355.4	-18.6	747
84.5	3.42	0.85	4.3	.08	-17.01	914	776.8	356.1	-18.6	739
85.0	3.47	0.83	4.3	.07	.01	915	776.8	356.8	-18.5	739
85.5	3.57	0.81	4.4	.06	.00	919	776.7	357.6	-18.4	741
86.0	3.76	0.80	4.6	.04	-16.98	927	776.6	358.3	-18.2	747
86.5	3.93	0.78	4.7	.03	.96	934	776.5	358.9	-17.9	752
87.0	3.85	0.77	4.6	.04	.97	930	776.3	359.6	-17.6	748
87.5	3.96	0.75	4.7	.03	.96	934	776.1	0.1	-17.2	750
88.0	3.93	0.73	4.7	.03	.97	932	775.8	0.7	-16.7	748
88.5	3.81	0.70	4.5	.05	.99	925	775.5	1.2	-16.1	742
89.0	4.06	0.67	4.7	.02	.96	934	775.2	1.7	-15.5	749
89.5	4.36	0.64	5.0	-16.99	.93	945	774.9	2.1	-14.8	757
90.0	4.72	0.61	5.3	.96	.90	957	774.6	2.4	-14.1	766
90.5	5.29	0.57	5.9	.91	.85	976	774.2	2.7	-13.3	780
91.0	5.42	0.52	5.9	.90	.85	978	773.8	3.0	-12.4	782
91.5	5.62	0.48	6.1	.89	.83	983	773.4	3.2	-11.5	785
92.0	5.76	0.41	6.2	.88	.83	985	773.0	3.3	-10.6	786
92.5	5.97	0.36	6.3	.87	.82	989	772.6	3.4	-9.6	789
93.0	6.13	0.30	6.4	.86	.81	992	772.2	3.4	-8.6	791
93.5	5.90	0.23	6.1	.88	.83	982	771.7	3.4	-7.5	783
94.0	5.80	0.15	5.9	.90	.85	976	771.3	3.4	-6.4	778
94.5	5.87	0.08	5.9	.90	.85	975	770.8	3.3	-5.3	778
95.0	5.86	0.00	5.9	.91	.86	972	770.4	3.1	-4.1	775
95.5	5.77	-0.10	5.7	.92	.88	965	769.9	3.0	-2.9	770
96.0	5.64	-0.19	5.4	.94	.90	957	769.4	2.7	-1.7	764
96.5	5.69	-0.29	5.4	.94	.91	955	769.0	2.5	-0.5	762
97.0	5.37	-0.39	5.0	.98	.95	938	768.5	2.2	0.8	750
97.5	5.55	-0.50	5.0	.98	.95	940	768.1	1.9	2.0	752
98.0	5.67	-0.60	5.1	.98	.94	941	767.6	1.6	3.3	752
98.5	5.85	-0.70	5.1	.97	.94	943	767.2	1.2	4.6	755
37699.0	6.02	-0.81	5.2	-16.96	-16.93	945	766.8	0.8	5.9	757
99.2	6.04	-0.86	5.2	.96	.94	944	766.7	0.7	6.4	756
99.4	6.57	-0.90	5.7	.92	.89	961	766.5	0.5	7.0	771
99.6	6.93	-0.95	6.0	.89	.86	971	766.4	0.4	7.5	779
99.8	8.14	-1.00	7.1	.80	.78	1005	766.2	0.2	8.0	807
37700.0	9.34	-1.03	8.3	.73	.70	1033	766.1	0.0	8.6	830
00.2	11.39	-1.08	10.3	.62	.59	1074	765.9	359.9	9.1	863
00.4	9.74	-1.13	8.6	.71	.68	1039	765.8	359.7	9.6	836
00.6	7.92	-1.18	6.7	.83	.81	993	765.7	359.5	10.2	799
00.8	6.43	-1.22	5.2	.96	.94	943	765.5	359.4	10.7	759
01.0	6.46	-1.28	5.2	.96	.94	942	765.4	359.2	11.2	758
37701.5	6.52	-1.39	5.1	-16.97	-16.95	939	765.1	358.7	12.6	757
02.0	6.65	-1.50	5.1	.97	.95	940	764.8	358.3	13.9	759
02.5	6.81	-1.62	5.2	.96	.94	941	764.5	357.9	15.3	761

Table 3 (Continued)

MJD	$-10^7\dot{P}$	$10^7\dot{P}_R$	$-10^7\dot{P}_A$	$\log \rho_\pi$ (g/cm^3)	$\log \rho_s$ (g/cm^3)	T_π (°K)	z (km)	$\alpha_\pi - \alpha_\odot$ (deg.)	$\delta_\pi - \delta_\odot$ (deg.)	T_N
37703.0	6.87	-1.71	5.2	-16.97	-16.95	939	764.3	357.4	16.6	761
03.5	6.77	-1.80	5.0	.99	.97	931	764.1	357.0	18.0	756
04.0	6.70	-1.90	4.8	-17.00	.99	924	763.9	356.5	19.3	751
04.5	6.64	-1.98	4.7	.02	-17.00	918	763.7	356.1	20.7	747
05.0	6.69	-2.05	4.6	.02	.01	916	763.6	355.7	22.0	747
05.5	6.64	-2.11	4.5	.03	.02	911	763.4	355.3	23.3	744
06.0	6.78	-2.19	4.6	.03	.01	913	763.4	354.9	24.6	748
06.5	7.52	-2.24	5.3	-16.96	-16.94	941	763.3	354.5	25.9	771
07.0	7.92	-2.29	5.6	.93	.91	953	763.2	354.2	27.2	783
07.5	8.48	-2.31	6.2	.88	.87	970	763.2	353.8	28.4	798
08.0	8.53	-2.34	6.2	.88	.87	970	763.2	353.5	29.7	800
08.5	8.40	-2.36	6.0	.89	.88	965	763.3	353.3	30.9	797
09.0	8.31	-2.37	5.9	.90	.89	962	763.3	353.0	32.1	796
09.5	8.28	-2.35	5.9	.90	.89	961	763.4	352.8	33.3	797
10.0	8.29	-2.32	6.0	.90	.89	962	763.4	352.6	34.4	799
37710.2	8.29	-2.30	6.0	-16.90	-16.89	963	763.5	352.6	34.9	800
10.4	8.33	-2.29	6.0	.90	.88	964	763.5	352.5	35.3	801
10.6	8.37	-2.28	6.1	.89	.88	966	763.6	352.5	35.8	803
10.8	8.58	-2.26	6.3	.87	.86	973	763.6	352.4	36.2	810
11.0	8.78	-2.23	6.5	.86	.84	980	763.6	352.4	36.6	816
11.2	10.16	-2.21	7.9	.76	.74	1017	763.7	352.4	37.1	847
11.4	10.36	-2.18	8.2	.75	.73	1022	763.7	352.4	37.5	851
11.6	11.23	-2.15	9.1	.69	.68	1042	763.8	352.3	37.9	868
11.8	12.09	-2.11	10.0	.65	.63	1059	763.8	352.3	38.3	884
12.0	11.44	-2.09	9.3	.68	.66	1047	763.9	352.3	38.7	874
12.2	10.11	-2.02	8.1	.75	.74	1020	763.9	352.4	39.1	851
12.4	9.78	-2.00	7.8	.77	.76	1012	764.0	352.4	39.5	845
12.6	8.95	-1.96	7.0	.83	.81	992	764.0	352.4	39.9	829
12.8	8.79	-1.90	6.9	.83	.82	989	764.1	352.4	40.2	827
37713.0	8.39	-1.86	6.5	-16.86	-16.84	979	764.1	352.5	40.6	819
13.5	8.06	-1.70	6.4	.88	.86	974	764.2	352.6	41.5	815
14.0	7.81	-1.53	6.3	.88	.86	971	764.3	352.8	42.4	813
14.5	7.94	-1.45	6.5	.87	.85	977	764.4	353.1	43.2	819
15.0	7.91	-1.20	6.7	.85	.83	984	764.6	353.4	43.9	825
15.5	8.02	-1.00	7.0	.83	.81	992	764.7	353.7	44.6	832
16.0	7.98	-0.76	7.2	.81	.79	998	764.8	354.1	45.2	837
16.5	8.44	-0.48	8.0	.77	.75	1016	764.8	354.6	45.8	852
17.0	8.64	-0.28	8.4	.74	.72	1025	764.9	355.1	46.3	860
17.5	8.72	-0.14	8.6	.73	.71	1030	765.0	355.7	46.8	864
18.0	8.70	-0.08	8.6	.73	.71	1031	765.1	356.3	47.1	864
18.5	8.84	-0.04	8.8	.72	.70	1035	765.1	356.9	47.4	867
19.0	8.75	-0.03	8.7	.72	.70	1033	765.2	357.6	47.6	865
19.5	8.99	-0.01	9.0	.71	.68	1039	765.2	358.3	47.8	869
20.0	9.13	0.00	9.1	.70	.68	1042	765.2	359.0	47.9	871
20.5	9.21	0.00	9.2	.70	.67	1043	765.2	359.8	47.9	871
21.0	9.31	0.01	9.3	.69	.67	1046	765.2	0.5	47.8	872
37721.4	9.39	0.02	9.4	-16.68	-16.66	1047	765.2	1.1	47.6	873
21.6	9.88	0.03	9.9	.66	.64	1057	765.2	1.5	47.6	881
21.8	10.20	0.04	10.2	.64	.62	1063	765.2	1.8	47.5	885
22.0	10.50	0.05	10.5	.63	.60	1069	765.2	2.1	47.4	890
22.2	11.99	0.07	12.1	.56	.54	1094	765.2	2.4	47.2	910
22.4	11.61	0.08	11.7	.58	.55	1089	765.1	2.7	47.1	905
22.6	11.40	0.06	11.5	.59	.56	1085	765.1	3.0	46.9	901
22.8	10.84	0.05	10.9	.61	.59	1075	765.1	3.3	46.8	892
37723.0	10.22	0.04	10.3	-16.64	-16.62	1064	765.1	3.6	46.6	883
23.5	9.09	0.02	9.1	.70	.68	1041	765.0	4.3	46.1	863

Table 3 (Continued)

MJD	$-10^7\dot{P}$	$10^7\dot{P}_R$	$-10^7\dot{P}_A$	$\log \rho_\pi$ (g/cm^3)	$\log \rho_s$ (g/cm^3)	T_π (°K)	z (km)	$\alpha_\pi - \alpha_\odot$ (deg.)	$\delta_\pi - \delta_\odot$ (deg.)	T_N
37724.0	8.78	0.01	8.8	-16.72	-16.70	1035	765.0	5.0	45.6	855
24.5	8.12	0.02	8.1	.76	.73	1020	764.9	5.7	44.9	842
25.0	7.94	0.19	8.1	.76	.73	1020	764.8	6.3	44.2	840
25.5	7.87	0.31	8.2	.75	.73	1021	764.7	6.9	43.4	840
26.0	7.78	0.45	8.2	.75	.73	1022	764.6	7.4	42.6	839
26.5	7.56	0.58	8.1	.75	.73	1020	764.5	7.9	41.7	836
27.0	7.33	0.70	8.0	.76	.74	1018	764.4	8.4	40.7	832
27.5	7.20	0.80	8.0	.76	.74	1017	764.3	8.8	39.7	830
28.0	6.88	0.90	7.8	.77	.76	1012	764.2	9.1	38.6	825
28.5	6.57	1.00	7.6	.79	.77	1007	764.0	9.4	37.4	819
29.0	6.43	1.08	7.5	.79	.77	1005	763.9	9.6	36.2	816
29.5	6.23	1.15	7.4	.80	.78	1002	763.7	9.8	35.0	812
30.0	5.89	1.19	7.1	.82	.80	995	763.5	10.0	33.7	804
30.5	5.40	1.20	6.6	.85	.84	981	763.4	10.0	32.4	792
31.0	5.02	1.21	6.2	.88	.87	970	763.2	10.1	31.0	782
31.5	4.19	1.20	5.4	.95	.94	943	763.0	10.1	29.6	759
32.0	3.70	1.20	4.9	-17.00	.99	924	762.9	10.0	28.1	743
32.5	3.34	1.18	4.5	.04	-17.03	908	762.7	9.9	26.7	729
33.0	3.69	1.14	4.8	.00	-16.99	921	762.6	9.8	25.2	738
33.5	4.27	1.09	5.4	-16.95	.94	942	762.4	9.6	23.6	754
34.0	5.27	1.02	6.3	.87	.86	973	762.3	9.4	22.1	778
37734.2	4.99	1.00	6.0	-16.89	-16.88	964	762.3	9.4	21.5	770
34.4	5.02	0.98	6.0	.89	.88	964	762.2	9.3	20.8	770
34.6	5.06	0.93	6.0	.89	.88	964	762.2	9.2	20.2	770
34.8	5.10	0.90	6.0	.89	.88	964	762.2	9.1	19.6	770
35.0	4.81	0.86	5.7	.92	.91	953	762.1	9.0	18.9	761
35.2	5.03	0.81	5.8	.90	.90	959	762.1	8.8	18.3	765
35.4	4.92	0.78	5.7	.92	.91	955	762.1	8.7	17.6	761
35.6	5.14	0.72	5.9	.90	.89	960	762.0	8.6	17.0	765
35.8	5.35	0.69	6.0	.89	.88	966	762.0	8.5	16.3	770
36.0	5.85	0.62	6.5	.85	.84	979	762.0	8.4	15.7	780
36.2	5.50	0.58	6.1	.88	.87	967	762.0	8.2	15.0	770
36.4	4.96	0.51	5.5	.94	.93	947	762.0	8.1	14.3	754
36.6	5.10	0.47	5.6	.93	.92	951	762.0	8.0	13.7	757
36.8	4.88	0.40	5.3	.95	.95	940	762.0	7.8	13.0	749
37.0	4.83	0.33	5.2	.96	.96	936	762.0	7.7	12.3	745
37.2	5.10	0.28	5.4	.94	.94	944	762.0	7.5	11.7	751
37.4	5.21	0.21	5.4	.94	.93	946	762.0	7.4	11.0	753
37737.5	5.30	0.19	5.5	-16.93	-16.92	948	762.0	7.3	10.7	755
38.0	5.73	0.03	5.8	.91	.90	958	762.0	7.0	9.0	762
38.5	5.96	-0.10	5.9	.90	.89	961	762.1	6.6	7.3	765
39.0	6.52	-0.23	6.3	.86	.85	975	762.2	6.2	5.6	776
39.5	6.79	-0.39	6.4	.85	.84	979	762.3	5.8	3.9	779
40.0	7.07	-0.51	6.6	.84	.83	984	762.5	5.4	2.2	783
40.5	7.28	-0.65	6.6	.84	.83	986	762.6	5.0	0.5	785
41.0	8.04	-0.79	7.2	.79	.78	1003	762.8	4.6	-1.2	799
41.5	8.71	-0.92	7.8	.76	.74	1017	763.0	4.2	-2.9	811
42.0	9.55	-1.08	8.5	.71	.70	1033	763.3	3.8	-4.6	824
42.5	10.61	-1.21	9.4	.66	.65	1053	763.5	3.4	-6.3	841
37742.6	10.90	-1.24	9.7	-16.65	-16.63	1058	763.6	3.3	-6.6	845
42.8	11.59	-1.30	10.3	.62	.60	1070	763.7	3.2	-7.3	855
43.0	11.76	-1.36	10.4	.61	.60	1072	763.8	3.0	-8.0	857
43.2	11.60	-1.40	10.2	.62	.61	1068	763.9	2.9	-8.6	855
43.4	12.10	-1.47	10.6	.60	.59	1076	764.0	2.8	-9.3	861
43.6	12.27	-1.52	10.7	.60	.58	1079	764.1	2.6	-10.0	864
43.8	12.76	-1.60	11.2	.58	.56	1086	764.2	2.5	-10.6	870
44.0	13.08	-1.63	11.5	.57	.55	1091	764.3	2.3	-11.3	874

Table 3 (Continued)

MJD	$-10^7\dot{P}$	$10^7\dot{P}_R$	$-10^7\dot{P}_A$	$\log \rho_\pi$ (g/cm^3)	$\log \rho_s$ (g/cm^3)	T_π (°K)	z (km)	$\alpha_\pi - \alpha_\odot$ (deg.)	$\delta_\pi - \delta_\odot$ (deg.)	T_N
37744.2	13.06	-1.70	11.4	-16.57	-16.55	1090	764.4	2.2	-12.0	874
44.4	13.20	-1.77	11.4	.57	.55	1091	764.6	2.1	-12.6	875
44.6	12.83	-1.82	11.0	.59	.57	1084	764.7	2.0	-13.3	870
44.8	13.13	-1.89	11.2	.58	.56	1088	764.8	1.9	-13.9	874
45.0	13.42	-1.93	11.5	.57	.54	1092	764.9	1.7	-14.6	878
45.2	13.87	-2.00	11.9	.55	.53	1099	765.1	1.6	-15.2	883
45.4	13.14	-2.05	11.1	.59	.56	1086	765.2	1.5	-15.9	873
37745.5	13.15	-2.08	11.1	-16.59	-16.56	1085	765.3	1.5	-16.2	873
46.0	13.03	-2.20	10.8	.60	.57	1082	765.6	1.2	-17.8	871
46.5	13.08	-2.31	10.8	.60	.57	1081	765.9	1.0	-19.4	872
47.0	13.35	-2.42	10.9	.59	.57	1084	766.2	0.9	-20.9	876
47.5	13.70	-2.52	11.2	.58	.55	1089	766.6	0.7	-22.5	881
48.0	14.09	-2.62	11.5	.57	.54	1094	766.9	0.6	-24.0	886
48.5	14.40	-2.73	11.7	.57	.53	1097	767.2	0.6	-25.5	890
49.0	13.21	-2.80	10.4	.62	.59	1076	767.5	0.5	-26.9	874
49.5	12.95	-2.87	10.1	.64	.60	1070	767.9	0.6	-28.3	870
50.0	12.11	-2.91	9.2	.68	.65	1053	768.2	0.7	-29.7	857
50.5	12.94	-2.92	10.0	.64	.60	1069	768.5	0.8	-31.0	872
51.0	12.09	-2.91	9.2	.69	.65	1053	768.8	1.0	-32.3	859
51.5	12.29	-2.90	9.4	.68	.64	1057	769.1	1.2	-33.5	864
52.0	12.98	-2.87	10.1	.64	.60	1072	769.4	1.5	-34.7	877
52.5	13.05	-2.82	10.2	.64	.59	1074	769.6	1.8	-35.9	879
53.0	12.08	-2.76	9.3	.68	.64	1057	769.9	2.2	-37.0	866
53.5	10.60	-2.70	7.9	.76	.72	1025	770.1	2.7	-38.0	841
54.0	10.13	-2.61	7.5	.79	.74	1016	770.3	3.2	-39.0	834
54.5	10.08	-2.51	7.6	.79	.74	1017	770.5	3.7	-39.8	835
55.0	9.85	-2.40	7.4	.80	.75	1014	770.7	4.3	-40.7	833
55.5	9.97	-2.27	7.7	.78	.73	1021	770.8	5.0	-41.4	839
56.0	9.61	-2.12	7.5	.79	.75	1016	770.9	5.6	-42.1	835
56.5	9.28	-1.98	7.3	.81	.76	1011	771.0	6.4	-42.7	831
57.0	8.87	-1.80	7.1	.82	.78	1005	771.1	7.1	-43.3	826
57.5	8.39	-1.64	6.7	.85	.80	996	771.1	7.9	-43.7	818
58.0	7.76	-1.48	6.3	.88	.84	982	771.1	8.7	-44.1	806
58.5	7.81	-1.29	6.5	.86	.82	989	771.0	9.5	-44.4	812
59.0	7.62	-1.09	6.5	.86	.82	989	771.0	10.3	-44.6	812
59.5	7.26	-0.90	6.4	.88	.83	983	770.8	11.1	-44.8	807
37759.8	7.16	-0.81	6.3	-16.88	-16.83	983	770.8	11.6	-44.8	806
60.0	7.25	-0.73	6.5	.86	.82	988	770.7	11.9	-44.8	810
60.2	7.02	-0.70	6.3	.88	.84	982	770.6	12.2	-44.8	805
60.4	6.79	-0.63	6.2	.89	.85	977	770.5	12.6	-44.8	801
60.6	7.08	-0.58	6.5	.87	.82	987	770.5	12.9	-44.8	809
60.8	7.38	-0.53	6.8	.84	.80	997	770.4	13.2	-44.7	817
61.0	7.35	-0.49	6.9	.84	.80	997	770.3	13.5	-44.7	817
61.2	8.00	-0.45	7.5	.79	.75	1015	770.2	13.8	-44.6	831
61.4	8.83	-0.41	8.4	.74	.69	1036	770.1	14.1	-44.5	848
61.6	9.66	-0.39	9.3	.69	.64	1054	770.0	14.4	-44.5	863
61.8	8.83	-0.37	8.5	.73	.69	1037	769.9	14.6	-44.4	848
62.0	7.66	-0.33	7.3	.81	.76	1009	769.8	14.9	-44.2	825
62.2	7.34	-0.31	7.0	.83	.78	1001	769.6	15.2	-44.1	818
62.4	7.19	-0.30	6.9	.84	.80	997	769.5	15.5	-44.0	814
62.6	7.22	-0.30	6.9	.83	.79	998	769.4	15.7	-43.8	815
62.8	7.09	-0.29	6.8	.84	.80	994	769.2	16.0	-43.7	811
63.0	6.96	-0.29	6.7	.85	.81	990	769.1	16.2	-43.5	808
63.2	6.51	-0.29	6.2	.89	.85	977	769.0	16.4	-43.3	796
63.4	6.06	-0.29	5.8	.92	.89	962	768.8	16.7	-43.1	784
63.6	5.95	-0.30	5.6	.93	.90	958	768.7	16.9	-42.9	780
63.8	6.35	-0.30	6.0	.90	.86	971	768.5	17.1	-42.7	791
64.0	6.42	-0.30	6.1	.89	.86	973	768.4	17.3	-42.5	792

Table 3 (Continued)

MJD	$-10^7\dot{P}$	$10^7\dot{P}_R$	$-10^7\dot{P}_A$	$\log \rho_\pi$ (g/cm^3)	$\log \rho_s$ (g/cm^3)	T_π (°K)	z (km)	$\alpha_\pi - \alpha_\odot$ (deg.)	$\delta_\pi - \delta_\odot$ (deg.)	T_N
37764.2	6.32	-0.31	6.0	-16.90	-16.87	969	768.2	17.5	-42.2	788
64.4	6.40	-0.32	6.1	.90	.86	971	768.1	17.7	-42.0	790
64.6	6.82	-0.31	6.5	.86	.83	984	767.9	17.9	-41.7	800
64.8	8.09	-0.30	7.8	.77	.74	1018	767.7	18.1	-41.5	827
65.0	9.19	-0.29	8.9	.71	.67	1043	767.6	18.2	-41.2	847
65.2	8.45	-0.28	8.2	.75	.72	1027	767.4	18.4	-40.9	833
65.4	7.54	-0.27	7.3	.81	.77	1005	767.2	18.5	-40.6	815
65.6	7.99	-0.26	7.7	.78	.74	1016	767.0	18.7	-40.3	824
65.8	7.26	-0.24	7.0	.82	.79	998	766.9	18.8	-40.0	808
66.0	7.37	-0.22	7.1	.81	.78	1001	766.7	18.9	-39.7	811
37766.5	7.54	-0.19	7.3	-16.80	-16.77	1006	766.2	19.2	-38.9	813
67.0	7.41	-0.15	7.3	.80	.78	1003	765.8	19.4	-38.0	810
67.5	7.90	-0.11	7.8	.77	.75	1016	765.3	19.5	-37.0	819
68.0	8.29	-0.08	8.2	.74	.72	1025	764.9	19.6	-36.1	826
68.5	8.78	-0.02	8.8	.71	.69	1037	764.4	19.7	-35.1	834
69.0	9.42	0.02	9.4	.67	.65	1051	763.9	19.7	-34.0	844
37769.6	10.16	0.08	10.2	-16.63	-16.61	1066	763.4	19.6	-32.7	854
69.8	11.00	0.09	11.1	.59	.58	1080	763.2	19.6	-32.3	865
70.0	11.50	0.10	11.6	.57	.55	1089	763.0	19.6	-31.8	872
70.2	13.01	0.10	13.1	.51	.50	1112	762.8	19.5	-31.4	890
70.4	13.68	0.10	13.8	.48	.47	1121	762.6	19.5	-30.9	897
70.6	13.68	0.11	13.8	.48	.47	1121	762.5	19.4	-30.5	896
70.8	13.85	0.12	14.0	.48	.47	1123	762.3	19.4	-30.0	898
71.0	13.68	0.12	13.8	.48	.47	1121	762.1	19.3	-29.5	895
71.2	13.67	0.12	13.8	.48	.47	1120	761.9	19.2	-29.0	894
71.4	13.67	0.12	13.8	.48	.47	1120	761.8	19.1	-28.6	894
71.6	13.83	0.13	14.0	.48	.47	1122	761.6	19.0	-28.1	895
71.8	13.99	0.13	14.1	.47	.46	1124	761.4	19.0	-27.6	896
72.0	13.98	0.13	14.1	.47	.46	1124	761.3	18.9	-27.1	896
72.2	13.62	0.12	13.7	.48	.48	1119	761.1	18.8	-26.6	891
72.4	13.61	0.12	13.7	.48	.48	1119	760.9	18.7	-26.1	890
72.6	13.75	0.12	13.9	.48	.47	1120	760.8	18.5	-25.6	891
72.8	13.39	0.11	13.5	.49	.49	1115	760.6	18.4	-25.1	887
37773.0	13.44	0.10	13.5	-16.49	-16.49	1115	760.5	18.3	-24.6	887
73.5	13.09	0.08	13.2	.50	.50	1110	760.1	18.0	-23.3	881
74.0	12.79	0.02	12.8	.51	.51	1104	759.7	17.7	-22.1	876
74.5	12.45	-0.02	12.4	.53	.53	1098	759.4	17.3	-20.8	871
75.0	12.96	-0.10	12.9	.51	.51	1104	759.0	16.9	-19.5	875
75.5	13.87	-0.19	13.7	.48	.49	1116	758.7	16.6	-18.1	883
37775.6	14.11	-0.20	13.9	-16.47	-16.48	1119	758.6	16.5	-17.9	886
75.8	14.49	-0.23	14.3	.46	.47	1123	758.5	16.3	-17.3	889
76.0	14.53	-0.27	14.3	.46	.47	1123	758.4	16.2	-16.8	889
76.2	16.24	-0.31	15.9	.41	.41	1144	758.3	16.0	-16.3	905
76.4	20.29	-0.34	19.9	.30	.31	1188	758.1	15.8	-15.8	940
76.6	19.45	-0.39	19.1	.32	.33	1179	758.0	15.7	-15.2	932
76.8	16.76	-0.41	16.3	.39	.40	1149	757.9	15.5	-14.7	908
77.0	15.74	-0.46	15.3	.42	.44	1136	757.8	15.3	-14.1	898
77.2	15.73	-0.50	15.2	.43	.44	1135	757.7	15.2	-13.6	897
77.4	14.99	-0.53	14.5	.45	.46	1125	757.6	15.0	-13.1	889
77.6	14.27	-0.58	13.7	.48	.49	1114	757.5	14.8	-12.5	880
77.8	11.87	-0.61	11.3	.57	.58	1077	757.4	14.7	-12.0	851
37778.0	11.56	-0.65	10.9	-16.59	-16.55	1071	757.3	14.5	-11.5	846
78.5	10.96	-0.75	10.2	.62	.59	1058	757.1	14.1	-10.1	836
79.0	10.93	-0.85	10.1	.63	.59	1056	757.0	13.7	-8.8	834
79.5	10.71	-0.94	9.8	.64	.61	1050	756.8	13.3	-7.5	829

Table 3 (Continued)

MJD	$-10^7\dot{P}$	$10^7\dot{P}_R$	$-10^7\dot{P}_A$	$\log \rho_\pi$ (g/cm^3)	$\log \rho_s$ (g/cm^3)	T_π (°K)	z (km)	$\alpha_\pi - \alpha_\odot$ (deg.)	$\delta_\pi - \delta_\odot$ (deg.)	T_N
37780.0	10.58	-1.04	9.5	-16.65	-16.62	1045	756.7	12.9	-6.1	825
80.5	10.69	-1.15	9.5	.65	.62	1045	756.6	12.5	-4.8	825
81.0	10.43	-1.25	9.2	.67	.64	1038	756.6	12.1	-3.5	820
81.5	10.18	-1.38	8.8	.69	.66	1030	756.5	11.8	-2.2	813
82.0	9.64	-1.47	8.2	.73	.70	1016	756.5	11.4	-0.9	803
82.5	9.15	-1.60	7.5	.77	.74	1001	756.5	11.1	0.4	791
83.0	8.76	-1.70	7.1	.80	.77	989	756.6	10.8	1.6	782
83.5	8.51	-1.80	6.7	.83	.80	979	756.6	10.6	2.9	774
84.0	8.30	-1.92	6.4	.85	.82	970	756.7	10.3	4.1	767
84.5	8.02	-2.02	6.0	.88	.86	958	756.7	10.1	5.3	758
85.0	7.94	-2.13	5.8	.90	.87	952	756.8	10.0	6.4	754
85.5	8.08	-2.23	5.8	.90	.87	954	756.9	9.8	7.6	755
86.0	8.16	-2.33	5.8	.90	.87	953	757.0	9.8	8.7	755
86.5	8.35	-2.43	5.9	.89	.86	956	757.1	9.7	9.8	758
87.0	8.78	-2.53	6.2	.87	.83	966	757.2	9.7	10.8	766
87.5	8.24	-2.63	5.6	.92	.89	946	757.3	9.7	11.9	750
88.0	7.94	-2.72	5.2	.96	.93	932	757.4	9.8	12.8	739
88.5	7.61	-2.81	4.8	-17.00	.97	916	757.5	10.0	13.8	727
89.0	7.37	-2.88	4.5	.03	-17.00	903	757.6	10.2	14.7	716
89.5	7.19	-2.91	4.3	.06	.03	893	757.7	10.4	15.5	709
90.0	7.63	-2.98	4.6	.02	-16.98	910	757.8	10.7	16.3	722
90.5	8.38	-3.02	5.4	-16.94	.91	937	757.9	11.1	17.0	744
91.0	9.71	-3.08	6.6	.84	.80	978	758.0	11.5	17.7	776
91.5	9.19	-3.10	6.1	.88	.85	962	758.0	11.9	18.3	764
92.0	8.72	-3.15	5.6	.93	.89	945	758.1	12.4	18.9	750
92.5	8.42	-3.19	5.2	.96	.92	933	758.1	13.0	19.4	741
93.0	8.19	-3.20	5.0	.98	.95	924	758.1	13.5	19.8	733
93.5	7.80	-3.23	4.6	-17.03	.99	906	758.1	14.2	20.2	719
94.0	7.59	-3.28	4.3	.06	-17.02	895	758.0	14.8	20.5	710
94.5	8.07	-3.30	4.8	.00	-16.97	915	758.0	15.5	20.7	725
95.0	8.35	-3.30	5.0	-16.97	.94	926	757.9	16.2	20.8	734
95.5	8.56	-3.30	5.3	.95	.92	934	757.8	17.0	20.9	740
96.0	9.06	-3.30	5.8	.91	.88	951	757.7	17.7	20.8	753
96.5	9.10	-3.30	5.8	.90	.87	952	757.6	18.5	20.7	754
97.0	9.12	-3.30	5.8	.90	.87	953	757.4	19.2	20.6	754
97.5	9.78	-3.30	6.5	.85	.82	973	757.2	20.0	20.3	769
98.0	10.26	-3.30	7.0	.81	.78	986	757.1	20.7	20.0	779
98.5	10.90	-3.30	7.6	.77	.74	1002	756.9	21.4	19.6	791
99.0	11.06	-3.30	7.8	.76	.73	1006	756.6	22.1	19.1	794
99.5	10.72	-3.30	7.4	.78	.75	997	756.4	22.7	18.5	786
37800.0	10.28	-3.30	7.0	.81	.78	985	756.2	23.3	17.9	776
00.5	10.18	-3.38	6.8	.82	.80	980	755.9	23.9	17.2	772
01.0	10.17	-3.39	6.8	.82	.80	979	755.6	24.4	16.4	771
01.5	10.21	-3.40	6.8	.82	.80	980	755.3	24.9	15.6	770
02.0	10.38	-3.40	7.0	.81	.79	984	755.0	25.3	14.7	773
02.5	10.49	-3.40	7.1	.80	.78	987	754.6	25.7	13.7	775
03.0	10.76	-3.41	7.3	.78	.76	993	754.3	26.0	12.7	779
03.5	10.92	-3.42	7.5	.77	.75	996	753.9	26.3	11.7	781
04.0	11.21	-3.46	7.7	.75	.74	1002	753.6	26.5	10.5	785
04.5	11.69	-3.51	8.2	.73	.71	1012	753.2	26.6	9.4	792
05.0	11.48	-3.57	7.9	.74	.73	1005	752.8	26.7	8.2	787
05.5	11.24	-3.62	7.6	.76	.75	998	752.5	26.8	7.0	781
06.0	11.11	-3.69	7.4	.77	.76	992	752.1	26.8	5.7	777
06.5	11.09	-3.74	7.3	.78	.77	990	751.7	26.8	4.4	775
07.0	11.02	-3.80	7.2	.78	.78	987	751.4	26.7	3.0	772
07.5	10.81	-3.88	6.9	.80	.80	979	751.0	26.5	1.6	765
08.0	10.77	-3.94	6.8	.81	.81	976	750.7	26.4	0.2	763
08.5	10.68	-4.02	6.7	.82	.82	971	750.3	26.2	-1.2	759
09.0	10.42	-4.10	6.3	.85	.85	960	750.0	25.9	-2.6	751
09.5	10.09	-4.20	5.9	.88	.89	947	749.7	25.7	-4.1	741

Table 3 (Continued)

MJD	$-10^7\dot{P}$	$10^7\dot{P}_R$	$-10^7\dot{P}_A$	$\log \rho_\pi$ (g/cm^3)	$\log \rho_s$ (g/cm^3)	T_π (°K)	z (km)	$\alpha_\pi - \alpha_\odot$ (deg.)	$\delta_\pi - \delta_\odot$ (deg.)	T_N
37810.0	9.79	-4.19	5.6	-16.91	-16.91	937	749.4	25.4	-5.6	734
10.5	10.27	-4.38	5.9	.88	.89	946	749.2	25.0	-7.1	741
11.0	10.94	-4.48	6.5	.84	.84	963	748.9	24.7	-8.6	755
37811.2	11.51	-4.52	7.0	-16.80	-16.80	978	748.9	24.5	-9.2	767
11.4	12.55	-4.56	8.0	.73	.74	1002	748.8	24.4	-9.9	786
11.6	12.57	-4.60	8.0	.73	.74	1002	748.7	24.2	-10.5	786
11.8	12.77	-4.65	8.1	.72	.73	1005	748.6	24.0	-11.1	789
12.0	12.80	-4.70	8.1	.72	.73	1004	748.5	23.9	-11.7	788
12.2	12.83	-4.73	8.1	.72	.73	1004	748.5	23.7	-12.3	789
12.4	13.03	-4.79	8.2	.72	.72	1007	748.4	23.6	-13.0	791
12.6	12.73	-4.82	7.9	.74	.74	1000	748.3	23.4	-13.6	786
12.8	12.43	-4.88	7.5	.76	.77	991	748.3	23.2	-14.2	779
37813.0	12.20	-4.92	7.3	-16.78	-16.79	984	748.2	23.0	-14.8	774
13.5	12.17	-5.04	7.1	.79	.80	980	748.1	22.6	-16.4	772
14.0	11.71	-5.16	6.5	.83	.84	964	748.0	22.2	-18.0	760
14.5	11.65	-5.28	6.4	.85	.85	959	747.9	21.7	-19.6	757
15.0	12.04	-5.38	6.7	.82	.83	967	747.9	21.2	-21.1	765
37815.2	13.05	-5.42	7.6	-16.76	-16.77	992	747.8	21.1	-21.8	785
15.4	13.27	-5.48	7.8	.75	.76	995	747.8	20.9	-22.4	788
15.6	13.32	-5.52	7.8	.74	.75	996	747.8	20.7	-23.0	789
15.8	14.20	-5.58	8.6	.70	.71	1014	747.8	20.5	-23.7	804
16.0	14.06	-5.60	8.5	.71	.71	1010	747.8	20.3	-24.3	802
16.2	13.91	-5.65	8.3	.72	.73	1006	747.8	20.1	-24.9	799
16.4	13.25	-5.70	7.5	.76	.77	989	747.8	20.0	-25.6	786
16.6	12.92	-5.74	7.2	.79	.80	980	747.8	19.8	-26.2	780
16.8	12.58	-5.80	6.8	.82	.83	969	747.9	19.6	-26.8	772
37817.0	12.67	-5.82	6.8	-16.81	-16.78	971	747.9	19.4	-27.4	773
17.5	12.52	-5.95	6.6	.83	.80	963	747.9	19.0	-29.0	769
18.0	12.29	-6.05	6.2	.86	.83	953	748.0	18.5	-30.5	763
18.5	12.42	-6.15	6.3	.86	.82	954	748.1	18.1	-32.1	765
19.0	12.51	-6.23	6.3	.86	.82	954	748.2	17.7	-33.6	767
19.5	12.80	-6.31	6.5	.84	.81	960	748.3	17.3	-35.1	773
20.0	12.96	-6.40	6.6	.84	.80	962	748.4	17.0	-36.6	776
20.5	12.98	-6.48	6.5	.84	.81	960	748.6	16.7	-38.1	777
21.0	13.03	-6.52	6.5	.85	.81	960	748.7	16.3	-39.6	779
21.5	13.05	-6.58	6.5	.85	.81	959	748.9	16.1	-41.0	779
22.0	12.85	-6.61	6.2	.87	.83	952	749.1	15.8	-42.4	776
22.5	12.64	-6.63	6.0	.89	.85	945	749.3	15.6	-43.8	772
23.0	12.15	-6.63	5.5	.93	.89	929	749.4	15.5	-45.2	760
23.5	12.13	-6.60	5.5	.93	.89	929	749.6	15.3	-46.5	762
24.0	12.57	-6.57	6.0	.89	.85	944	749.8	15.2	-47.8	777
24.5	13.35	-6.53	6.8	.83	.78	968	750.0	15.2	-49.0	798
25.0	13.74	-6.47	7.3	.80	.75	980	750.2	15.2	-50.2	809
25.5	13.79	-6.35	7.4	.79	.74	984	750.4	15.3	-51.4	814
26.0	13.29	-6.20	7.1	.81	.77	975	750.6	15.4	-52.6	809
26.5	12.69	-6.00	6.7	.84	.80	964	750.7	15.5	-53.6	801
27.0	12.31	-5.72	6.6	.85	.80	961	750.9	15.7	-54.7	800
27.5	12.02	-5.40	6.6	.85	.80	962	751.0	16.0	-55.7	802
28.0	11.66	-5.07	6.6	.85	.80	961	751.1	16.3	-56.6	803
28.5	11.22	-4.67	6.5	.86	.81	960	751.2	16.7	-57.4	803
29.0	10.74	-4.20	6.5	.86	.81	959	751.3	17.1	-58.2	803
29.5	10.39	-2.70	7.7	.78	.73	989	751.3	17.6	-59.0	830
30.0	9.77	-1.30	8.5	.73	.68	1007	751.4	18.1	-59.6	845
30.5	9.23	-0.15	9.1	.70	.64	1020	751.4	18.7	-60.2	857
31.0	8.00	-0.15	7.8	.77	.72	993	751.4	19.3	-60.8	835
31.5	6.94	-0.15	6.8	.84	.79	965	751.3	19.9	-61.2	812

Table 3 (Continued)

MJD	$-10^7\dot{P}$	$10^7\dot{P}_R$	$-10^7\dot{P}_A$	$\log \rho_\pi$ (g/cm^3)	$\log \rho_s$ (g/cm^3)	T_π (°K)	z (km)	$a_\pi - a_\odot$ (deg.)	$\delta_\pi - \delta_\odot$ (deg.)	T_N
37832.0	6.79	-0.16	6.6	-16.85	-16.80	961	751.3	20.6	-61.6	809
32.5	6.80	-0.16	6.6	.85	.80	961	751.2	21.3	-61.9	809
33.0	6.84	-0.16	6.7	.85	.80	962	751.0	22.0	-62.1	810
33.5	6.78	-0.15	6.6	.85	.81	960	750.9	22.8	-62.2	808
34.0	6.80	-0.10	6.7	.85	.80	962	750.7	23.5	-62.2	809
34.5	6.59	-0.06	6.5	.86	.82	956	750.5	24.3	-62.2	805
35.0	6.72	-0.02	6.7	.85	.80	961	750.2	25.0	-62.1	808
35.5	6.69	0.00	6.7	.85	.81	960	750.0	25.7	-61.9	807
36.0	6.61	0.01	6.6	.86	.81	958	749.7	26.4	-61.6	805
36.5	6.72	0.04	6.8	.84	.80	961	749.4	27.1	-61.2	807
37836.6	6.72	0.05	6.8	-16.84	-16.85	962	749.3	27.2	-61.1	807
36.8	6.66	0.07	6.7	.85	.85	961	749.2	27.5	-61.0	806
37.0	6.76	0.08	6.8	.84	.84	964	749.0	27.7	-60.8	808
37.2	6.70	0.09	6.8	.84	.85	962	748.9	27.9	-60.6	806
37.4	6.65	0.10	6.7	.84	.85	961	748.7	28.2	-60.4	805
37.6	7.44	0.10	7.5	.79	.79	981	748.6	28.4	-60.2	821
37.8	7.05	0.11	7.2	.81	.82	971	748.4	28.6	-59.9	813
37838.0	7.03	0.12	7.1	-16.82	-16.78	970	748.3	28.9	-59.7	811
38.5	6.66	0.15	6.8	.84	.80	961	747.9	29.4	-59.0	802
39.0	6.42	0.19	6.6	.85	.82	955	747.4	29.8	-58.3	796
39.5	6.12	0.20	6.3	.88	.84	946	747.0	30.2	-57.5	788
40.0	5.88	0.23	6.1	.89	.86	939	746.5	30.6	-56.6	781
40.5	5.49	0.28	5.8	.92	.89	928	746.1	30.9	-55.7	770
41.0	5.40	0.30	5.7	.92	.90	925	745.6	31.2	-54.7	766
41.5	5.49	0.33	5.8	.91	.89	929	745.1	31.4	-53.7	767
42.0	5.54	0.37	5.9	.90	.88	931	744.6	31.5	-52.6	768
42.5	6.56	0.40	7.0	.82	.80	961	744.1	31.6	-51.5	791
43.0	6.70	0.42	7.1	.81	.79	965	743.7	31.7	-50.3	792
43.5	6.36	0.45	6.8	.83	.82	957	743.2	31.6	-49.1	784
44.0	5.73	0.48	6.2	.88	.86	939	742.7	31.6	-47.9	768
44.5	5.65	0.49	6.1	.88	.87	937	742.2	31.5	-46.6	764
45.0	5.31	0.49	5.8	.91	.90	926	741.8	31.4	-45.3	753
45.5	5.04	0.50	5.5	.93	.92	917	741.3	31.2	-43.9	745
46.0	4.89	0.50	5.4	.94	.94	912	740.9	31.0	-42.6	738
46.5	4.56	0.50	5.1	.97	.97	900	740.4	30.7	-41.2	727
47.0	4.46	0.42	4.9	.99	.99	892	740.0	30.4	-39.7	720
47.5	4.69	0.30	5.0	.98	.98	896	739.6	30.1	-38.3	721
48.0	4.94	0.17	5.1	.96	.97	901	739.2	29.8	-36.8	723
48.5	5.05	0.00	5.0	.97	.97	898	738.8	29.4	-35.3	720
49.0	5.41	-0.25	5.2	.96	.96	902	738.4	29.0	-33.8	722
49.5	5.73	-0.26	5.5	.93	.93	913	738.0	28.6	-32.3	729
37849.8	5.93	-0.27	5.7	-16.91	-16.96	920	737.8	28.4	-31.4	734
50.0	6.13	-0.28	5.8	.89	.94	926	737.7	28.2	-30.8	738
50.2	6.84	-0.29	6.5	.83	.89	947	737.5	28.0	-30.2	754
50.4	6.55	-0.30	6.2	.86	.91	939	737.4	27.9	-29.6	747
50.6	6.42	-0.30	6.1	.87	.92	935	737.3	27.7	-29.0	743
50.8	6.63	-0.30	6.3	.85	.90	941	737.2	27.5	-28.3	748
37851.0	6.51	-0.30	6.2	-16.86	-16.91	937	737.0	27.3	-27.7	744
51.5	6.01	-0.38	5.6	.91	.96	919	736.7	26.9	-26.2	729
52.0	6.13	-0.46	5.7	.90	.96	920	736.5	26.4	-24.6	729
52.5	6.23	-0.56	5.7	.90	.96	920	736.2	26.0	-23.1	727
53.0	6.38	-0.68	5.7	.90	.96	921	736.0	25.5	-21.5	727
53.5	6.67	-0.80	5.9	.88	.94	926	735.8	25.0	-19.9	731
54.0	6.61	-0.93	5.7	.90	.96	920	735.6	24.6	-18.4	725
54.5	6.73	-1.06	5.7	.90	.96	920	735.5	24.1	-16.8	724
55.0	6.56	-1.21	5.3	.93	.99	909	735.4	23.7	-15.3	715

Table 3 (Continued)

MJD	$-10^7\dot{P}$	$10^7\dot{P}_R$	$-10^7\dot{P}_A$	$\log \rho_\pi$ (g/cm^3)	$\log \rho_s$ (g/cm^3)	T_π (°K)	z (km)	$\alpha_\pi - \alpha_\odot$ (deg.)	$\delta_\pi - \delta_\odot$ (deg.)	T_N
37855.5	6.59	-1.27	5.3	-16.93	-16.99	908	735.3	23.3	-13.7	713
56.0	6.67	-1.52	5.1	.95	-17.01	902	735.2	22.8	-12.2	708
56.5	6.88	-1.69	5.2	.94	-16.96	902	735.1	22.4	-10.6	708
57.0	7.04	-1.83	5.2	.94	.96	903	735.1	22.1	-9.1	709
57.5	7.19	-1.98	5.2	.94	.96	903	735.1	21.7	-7.6	708
58.0	7.37	-2.10	5.3	.94	.96	905	735.1	21.4	-6.1	710
58.5	7.53	-2.27	5.3	.94	.96	905	735.1	21.1	-4.7	709
59.0	7.74	-2.42	5.3	.93	.95	907	735.2	20.8	-3.2	711
59.5	8.23	-2.58	5.6	.90	.92	918	735.2	20.6	-1.8	720
60.0	7.83	-2.63	5.2	.94	.96	903	735.3	20.4	-0.4	708
60.5	7.94	-2.90	5.0	.96	.98	897	735.4	20.2	1.0	703
61.0	8.06	-3.06	5.0	.96	.98	895	735.5	20.1	2.4	702
61.5	8.00	-3.21	4.8	.99	-17.00	887	735.6	20.0	3.7	696
62.0	8.03	-3.40	4.6	-17.00	.02	881	735.7	20.0	5.0	691
62.5	7.89	-3.56	4.3	.04	.05	868	735.8	20.0	6.2	681
63.0	8.09	-3.70	4.4	.03	.05	870	735.9	20.1	7.4	683
63.5	8.37	-3.86	4.5	.02	.03	876	735.9	20.2	8.6	688
64.0	8.61	-4.00	4.6	.01	.02	880	736.0	20.4	9.7	691
64.5	8.94	-4.12	4.8	-16.98	.00	889	736.1	20.6	10.8	698
65.0	9.28	-4.23	5.0	.96	-16.98	898	736.1	20.9	11.8	705
65.5	9.56	-4.33	5.2	.94	.96	904	736.1	21.2	12.8	711
66.0	9.79	-4.42	5.4	.93	.95	909	736.2	21.6	13.7	715
66.5	9.50	-4.51	5.0	.97	.98	895	736.2	22.0	14.6	704
67.0	9.44	-4.60	4.8	.98	-17.00	889	736.1	22.5	15.4	700
67.5	9.28	-4.68	4.6	-17.01	.02	879	736.1	23.0	16.1	692
68.0	9.27	-4.72	4.5	.02	.03	877	736.1	23.6	16.8	690
68.5	8.96	-4.80	4.2	.06	.08	859	736.0	24.2	17.4	676
69.0	9.31	-4.88	4.4	.03	.05	871	735.9	24.9	17.9	686
37869.4	9.18	-4.90	4.3	-17.05	-17.10	865	735.8	25.4	18.2	681
69.6	9.70	-4.92	4.8	-16.99	.04	887	735.8	25.7	18.4	698
69.8	9.56	-4.95	4.6	-17.01	.06	879	735.7	26.0	18.6	693
70.0	9.57	-4.98	4.6	.01	.07	878	735.6	26.3	18.7	692
70.2	10.26	-5.00	5.3	-16.94	.00	905	735.6	26.6	18.8	713
70.4	9.94	-5.01	4.9	.97	.03	892	735.5	26.9	18.9	703
70.6	10.29	-5.02	5.3	.94	.00	905	735.5	27.2	19.0	713
70.8	10.48	-5.03	5.4	.92	-16.98	911	735.4	27.5	19.1	718
71.0	10.66	-5.08	5.6	.91	.97	915	735.3	27.8	19.2	721
71.2	11.17	-5.09	6.1	.87	.93	931	735.2	28.1	19.3	733
71.4	10.85	-5.10	5.7	.90	.96	921	735.2	28.4	19.3	725
71.6	10.85	-5.11	5.7	.90	.96	920	735.1	28.7	19.4	725
71.8	10.53	-5.11	5.4	.93	.99	909	735.0	29.0	19.4	716
72.0	10.36	-5.12	5.2	.94	-17.00	903	734.9	29.3	19.4	711
72.2	10.20	-5.13	5.1	.96	.02	897	734.8	29.6	19.4	706
72.4	10.53	-5.14	5.4	.93	-16.99	908	734.7	29.9	19.4	715
72.6	10.03	-5.15	4.9	.98	-17.04	889	734.6	30.2	19.4	700
72.8	9.86	-5.16	4.7	-17.00	.06	881	734.5	30.4	19.3	694
73.0	9.68	-5.17	4.5	.02	.08	873	734.4	30.7	19.3	688
37873.5	9.18	-5.19	4.0	-17.08	-17.14	848	734.1	31.4	19.1	668
74.0	9.04	-5.20	3.8	.10	.16	840	733.8	32.1	18.8	661
74.5	8.95	-5.20	3.7	.12	.17	835	733.5	32.8	18.5	657
75.0	8.87	-5.20	3.7	.13	.18	830	733.2	33.4	18.1	652
75.5	8.37	-5.22	3.1	.21	.26	795	732.8	34.0	17.7	625
76.0	8.68	-5.22	3.5	.16	.22	816	732.5	34.5	17.1	641
76.5	9.27	-5.22	4.0	.07	.02	850	732.1	35.0	16.5	668
77.0	9.40	-5.22	4.2	.06	.01	855	731.7	35.4	15.9	672
77.5	9.96	-5.21	4.7	-16.99	-16.94	879	731.3	35.8	15.1	690
78.0	10.60	-5.20	5.4	.93	.88	903	730.9	36.1	14.4	708
78.5	10.71	-5.19	5.5	.91	.87	906	730.5	36.4	13.5	711

Table 3 (Continued)

MJD	$-10^7\dot{P}$	$10^7\dot{P}_R$	$-10^7\dot{P}_A$	$\log \rho_\pi$ (g/cm^3)	$\log \rho_s$ (g/cm^3)	T_π (°K)	z (km)	$\alpha_\pi - \alpha_\odot$ (deg.)	$\delta_\pi - \delta_\odot$ (deg.)	T_N
37879.0	9.88	-5.18	4.7	-16.99	-16.95	876	730.1	36.6	12.7	687
79.5	9.59	-5.16	4.4	-17.02	.98	864	729.7	36.8	11.7	677
80.0	9.56	-5.14	4.4	.02	.99	863	729.3	36.9	10.8	676
80.5	9.50	-5.13	4.4	.03	.99	861	728.9	37.0	9.8	674
81.0	9.52	-5.16	4.4	.03	.99	860	728.5	37.0	8.7	673
81.5	9.60	-5.18	4.4	.02	.99	862	728.0	36.9	7.6	674
82.0	9.69	-5.20	4.5	.01	.98	865	727.6	36.9	6.5	676
82.5	9.73	-5.21	4.5	.01	.98	865	727.2	36.8	5.4	677
83.0	9.94	-5.22	4.7	-16.99	.96	873	726.8	36.6	4.2	683
83.5	10.09	-5.28	4.8	.98	.95	876	726.5	36.4	3.0	685
84.0	10.22	-5.31	4.9	.97	.94	880	726.1	36.2	1.8	687
84.5	10.60	-5.38	5.2	.94	.91	891	725.8	36.0	0.5	696
85.0	10.59	-5.41	5.2	.94	.91	889	725.4	35.7	-0.7	695
85.5	10.56	-5.48	5.1	.95	.93	885	725.1	35.4	-2.0	691
86.0	10.49	-5.52	5.0	.96	.94	881	724.8	35.1	-3.3	688
86.5	10.44	-5.60	4.8	.97	.95	875	724.6	34.7	-4.6	684
87.0	10.38	-5.65	4.7	.98	.97	871	724.3	34.3	-5.9	681
87.5	10.16	-5.71	4.4	-17.02	-17.00	859	724.1	34.0	-7.3	672
88.0	9.92	-5.79	4.1	.05	.04	844	723.9	33.6	-8.6	660
88.5	10.35	-5.86	4.5	.01	-16.99	860	723.8	33.2	-10.0	673
89.0	10.64	-5.95	4.7	-16.99	.97	868	723.6	32.7	-11.3	680
89.5	11.22	-6.00	5.2	.93	.92	888	723.5	32.3	-12.7	696
90.0	11.71	-6.09	5.6	.90	.88	901	723.4	31.9	-14.0	707
90.5	12.04	-6.18	5.9	.88	.86	908	723.4	31.5	-15.4	713
91.0	13.18	-6.28	6.9	.79	.78	937	723.3	31.1	-16.7	736
91.5	13.61	-6.35	7.3	.77	.75	946	723.3	30.6	-18.1	744
37891.6	13.83	-6.37	7.5	-16.76	-16.74	951	723.3	30.6	-18.3	748
91.8	14.09	-6.40	7.7	.74	.72	956	723.3	30.4	-18.9	752
92.0	14.35	-6.45	7.9	.73	.71	961	723.3	30.2	-19.4	756
92.2	14.45	-6.48	8.0	.72	.71	962	723.3	30.1	-20.0	758
92.4	14.38	-6.51	7.9	.73	.71	960	723.3	29.9	-20.5	757
92.6	14.47	-6.58	7.9	.73	.71	960	723.4	29.8	-21.0	757
92.8	15.07	-6.61	8.5	.69	.68	972	723.4	29.6	-21.6	767
93.0	15.17	-6.65	8.5	.69	.67	974	723.4	29.4	-22.1	769
93.2	14.43	-6.70	7.7	.74	.72	957	723.4	29.3	-22.6	755
93.4	14.86	-6.74	8.1	.72	.70	965	723.5	29.2	-23.1	763
37893.5	14.83	-6.76	8.1	-16.72	-16.70	964	723.5	29.1	-23.4	762
94.0	14.80	-6.86	7.9	.73	.71	961	723.6	28.7	-24.7	761
94.5	14.70	-6.95	7.7	.74	.72	957	723.7	28.4	-26.0	758
95.0	14.75	-7.04	7.7	.74	.73	956	723.8	28.1	-27.3	759
95.5	14.30	-7.11	7.2	.78	.76	944	723.9	27.8	-28.6	750
96.0	13.89	-7.20	6.7	.82	.80	931	724.1	27.6	-29.8	741
96.5	13.59	-7.26	6.3	.84	.82	921	724.2	27.3	-31.0	734
97.0	12.84	-7.32	5.5	.91	.89	896	724.4	27.1	-32.2	716
97.5	13.31	-7.40	5.9	.88	.86	909	724.6	27.0	-33.4	727
37897.8	13.13	-7.44	5.7	-16.90	-16.88	902	724.7	26.9	-34.1	722
98.0	14.27	-7.47	6.8	.81	.79	934	724.8	26.9	-34.5	748
98.2	14.23	-7.49	6.7	.82	.79	932	724.8	26.9	-35.0	747
98.4	15.37	-7.51	7.9	.74	.72	959	724.9	26.8	-35.4	769
98.6	14.51	-7.54	7.0	.80	.78	938	725.0	26.8	-35.9	753
98.8	15.15	-7.57	7.6	.76	.73	953	725.0	26.8	-36.3	765
99.0	15.12	-7.59	7.5	.76	.74	952	725.1	26.8	-36.7	765
99.2	14.92	-7.60	7.3	.78	.75	947	725.2	26.8	-37.1	761
99.4	15.06	-7.61	7.4	.77	.74	950	725.2	26.8	-37.6	764
99.6	15.37	-7.62	7.7	.75	.72	957	725.3	26.8	-38.0	770
99.8	15.01	-7.64	7.4	.77	.75	948	725.4	26.9	-38.4	763
37900.0	14.81	-7.66	7.1	.79	.76	942	725.4	26.9	-38.8	759

Table 3 (Continued)

MJD	$-10^7\dot{P}$	$10^7\dot{P}_R$	$-10^7\dot{P}_A$	$\log \rho_\pi$ (g/cm^3)	$\log \rho_s$ (g/cm^3)	T_π (°K)	z (km)	$\alpha_\pi - \alpha_\odot$ (deg.)	$\delta_\pi - \delta_\odot$ (deg.)	T_N
37900.2	14.62	-7.68	6.9	-16.80	-16.78	937	725.5	26.9	-39.2	756
00.4	14.77	-7.69	7.1	.79	.77	941	725.5	27.0	-39.6	759
00.6	14.41	-7.69	6.7	.82	.79	931	725.6	27.0	-39.9	752
00.8	14.39	-7.70	6.7	.82	.80	931	725.7	27.1	-40.3	752
37901.0	14.27	-7.70	6.6	-16.83	-16.81	927	725.7	27.2	-40.7	749
01.5	14.20	-7.70	6.5	.84	.81	925	725.8	27.4	-41.5	749
02.0	14.03	-7.70	6.3	.85	.83	921	725.9	27.7	-42.4	746
02.5	13.98	-7.68	6.3	.86	.83	920	726.0	28.0	-43.1	746
03.0	13.43	-7.64	5.8	.90	.87	904	726.1	28.4	-43.8	734
03.5	13.22	-7.60	5.6	.91	.89	899	726.1	28.9	-44.5	731
04.0	12.72	-7.54	5.2	.96	.93	884	726.2	29.4	-45.1	719
04.5	12.82	-7.49	5.3	.94	.92	889	726.2	29.9	-45.6	724
05.0	13.01	-7.40	5.6	.92	.89	898	726.1	30.5	-46.1	732
05.5	13.35	-7.30	6.0	.88	.85	912	726.1	31.1	-46.5	743
06.0	13.61	-7.20	6.4	.85	.82	922	726.0	31.8	-46.8	752
06.5	13.83	-7.10	6.7	.83	.80	930	725.9	32.5	-47.0	759
07.0	13.91	-6.97	6.9	.81	.78	935	725.8	33.3	-47.2	763
37907.2	14.38	-6.90	7.5	-16.77	-16.75	949	725.7	33.6	-47.2	774
07.4	14.24	-6.83	7.4	.78	.75	947	725.6	33.9	-47.2	773
07.6	14.43	-6.78	7.6	.76	.74	952	725.6	34.2	-47.3	777
07.8	14.62	-6.70	7.9	.74	.72	958	725.5	34.5	-47.3	782
08.0	14.48	-6.64	7.8	.75	.72	956	725.4	34.9	-47.3	781
08.2	14.51	-6.58	7.9	.74	.72	958	725.3	35.2	-47.2	782
08.4	14.53	-6.50	8.0	.74	.71	960	725.2	35.5	-47.2	784
08.6	14.72	-6.42	8.3	.72	.70	966	725.1	35.8	-47.2	788
08.8	14.58	-6.35	8.2	.73	.70	964	725.0	36.2	-47.1	787
09.0	14.60	-6.29	8.3	.72	.70	966	724.9	36.5	-47.0	788
09.2	14.79	-6.20	8.6	.70	.68	971	724.8	36.8	-46.9	793
09.4	14.98	-6.11	8.9	.69	.67	977	724.7	37.1	-46.8	797
09.6	14.49	-6.03	8.5	.71	.69	968	724.5	37.5	-46.7	790
09.8	15.01	-5.96	9.0	.68	.66	980	724.4	37.8	-46.6	799
10.0	14.69	-5.88	8.8	.69	.67	975	724.2	38.1	-46.4	795
10.2	14.87	-5.79	9.1	.68	.66	980	724.1	38.4	-46.3	799
10.4	15.38	-5.70	9.7	.64	.63	991	723.9	38.7	-46.1	808
10.6	14.72	-5.60	9.1	.67	.66	980	723.8	39.0	-45.9	799
10.8	15.40	-5.50	9.9	.63	.62	995	723.6	39.3	-45.7	810
11.0	15.07	-5.38	9.7	.64	.63	991	723.4	39.6	-45.5	807
11.2	15.57	-5.28	10.3	.61	.60	1001	723.3	39.9	-45.3	815
11.4	15.57	-5.19	10.4	.61	.59	1002	723.1	40.2	-45.1	816
11.6	15.06	-5.09	10.0	.63	.61	995	722.9	40.5	-44.9	809
37912.0	13.92	-4.90	9.0	-16.68	-16.67	977	722.5	41.1	-44.3	794
12.5	13.34	-4.69	8.6	.70	.69	969	722.0	41.7	-43.6	787
13.0	13.33	-4.48	8.8	.69	.68	972	721.5	42.4	-42.8	789
13.5	13.63	-4.27	9.4	.66	.65	981	720.9	42.9	-42.0	795
14.0	13.74	-4.08	9.7	.64	.64	986	720.3	43.5	-41.0	798
14.5	13.86	-3.90	10.0	.63	.63	990	719.7	43.9	-40.0	801
15.0	13.48	-3.20	10.3	.61	.61	995	719.1	44.4	-39.0	803
15.5	13.16	-3.56	9.6	.64	.65	983	718.5	44.7	-37.9	792
16.0	13.16	-3.48	9.7	.64	.65	983	717.8	45.0	-36.7	791
16.5	13.21	-3.41	9.8	.63	.64	985	717.2	45.3	-35.5	791
17.0	13.21	-3.40	9.8	.63	.64	984	716.5	45.5	-34.3	789
17.5	13.08	-3.43	9.6	.64	.55	980	715.8	45.7	-32.9	785
18.0	12.84	-3.49	9.3	.65	.57	974	715.2	45.8	-31.6	779
18.5	13.16	-3.55	9.6	.64	.56	978	714.5	45.8	-30.2	781
37919.0	13.86	-3.63	10.2	-16.60	-16.53	988	713.8	45.8	-28.8	787
19.2	14.42	-3.67	10.7	.58	.51	996	713.5	45.8	-28.2	793

Table 3 (Continued)

MJD	$-10^6\dot{P}$	$10^6\dot{P}_R$	$-10^6\dot{P}_A$	$\log \rho_\pi$ (g/cm^3)	$\log \rho_s$ (g/cm^3)	T_π (°K)	z (km)	$\alpha_\pi - \alpha_\odot$ (deg.)	$\delta_\pi - \delta_\odot$ (deg.)	T_N
37919.4	1.60	-0.37	1.2	16.51	-16.44	1019	713.2	45.8	-27.6	811
19.6	1.87	-0.37	1.5	.42	.35	1053	713.0	45.8	-27.0	838
19.8	1.91	-0.38	1.5	.41	.34	1057	712.7	45.8	-26.4	840
20.0	1.68	-0.38	1.3	.49	.42	1027	712.4	45.7	-25.8	816
37920.5	1.62	-0.39	1.2	-16.51	-16.45	1017	711.8	45.6	-24.3	807
21.0	1.56	-0.40	1.2	.54	.48	1006	711.1	45.4	-22.8	797
21.5	1.55	-0.41	1.1	.55	.49	1002	710.5	45.2	-21.2	793
22.0	1.57	-0.42	1.1	.54	.49	1001	709.9	45.0	-19.6	791
22.5	1.57	-0.43	1.1	.54	.50	1001	709.2	44.8	-18.0	789
23.0	1.58	-0.45	1.1	.55	.50	998	708.6	44.5	-16.4	786
23.5	1.58	-0.46	1.1	.55	.51	996	708.1	44.2	-14.7	784
24.0	1.57	-0.47	1.1	.56	.52	992	707.5	43.9	-13.1	780
24.5	1.56	-0.48	1.1	.57	.53	988	706.9	43.5	-11.4	776
25.0	1.53	-0.50	1.0	.59	.56	980	706.4	43.2	-9.7	769
25.5	1.49	-0.51	1.0	.61	.58	971	705.9	42.8	-8.0	761
26.0	1.52	-0.52	1.0	.60	.57	973	705.4	42.4	-6.3	762
37926.4	1.64	-0.53	1.1	-16.55	-16.52	990	705.0	42.1	-5.0	775
26.6	1.71	-0.54	1.2	.53	.50	999	704.8	41.9	-4.3	782
26.8	1.97	-0.54	1.4	.43	.40	1033	704.6	41.8	-3.6	808
27.0	1.82	-0.55	1.3	.49	.46	1012	704.4	41.6	-2.9	792
27.2	1.74	-0.56	1.2	.52	.50	1000	704.2	41.4	-2.2	782
37927.5	1.64	-0.56	1.1	-16.56	-16.54	984	704.0	41.2	-1.2	770
28.0	1.58	-0.58	1.0	.60	.58	971	703.5	40.8	0.5	759
28.5	1.60	-0.59	1.0	.60	.58	972	703.1	40.4	2.2	760
29.0	1.65	-0.61	1.0	.58	.57	976	702.8	40.0	3.9	763
29.5	1.79	-0.62	1.2	.52	.51	995	702.4	39.6	5.6	779
30.0	1.75	-0.64	1.1	.55	.54	986	702.1	39.2	7.3	771
30.5	1.71	-0.65	1.1	.57	.56	977	701.8	38.9	9.0	765
31.0	1.69	-0.66	1.0	.59	.58	972	701.5	38.5	10.6	762
31.5	1.67	-0.68	1.0	.61	.60	965	701.3	38.2	12.3	756
32.0	1.70	-0.70	1.0	.60	.60	966	701.1	37.9	13.9	758
32.5	1.75	-0.71	1.0	.58	.58	972	700.9	37.6	15.6	763
33.0	1.86	-0.73	1.1	.54	.54	985	700.7	37.3	17.2	775
33.5	1.98	-0.74	1.2	.50	.50	1000	700.5	37.1	18.8	788
34.0	1.94	-0.76	1.2	.52	.52	992	700.4	36.9	20.3	782
34.5	1.93	-0.77	1.2	.53	.53	988	700.3	36.7	21.9	780
35.0	1.89	-0.78	1.1	.55	.55	980	700.2	36.6	23.4	775
35.5	1.89	-0.79	1.1	.56	.56	979	700.1	36.5	24.9	774
36.0	1.99	-0.81	1.2	.53	.53	990	700.0	36.4	26.4	785
36.5	2.07	-0.82	1.2	.50	.50	999	699.9	36.4	27.8	793
37936.8	2.15	-0.82	1.3	-16.47	-16.47	1009	699.8	36.4	28.6	802
37.0	2.34	-0.83	1.5	.41	.41	1032	699.8	36.4	29.2	820
37.2	2.51	-0.83	1.7	.36	.36	1049	699.7	36.5	29.7	834
37.4	2.44	-0.84	1.6	.38	.38	1040	699.7	36.5	30.3	828
37.6	2.37	-0.84	1.5	.40	.41	1032	699.7	36.5	30.8	822
37.8	2.34	-0.84	1.5	.41	.42	1029	699.6	36.6	31.3	820
38.0	2.27	-0.85	1.4	.44	.44	1019	699.6	36.6	31.8	813
38.2	2.18	-0.85	1.3	.47	.47	1008	699.6	36.7	32.3	805
38.4	2.17	-0.86	1.3	.48	.48	1005	699.5	36.8	32.8	803
38.6	2.25	-0.86	1.4	.45	.45	1015	699.5	36.9	33.3	811
38.8	2.29	-0.86	1.4	.44	.44	1020	699.4	37.0	33.8	816
39.0	2.26	-0.87	1.4	.45	.45	1015	699.4	37.1	34.3	812
39.2	2.20	-0.87	1.3	.47	.48	1007	699.3	37.2	34.8	807
37939.5	2.22	-0.87	1.3	-16.47	-16.47	1008	699.3	37.3	35.5	808
40.0	2.08	-0.88	1.2	.52	.53	989	699.1	37.7	36.6	794

Table 3 (Continued)

MJD	$-10^6\dot{P}$	$10^6\dot{P}_R$	$-10^6\dot{P}_A$	$\log \rho_\pi$ (g/cm^3)	$\log \rho_s$ (g/cm^3)	T_π (°K)	z (km)	$\alpha_\pi - \alpha_\odot$ (deg.)	$\delta_\pi - \delta_\odot$ (deg.)	T_N
37940.5	2.02	-0.89	1.1	-16.55	-16.56	979	699.0	38.1	37.7	787
41.0	1.97	-0.89	1.1	.58	.58	971	698.9	38.5	38.7	782
41.5	1.93	-0.89	1.0	.59	.60	964	698.7	39.0	39.6	778
42.0	1.92	-0.89	1.0	.60	.61	962	698.5	39.5	40.5	777
42.5	1.95	-0.89	1.1	.59	.59	966	698.3	40.1	41.3	782
43.0	1.98	-0.89	1.1	.57	.58	970	698.0	40.7	42.0	786
43.5	2.02	-0.89	1.1	.56	.57	976	697.8	41.4	42.7	791
44.0	1.99	-0.89	1.1	.57	.58	971	697.5	42.1	43.3	788
44.5	2.04	-0.89	1.1	.55	.56	978	697.2	42.8	43.8	795
37944.8	2.03	-0.88	1.1	-16.55	-16.56	977	697.0	43.3	44.0	795
45.0	2.17	-0.88	1.3	.49	.51	996	696.9	43.6	44.2	811
45.2	2.16	-0.87	1.3	.50	.51	995	696.8	43.9	44.4	810
45.4	2.16	-0.87	1.3	.49	.51	996	696.6	44.2	44.5	811
45.6	2.23	-0.86	1.4	.47	.48	1004	696.5	44.5	44.6	818
45.8	2.29	-0.86	1.4	.44	.46	1012	696.4	44.8	44.7	825
46.0	2.29	-0.85	1.4	.44	.46	1013	696.2	45.1	44.8	826
46.2	2.36	-0.85	1.5	.42	.44	1021	696.1	45.4	44.9	832
46.4	2.33	-0.84	1.5	.42	.44	1019	695.9	45.7	45.0	831
46.6	2.23	-0.84	1.4	.46	.48	1007	695.8	46.1	45.0	821
46.8	2.18	-0.83	1.3	.47	.49	1002	695.6	46.4	45.1	817
37947.0	2.18	-0.83	1.3	-16.47	-16.49	1001	695.5	46.7	45.1	817
47.5	2.15	-0.81	1.3	.47	.50	999	695.1	47.4	45.2	816
48.0	2.13	-0.84	1.3	.49	.52	992	694.7	48.2	45.1	810
48.5	2.09	-0.77	1.3	.48	.51	996	694.3	48.9	45.0	813
49.0	2.09	-0.75	1.3	.47	.50	997	693.8	49.6	44.8	815
49.5	2.05	-0.72	1.3	.47	.51	997	693.4	50.3	44.5	814
50.0	2.01	-0.69	1.3	.48	.52	993	692.9	50.9	44.1	811
37950.2	2.00	-0.68	1.3	-16.48	-16.51	994	692.8	51.1	44.0	812
50.4	2.00	-0.66	1.3	.47	.51	995	692.6	51.4	43.8	813
50.6	1.90	-0.65	1.2	.50	.54	984	692.4	51.6	43.6	803
50.8	2.01	-0.64	1.4	.46	.50	999	692.2	51.8	43.4	815
51.0	2.07	-0.62	1.4	.43	.48	1008	692.0	52.0	43.2	822
51.2	2.15	-0.60	1.5	.40	.45	1017	691.8	52.2	43.0	830
51.4	2.34	-0.59	1.7	.34	.39	1039	691.6	52.4	42.8	847
51.6	2.22	-0.57	1.6	.37	.42	1028	691.4	52.6	42.6	838
51.8	2.25	-0.56	1.7	.36	.41	1032	691.2	52.7	42.3	841
52.0	2.16	-0.54	1.6	.38	.43	1025	691.0	52.9	42.1	835
52.2	2.10	-0.52	1.6	.39	.44	1020	690.8	53.0	41.8	831
52.4	2.06	-0.51	1.5	.40	.45	1017	690.7	53.2	41.5	828
52.6	2.08	-0.49	1.6	.39	.44	1021	690.5	53.3	41.2	831
52.8	1.84	-0.47	1.4	.46	.51	996	690.3	53.5	41.0	811
53.0	1.85	-0.45	1.4	.45	.50	998	690.1	53.6	40.6	812
53.2	1.85	-0.44	1.4	.44	.50	1000	689.9	53.7	40.3	813
53.4	1.84	-0.42	1.4	.44	.49	1001	689.7	53.8	40.0	814
53.6	1.91	-0.40	1.5	.41	.46	1012	689.5	53.9	39.7	822
53.8	1.85	-0.37	1.5	.42	.48	1007	689.3	54.0	39.4	818
54.0	1.87	-0.35	1.5	.41	.46	1012	689.1	54.1	39.0	821
54.2	1.86	-0.32	1.5	.40	.46	1014	688.9	54.1	38.7	822
54.4	1.88	-0.30	1.6	.39	.45	1018	688.7	54.2	38.3	825
54.6	1.88	-0.27	1.6	.38	.44	1020	688.5	54.2	38.0	827
54.8	1.86	-0.25	1.6	.38	.44	1020	688.3	54.3	37.6	827
55.0	1.78	-0.22	1.6	.39	.46	1015	688.1	54.3	37.2	822
55.2	1.76	-0.20	1.6	.39	.46	1014	687.9	54.4	36.8	821
55.4	1.74	-0.19	1.5	.39	.46	1013	687.7	54.4	36.4	820
55.6	1.75	-0.17	1.6	.39	.45	1016	687.5	54.4	36.0	822
55.8	1.70	-0.16	1.5	.40	.46	1012	687.3	54.4	35.6	818
56.0	1.71	-0.15	1.6	.39	.46	1014	687.1	54.4	35.2	819

Table 3 (Continued)

MJD	$-10^6\dot{P}$	$10^6\dot{P}_R$	$-10^6\dot{P}_A$	$\log \rho_\pi$ (g/cm^3)	$\log \rho_s$ (g/cm^3)	T_π (°K)	z (km)	$\alpha_\pi - \alpha_\odot$ (deg.)	$\delta_\pi - \delta_\odot$ (deg.)	T_N
37956.2	1.72	-0.13	1.6	-16.38	-16.45	1017	686.9	54.4	34.8	821
56.4	1.70	-0.05	1.6	.36	.43	1022	686.7	54.4	34.4	825
56.6	1.74	0.00	1.7	.34	.41	1031	686.6	54.4	34.0	832
56.8	1.70	0.02	1.7	.34	.42	1029	686.4	54.3	33.5	829
57.0	1.68	0.02	1.7	.35	.42	1027	686.2	54.3	33.1	827
57.2	1.67	0.02	1.7	.35	.42	1026	686.0	54.2	32.7	826
57.4	1.68	0.02	1.7	.35	.42	1026	685.8	54.2	32.2	826
57.6	1.63	0.02	1.6	.36	.44	1021	685.7	54.1	31.8	821
57.8	1.63	0.02	1.6	.36	.44	1021	685.5	54.1	31.3	821
37958.0	1.52	0.02	1.5	-16.39	-16.30	1010	685.4	54.0	30.8	811
58.5	1.57	0.03	1.6	.38	.29	1015	684.9	53.8	29.7	814
59.0	1.62	-0.02	1.6	.37	.29	1014	684.5	53.6	28.5	812
59.5	1.75	-0.08	1.7	.35	.27	1021	684.1	53.3	27.2	816
60.0	1.81	-0.13	1.7	.35	.27	1022	683.8	53.0	26.0	816
60.5	1.83	-0.18	1.6	.36	.28	1018	683.5	52.7	24.7	812
61.0	1.86	-0.22	1.6	.36	.28	1017	683.2	52.4	23.5	809
61.5	1.97	-0.25	1.7	.34	.26	1025	682.9	52.0	22.2	814
62.0	2.20	-0.28	1.9	.29	.22	1042	682.6	51.6	20.9	827
62.5	2.30	-0.31	2.0	.27	.20	1049	682.4	51.3	19.6	831
37962.6	2.35	-0.32	2.0	-16.26	-16.19	1052	682.4	51.2	19.3	834
62.8	2.38	-0.33	2.0	.25	.18	1054	682.3	51.0	18.8	835
63.0	2.37	-0.34	2.0	.26	.19	1052	682.3	50.8	18.2	833
63.2	2.38	-0.35	2.0	.26	.19	1052	682.2	50.7	17.7	832
63.4	2.45	-0.36	2.1	.24	.18	1057	682.2	50.5	17.2	836
63.6	2.41	-0.37	2.0	.25	.19	1053	682.1	50.3	16.6	832
63.8	2.40	-0.38	2.0	.26	.19	1051	682.1	50.2	16.1	830
64.0	2.48	-0.39	2.1	.24	.17	1057	682.0	50.0	15.6	835
64.2	2.50	-0.40	2.1	.24	.17	1057	682.0	49.8	15.0	835
64.4	2.47	-0.40	2.1	.25	.18	1054	682.0	49.6	14.5	832
64.6	2.39	-0.41	2.0	.27	.20	1047	681.9	49.5	14.0	825
37965.0	2.27	-0.43	1.8	-16.30	-16.23	1035	681.9	49.1	12.9	816
65.5	2.13	-0.45	1.7	.34	.28	1020	681.9	48.7	11.5	803
66.0	2.07	-0.46	1.6	.36	.30	1013	681.9	48.3	10.2	797
66.5	2.05	-0.48	1.6	.38	.31	1009	681.9	47.8	8.8	793
67.0	1.97	-0.50	1.5	.41	.34	998	682.0	47.4	7.5	784
67.5	2.00	-0.51	1.5	.40	.33	1000	682.1	47.0	6.2	785
68.0	2.02	-0.53	1.5	.40	.33	1001	682.2	46.6	4.8	785
68.5	2.01	-0.54	1.5	.41	.34	999	682.3	46.2	3.5	783
69.0	2.02	-0.56	1.5	.41	.34	998	682.4	45.8	2.2	782
69.5	1.99	-0.57	1.4	.42	.35	993	682.6	45.5	0.9	779
70.0	1.98	-0.59	1.4	.43	.36	990	682.7	45.2	-0.4	776
70.5	1.99	-0.60	1.4	.43	.36	990	682.9	44.9	-1.6	776
71.0	2.01	-0.62	1.4	.43	.36	992	683.1	44.6	-2.9	777
71.5	2.03	-0.63	1.4	.43	.36	992	683.2	44.4	-4.1	777
72.0	2.08	-0.65	1.4	.42	.34	997	683.4	44.2	-5.3	781
72.5	2.12	-0.66	1.4	.42	.34	998	683.6	44.0	-6.5	782
37972.6	2.14	-0.66	1.5	-16.41	-16.33	1000	683.6	44.0	-6.7	784
72.8	2.10	-0.67	1.4	.42	.35	996	683.7	43.9	-7.2	781
73.0	2.15	-0.68	1.5	.41	.33	1000	683.8	43.9	-7.6	784
73.2	2.13	-0.68	1.4	.42	.34	998	683.9	43.8	-8.1	783
73.4	2.10	-0.69	1.4	.43	.35	994	683.9	43.8	-8.5	779
73.6	2.10	-0.70	1.4	.43	.35	994	684.0	43.8	-9.0	779
73.8	2.10	-0.70	1.4	.43	.36	993	684.1	43.8	-9.4	779
74.0	2.09	-0.71	1.4	.44	.36	990	684.1	43.8	-9.8	777
74.2	2.16	-0.71	1.4	.42	.34	998	684.2	43.8	-10.3	783
74.4	2.15	-0.72	1.4	.42	.34	996	684.3	43.8	-10.7	782

Table 3 (Continued)

MJD	$-10^6\dot{P}$	$10^6\dot{P}_R$	$-10^6\dot{P}_A$	$\log \rho_\pi$ (g/cm^3)	$\log \rho_s$ (g/cm^3)	T_π (°K)	z (km)	$\alpha_\pi - \alpha_\odot$ (deg.)	$\delta_\pi - \delta_\odot$ (deg.)	T_N
37974.6	2.22	-0.72	1.5	-16.40	-16.32	1004	684.4	43.8	-11.1	788
74.8	2.19	-0.73	1.5	.42	.33	1000	684.4	43.8	-11.5	785
75.0	2.28	-0.73	1.5	.39	.31	1010	684.5	43.8	-11.9	793
75.2	2.18	-0.73	1.4	.42	.34	999	684.6	43.9	-12.3	784
75.4	2.24	-0.74	1.5	.40	.32	1004	684.6	43.9	-12.7	789
75.6	2.23	-0.74	1.5	.41	.32	1003	684.7	44.0	-13.1	788
75.8	2.24	-0.75	1.5	.40	.32	1004	684.7	44.0	-13.4	789
76.0	2.15	-0.75	1.4	.44	.35	993	684.8	44.1	-13.8	781
76.2	2.16	-0.75	1.4	.43	.35	994	684.8	44.2	-14.2	782
76.4	2.18	-0.76	1.4	.43	.35	995	684.9	44.3	-14.5	783
37976.5	2.19	-0.76	1.4	-16.43	-16.34	997	684.9	44.3	-14.7	784
77.0	2.10	-0.77	1.3	.46	.38	985	685.0	44.6	-15.5	775
77.5	2.00	-0.78	1.2	.50	.42	971	685.1	44.9	-16.3	764
78.0	2.00	-0.80	1.2	.51	.42	969	685.1	45.3	-17.0	764
78.5	1.99	-0.81	1.2	.52	.44	965	685.1	45.7	-17.7	761
79.0	2.01	-0.82	1.2	.52	.43	966	685.1	46.2	-18.3	762
79.5	2.06	-0.83	1.2	.50	.42	971	685.1	46.7	-18.8	767
80.0	2.12	-0.84	1.3	.48	.40	978	685.1	47.3	-19.3	772
80.5	2.11	-0.85	1.3	.49	.41	975	685.0	47.9	-19.7	771
81.0	2.04	-0.86	1.2	.52	.44	965	684.9	48.6	-20.0	763
81.5	2.06	-0.86	1.2	.52	.43	966	684.7	49.3	-20.2	765
82.0	2.08	-0.87	1.2	.51	.43	967	684.5	50.0	-20.4	766
82.5	2.14	-0.87	1.3	.49	.41	973	684.3	50.7	-20.5	771
83.0	2.24	-0.88	1.4	.46	.38	985	684.0	51.5	-20.5	781
37983.2	2.31	-0.88	1.4	-16.43	-16.35	993	683.9	51.8	-20.5	787
83.4	2.55	-0.88	1.7	.36	.28	1018	683.8	52.1	-20.4	807
83.6	2.87	-0.88	2.0	.28	.20	1048	683.7	52.4	-20.4	831
83.8	2.69	-0.88	1.8	.32	.24	1031	683.5	52.7	-20.3	818
84.0	2.68	-0.88	1.8	.32	.25	1030	683.4	53.0	-20.3	817
84.2	2.72	-0.88	1.8	.31	.24	1034	683.2	53.3	-20.2	820
84.4	2.82	-0.89	1.9	.29	.21	1042	683.1	53.6	-20.1	827
84.6	2.75	-0.89	1.9	.31	.24	1035	682.9	53.9	-20.0	821
84.8	2.75	-0.89	1.9	.31	.24	1034	682.7	54.2	-19.8	821
85.0	2.64	-0.89	1.7	.34	.27	1024	682.6	54.5	-19.7	812
37985.5	2.33	-0.89	1.4	-16.43	-16.36	991	682.1	55.2	-19.3	787
86.0	2.20	-0.89	1.3	.47	.41	975	681.6	55.9	-18.8	774
86.5	2.12	-0.90	1.2	.51	.44	962	681.0	56.5	-18.3	764
87.0	2.08	-0.90	1.2	.52	.46	956	680.5	57.2	-17.7	759
87.5	2.06	-0.90	1.2	.53	.47	952	679.8	57.7	-17.0	756
88.0	2.07	-0.90	1.2	.52	.47	953	679.2	58.3	-16.2	756
88.5	2.09	-0.90	1.2	.52	.47	953	678.5	58.7	-15.4	757
89.0	2.13	-0.90	1.2	.50	.46	958	677.8	59.2	-14.5	761
89.5	2.29	-0.90	1.4	.44	.40	976	677.1	59.5	-13.5	774
37990.0	2.63	-0.90	1.7	-16.34	-16.30	1011	676.3	59.8	-12.5	802
90.2	2.73	-0.90	1.8	.31	.28	1020	676.0	59.9	-12.1	809
90.4	2.68	-0.90	1.8	.33	.29	1014	675.7	60.0	-11.6	804
90.6	2.64	-0.90	1.7	.33	.30	1011	675.4	60.1	-11.2	802
90.8	2.60	-0.90	1.7	.34	.32	1006	675.1	60.2	-10.8	798
91.0	2.58	-0.90	1.7	.35	.32	1003	674.8	60.3	-10.3	796
91.2	2.47	-0.91	1.6	.38	.36	991	674.5	60.4	-9.8	786
91.4	2.40	-0.91	1.5	.40	.38	984	674.2	60.4	-9.4	780
37991.5	2.39	-0.91	1.5	-16.41	-16.39	982	674.0	60.4	-9.1	779
92.0	2.32	-0.91	1.4	.43	.41	974	673.2	60.5	-7.9	772
92.5	2.27	-0.91	1.4	.45	.43	966	672.4	60.6	-6.7	766
93.0	2.24	-0.91	1.3	.46	.45	961	671.6	60.6	-5.4	762

Table 3 (Continued)

MJD	$-10^6\dot{P}$	$10^6\dot{P}_R$	$-10^6\dot{P}_A$	$\log \rho_\pi$ (g/cm^3)	$\log \rho_s$ (g/cm^3)	T_π (°K)	z (km)	$\alpha_\pi - \alpha_\odot$ (deg.)	$\delta_\pi - \delta_\odot$ (deg.)	T_N
37993.5	2.19	-0.91	1.3	-16.47	-16.47	955	670.8	60.5	-4.1	757
94.0	2.16	-0.91	1.2	.48	.48	949	669.9	60.4	-2.7	752
94.5	2.13	-0.91	1.2	.50	.50	944	669.1	60.3	-1.3	748
95.0	2.07	-0.91	1.2	.52	.53	935	668.3	60.1	0.1	740
95.5	2.04	-0.91	1.1	.53	.54	929	667.5	59.8	1.6	736
96.0	2.04	-0.92	1.1	.53	.55	928	666.7	59.6	3.0	735
96.5	2.07	-0.92	1.1	.52	.54	930	665.9	59.3	4.5	736
97.0	2.07	-0.92	1.1	.52	.55	929	665.1	58.9	6.0	735
97.5	2.05	-0.93	1.1	.53	.56	923	664.3	58.6	7.6	731
98.0	2.22	-0.93	1.3	.46	.50	944	663.5	58.2	9.1	748
37998.2	2.23	-0.93	1.3	-16.46	-16.50	945	663.2	58.0	9.7	748
98.4	2.43	-0.93	1.5	.40	.43	966	662.9	57.8	10.3	765
98.6	2.77	-0.94	1.8	.30	.34	999	662.7	57.7	10.9	791
98.8	2.70	-0.94	1.8	.32	.36	991	662.4	57.5	11.6	785
99.0	2.29	-0.94	1.3	.44	.49	949	662.1	57.3	12.2	752
37999.5	2.25	-0.95	1.3	-16.46	-16.51	942	661.4	56.9	13.8	747
38000.0	2.23	-0.95	1.3	.47	.52	938	660.7	56.4	15.3	744
00.5	2.21	-0.96	1.2	.48	.53	933	660.0	55.9	16.9	741
01.0	2.14	-0.96	1.2	.51	.56	923	659.4	55.4	18.5	734
01.5	2.23	-0.97	1.3	.47	.54	932	658.8	54.9	20.1	741
02.0	2.30	-0.98	1.3	.45	.52	938	658.2	54.4	21.7	747
38002.2	2.33	-0.98	1.3	-16.44	-16.51	942	658.0	54.2	22.3	750
02.4	2.44	-0.98	1.5	.40	.47	953	657.8	54.0	22.9	759
02.6	2.53	-0.98	1.5	.38	.45	961	657.6	53.8	23.6	766
02.8	2.90	-0.99	1.9	.28	.35	994	657.4	53.6	24.2	793
03.0	2.81	-0.99	1.8	.30	.37	986	657.1	53.4	24.8	787
03.2	2.75	-0.99	1.8	.32	.39	981	656.9	53.2	25.5	782
03.4	2.69	-1.00	1.7	.34	.41	974	656.7	53.0	26.1	777
03.6	2.68	-1.00	1.7	.34	.41	973	656.5	52.8	26.7	777
03.8	2.67	-1.00	1.7	.34	.42	970	656.4	52.6	27.4	775
38004.0	2.55	-1.00	1.5	-16.38	-16.46	958	656.2	52.4	28.0	766
04.5	2.37	-1.01	1.3	.44	.52	937	655.7	51.9	29.6	750
05.0	2.31	-1.02	1.3	.46	.55	929	655.3	51.5	31.1	745
05.5	2.29	-1.03	1.3	.47	.56	926	654.9	51.0	32.7	744
06.0	2.39	-1.03	1.4	.44	.53	936	654.5	50.6	34.2	753
06.5	2.45	-1.04	1.4	.42	.51	940	654.2	50.1	35.7	758
07.0	2.67	-1.04	1.6	.36	.45	961	653.9	49.7	37.2	776
07.5	2.50	-1.05	1.4	.41	.50	943	653.5	49.4	38.7	763
08.0	2.41	-1.06	1.4	.44	.54	932	653.3	49.0	40.1	756
08.5	2.42	-1.06	1.4	.44	.54	932	653.0	48.7	41.5	757
09.0	2.50	-1.07	1.4	.42	.52	939	652.8	48.4	43.0	764
38009.4	2.65	-1.07	1.6	-16.37	-16.47	954	652.6	48.2	44.1	777
09.6	2.73	-1.08	1.7	.35	.45	961	652.5	48.1	44.6	784
09.8	2.99	-1.08	1.9	.29	.38	982	652.4	48.0	45.1	802
10.0	2.94	-1.08	1.9	.30	.40	978	652.3	48.0	45.7	799
10.2	2.77	-1.08	1.7	.34	.44	963	652.2	47.9	46.2	788
10.4	2.77	-1.08	1.7	.34	.44	963	652.1	47.8	46.7	788
38010.5	2.75	-1.09	1.7	-16.35	-16.45	961	652.1	47.8	47.0	787
11.0	2.64	-1.09	1.5	.38	.49	949	651.9	47.6	48.3	779
11.5	2.60	-1.10	1.5	.40	.50	944	651.7	47.6	49.5	777
12.0	2.59	-1.10	1.5	.40	.51	942	651.5	47.5	50.7	776
12.5	2.52	-1.10	1.4	.43	.53	934	651.3	47.5	51.9	771
13.0	2.48	-1.10	1.4	.44	.55	929	651.1	47.6	53.0	769
13.5	2.40	-1.10	1.3	.47	.58	919	650.9	47.7	54.1	763

Table 3 (Continued)

MJD	$-10^6\dot{P}$	$10^6\dot{P}_R$	$-10^6\dot{P}_A$	$\log \rho_\pi$ (g/cm^3)	$\log \rho_s$ (g/cm^3)	T_π (°K)	z (km)	$\alpha_\pi - \alpha_\odot$ (deg.)	$\delta_\pi - \delta_\odot$ (deg.)	T_N
38014.0	2.27	-1.10	1.2	-16.52	-16.63	903	650.7	47.9	55.1	751
14.5	2.21	-1.10	1.1	.55	.65	895	650.5	48.1	56.0	745
15.0	2.04	-1.10	0.9	.63	.73	869	650.3	48.4	56.9	725
38015.4	2.32	-1.09	1.2	-16.50	-16.61	908	650.1	48.6	57.6	759
15.6	2.71	-1.09	1.6	.37	.48	951	650.0	48.8	57.9	795
15.8	2.81	-1.09	1.7	.34	.45	960	649.9	48.9	58.3	803
16.0	3.01	-1.09	1.9	.29	.40	977	649.8	49.1	58.6	818
16.2	2.99	-1.08	1.9	.29	.41	975	649.7	49.2	58.9	817
16.4	2.87	-1.08	1.8	.32	.44	965	649.6	49.4	59.1	809
16.6	2.76	-1.08	1.7	.35	.46	956	649.5	49.6	59.4	802
16.8	2.79	-1.07	1.7	.34	.46	959	649.4	49.8	59.7	805
17.0	2.89	-1.07	1.8	.31	.43	967	649.3	50.0	59.9	813
17.2	2.85	-1.06	1.8	.32	.44	964	649.2	50.2	60.2	811
17.4	2.62	-1.05	1.6	.39	.50	943	649.1	50.4	60.4	793
17.6	2.60	-1.05	1.5	.39	.51	942	649.0	50.6	60.6	793
17.8	2.50	-1.04	1.4	.42	.37	930	648.9	50.8	60.8	783
38018.0	2.44	-1.04	1.4	-16.44	-16.39	924	648.7	51.0	61.0	779
18.5	2.45	-1.02	1.4	.43	.38	926	648.5	51.6	61.4	781
19.0	2.45	-1.01	1.4	.43	.38	928	648.2	52.2	61.7	783
19.5	2.34	-0.99	1.3	.46	.41	917	647.8	52.9	62.0	775
20.0	2.19	-0.97	1.2	.50	.46	902	647.5	53.6	62.2	762
20.5	2.04	-0.95	1.1	.56	.52	884	647.2	54.2	62.3	748
21.0	1.95	-0.93	1.0	.59	.55	873	646.8	54.9	62.3	739
21.5	1.90	-0.90	1.0	.60	.56	870	646.4	55.6	62.2	736
22.0	1.84	-0.88	1.0	.62	.59	863	646.0	56.3	62.1	731
22.5	1.74	-0.84	0.9	.65	.62	853	645.6	56.9	61.8	722
23.0	1.66	-0.76	0.9	.65	.62	852	645.2	57.5	61.5	721
23.5	1.61	-0.64	1.0	.62	.59	861	644.7	58.1	61.1	729
38024.0	1.60	-0.50	1.1	-16.55	-16.53	881	644.3	58.7	60.7	745
24.2	1.62	-0.45	1.2	.52	.50	889	644.1	58.9	60.4	752
24.4	1.72	-0.40	1.3	.46	.44	908	643.9	59.1	60.2	768
24.6	1.76	-0.36	1.4	.43	.41	917	643.7	59.3	60.0	775
24.8	1.66	-0.31	1.3	.45	.43	910	643.5	59.5	59.7	769
38025.0	1.54	-0.27	1.3	-16.48	-16.46	902	643.3	59.7	59.5	761
25.5	1.28	-0.17	1.1	.55	.53	879	642.8	60.2	58.8	742
26.0	0.92	-0.09	0.8	.69	.67	837	642.4	60.6	58.0	705
26.5	0.74	-0.02	0.7	.76	.75	814	641.9	60.9	57.2	685
27.0	0.84	0.01	0.8	.67	.66	839	641.4	61.2	56.3	705
27.5	0.82	0.02	0.8	.68	.67	837	640.9	61.4	55.4	702
28.0	0.75	0.02	0.8	.72	.72	823	640.4	61.6	54.4	689
28.5	0.76	0.02	0.8	.71	.71	824	639.9	61.7	53.4	689
29.0	0.82	0.02	0.8	.67	.68	835	639.4	61.8	52.3	697
29.5	0.92	0.02	0.9	.61	.62	853	639.0	61.8	51.1	711
30.0	1.02	0.03	1.0	.56	.57	868	638.5	61.8	49.9	721
30.5	1.05	0.03	1.1	.55	.56	871	638.1	61.7	48.7	723
31.0	0.90	0.03	0.9	.62	.63	849	637.6	61.6	47.4	703
31.5	0.84	0.03	0.9	.65	.67	839	637.2	61.5	46.1	692
32.0	0.87	0.03	0.9	.63	.65	843	636.8	61.3	44.8	695
32.5	0.89	0.03	0.9	.62	.64	848	636.4	61.0	43.4	697
33.0	0.94	0.04	1.0	.59	.61	855	636.1	60.7	42.0	701
33.5	1.02	0.04	1.1	.55	.57	867	635.7	60.4	40.5	709
34.0	1.10	0.04	1.1	.51	.54	877	635.4	60.1	39.1	716
34.5	1.09	0.04	1.1	.52	.54	876	635.1	59.7	37.6	713
35.0	1.09	0.04	1.1	.51	.54	875	634.8	59.4	36.1	711
35.5	1.05	0.04	1.1	.53	.56	870	634.6	58.9	34.6	705
36.0	1.06	0.04	1.1	.52	.55	872	634.4	58.5	33.1	705

Table 3 (Continued)

MJD	$-10^6\dot{P}$	$10^6\dot{P}_R$	$-10^6\dot{P}_A$	$\log \rho_\pi$ (g/cm^3)	$\log \rho_s$ (g/cm^3)	T_π (°K)	z (km)	$\alpha_\pi - \alpha_\odot$ (deg.)	$\delta_\pi - \delta_\odot$ (deg.)	T_N
38036.5	1.09	0.04	1.1	-16.51	-16.54	876	634.2	58.1	31.5	707
37.0	1.12	0.04	1.2	.49	.53	880	634.0	57.6	30.0	708
37.5	1.14	0.04	1.2	.49	.52	882	633.8	57.1	28.4	709
38.0	1.08	0.05	1.1	.51	.55	875	633.7	56.6	26.8	701
38.5	1.06	0.05	1.1	.52	.55	872	633.6	56.1	25.2	697
39.0	1.09	0.05	1.1	.50	.54	876	633.5	55.6	23.6	699
39.5	1.13	0.05	1.2	.48	.52	883	633.5	55.1	22.0	703
40.0	1.06	0.06	1.1	.51	.55	874	633.5	54.6	20.4	695
40.5	1.20	-0.01	1.2	.49	.52	882	633.5	54.1	18.8	700
41.0	1.49	-0.18	1.3	.44	.47	897	633.6	53.6	17.3	711
41.5	1.57	-0.28	1.3	.44	.48	895	633.6	53.1	15.7	708
42.0	1.75	-0.34	1.4	.40	.44	908	633.7	52.7	14.1	718
38042.2	1.90	-0.36	1.5	-16.36	-16.40	921	633.8	52.5	13.4	728
42.4	1.95	-0.38	1.6	.35	.39	924	633.8	52.3	12.8	730
42.6	2.07	-0.40	1.7	.32	.36	934	633.9	52.1	12.2	737
42.8	2.10	-0.42	1.7	.32	.36	935	634.0	51.9	11.5	737
43.0	2.16	-0.43	1.7	.31	.34	938	634.0	51.8	10.9	740
43.2	2.17	-0.45	1.7	.31	.34	938	634.1	51.6	10.3	740
43.4	2.22	-0.46	1.8	.30	.33	942	634.1	51.4	9.7	742
43.6	2.20	-0.48	1.7	.31	.34	938	634.2	51.3	9.0	739
43.8	2.15	-0.49	1.7	.32	.36	933	634.3	51.1	8.4	735
44.0	2.23	-0.50	1.7	.31	.34	940	634.3	51.0	7.8	740
44.2	2.25	-0.51	1.7	.31	.34	940	634.4	50.8	7.2	739
44.4	2.19	-0.53	1.7	.32	.36	934	634.5	50.7	6.6	735
44.6	2.17	-0.54	1.6	.33	.37	931	634.5	50.5	6.0	732
44.8	2.15	-0.55	1.6	.34	.37	928	634.6	50.4	5.3	730
45.0	2.11	-0.56	1.5	.36	.39	924	634.7	50.2	4.7	726
45.2	2.05	-0.57	1.5	.38	.41	917	634.7	50.1	4.1	721
45.4	2.06	-0.58	1.5	.38	.41	917	634.8	50.0	3.5	720
45.6	2.09	-0.59	1.5	.37	.40	919	634.9	49.9	2.9	722
45.8	2.08	-0.60	1.5	.38	.41	917	635.0	49.8	2.3	720
38046.0	2.08	-0.61	1.5	-16.38	-16.41	916	635.0	49.6	1.7	720
46.5	2.02	-0.64	1.4	.41	.44	907	635.2	49.4	0.3	712
47.0	1.98	-0.66	1.3	.44	.46	901	635.4	49.2	-1.2	707
47.5	1.99	-0.68	1.3	.44	.47	900	635.6	49.0	-2.6	706
48.0	1.98	-0.70	1.3	.45	.48	896	635.7	48.9	-3.9	704
48.5	2.03	-0.72	1.3	.44	.47	900	635.9	48.9	-5.3	707
49.0	2.00	-0.74	1.3	.46	.48	894	636.0	48.8	-6.6	702
49.5	1.94	-0.76	1.2	.49	.51	885	636.2	48.9	-7.9	695
50.0	1.88	-0.78	1.1	.53	.55	874	636.3	49.0	-9.1	687
50.5	1.81	-0.80	1.0	.57	.59	862	636.4	49.1	-10.3	678
51.0	1.74	-0.81	0.9	.62	.64	848	636.5	49.3	-11.4	667
51.5	1.72	-0.83	0.9	.63	.65	843	636.6	49.5	-12.5	664
52.0	1.83	-0.85	1.0	.59	.60	857	636.7	49.8	-13.6	676
52.5	1.89	-0.86	1.0	.56	.58	864	636.7	50.2	-14.5	682
53.0	1.90	-0.88	1.0	.56	.58	864	636.8	50.6	-15.5	682
53.5	1.91	-0.89	1.0	.57	.59	863	636.7	51.1	-16.3	682
54.0	1.98	-0.91	1.1	.54	.56	870	636.7	51.6	-17.1	687
54.5	2.18	-0.92	1.3	.47	.49	893	636.6	52.2	-17.8	707
55.0	2.07	-0.93	1.1	.51	.54	878	636.5	52.8	-18.5	696
55.5	1.88	-0.94	0.9	.61	.63	850	636.4	53.5	-19.0	673
56.0	1.81	-0.95	0.9	.65	.67	836	636.2	54.1	-19.5	663
56.5	1.83	-0.96	0.9	.65	.67	837	636.0	54.9	-19.9	665
57.0	1.84	-0.97	0.9	.65	.67	837	635.8	55.6	-20.3	665
57.5	1.84	-0.98	0.9	.65	.62	836	635.5	56.3	-20.5	665
58.0	1.91	-0.99	0.9	.62	.59	844	635.2	57.1	-20.7	672
58.5	2.15	-0.99	1.2	.51	.48	877	634.8	57.9	-20.8	699
59.0	2.16	-1.00	1.2	.51	.48	877	634.4	58.6	-20.8	698

Table 3 (Continued)

MJD	$-10^6\dot{P}$	$10^6\dot{P}_R$	$-10^6\dot{P}_A$	$\log \rho_\pi$ (g/cm^3)	$\log \rho_s$ (g/cm^3)	T_π (°K)	z (km)	$a_\pi - a_\odot$ (deg.)	$\delta_\pi - \delta_\odot$ (deg.)	T_N
38077.5	2.57	-1.01	1.6	-16.34	-16.29	876	608.0	59.1	15.2	697
78.0	2.58	-1.01	1.6	.34	.29	876	607.5	58.7	16.6	697
78.5	2.57	-1.02	1.5	.35	.30	873	607.0	58.3	17.9	695
79.0	2.52	-1.03	1.5	.37	.32	867	606.6	57.8	19.2	691
79.5	2.60	-1.03	1.6	.34	.30	873	606.2	57.4	20.6	696
80.0	2.66	-1.04	1.6	.33	.29	877	605.8	57.0	21.9	700
80.5	2.73	-1.05	1.7	.31	.28	881	605.5	56.7	23.2	704
81.0	2.78	-1.05	1.7	.30	.26	885	605.2	56.3	24.4	707
81.5	2.81	-1.06	1.7	.29	.26	885	604.9	56.0	25.7	708
82.0	2.81	-1.07	1.7	.30	.27	884	604.6	55.7	27.0	708
82.5	2.83	-1.08	1.7	.29	.27	884	604.3	55.4	28.2	709
83.0	2.78	-1.08	1.7	.31	.28	878	604.0	55.2	29.4	705
83.5	2.75	-1.09	1.7	.32	.30	875	603.8	55.0	30.6	703
84.0	2.73	-1.10	1.6	.33	.31	872	603.5	54.9	31.7	702
84.5	2.71	-1.11	1.6	.34	.32	869	603.3	54.7	32.8	700
85.0	2.69	-1.11	1.6	.35	.33	866	603.1	54.7	33.9	698
85.5	2.70	-1.12	1.6	.35	.33	866	602.9	54.6	35.0	699
86.0	2.75	-1.13	1.6	.33	.32	869	602.6	54.7	36.0	703
86.5	2.72	-1.13	1.6	.34	.33	866	602.4	54.7	37.0	701
87.0	2.66	-1.14	1.5	.37	.35	859	602.2	54.8	37.9	696
87.5	2.62	-1.14	1.5	.38	.37	855	602.0	55.0	38.8	694
88.0	2.54	-1.15	1.4	.41	.40	845	601.8	55.2	39.6	688
38088.8	2.42	-1.16	1.3	-16.45	-16.44	832	601.5	55.7	40.8	678
89.0	2.70	-1.16	1.5	.36	.35	859	601.4	55.8	41.1	701
89.2	2.79	-1.16	1.6	.33	.33	866	601.4	56.0	41.4	707
89.4	3.02	-1.16	1.9	.27	.26	884	601.3	56.2	41.7	722
89.6	3.02	-1.16	1.9	.27	.27	884	601.2	56.3	41.9	722
89.8	2.79	-1.16	1.6	.33	.33	866	601.1	56.5	42.2	707
90.0	2.79	-1.16	1.6	.34	.33	865	601.0	56.7	42.4	707
90.2	2.74	-1.16	1.6	.35	.34	861	601.0	56.9	42.6	704
38090.5	2.75	-1.16	1.6	-16.35	-16.34	862	600.8	57.2	42.9	705
91.0	2.71	-1.17	1.5	.36	.36	857	600.6	57.7	43.4	702
91.5	2.67	-1.17	1.5	.37	.37	853	600.4	58.3	43.8	699
92.0	2.66	-1.17	1.5	.38	.38	851	600.1	58.9	44.2	699
92.5	2.65	-1.17	1.5	.38	.38	850	599.8	59.6	44.4	698
93.0	2.64	-1.17	1.5	.38	.39	848	599.5	60.3	44.6	698
93.5	2.67	-1.17	1.5	.37	.38	850	599.1	61.1	44.7	700
94.0	2.73	-1.16	1.6	.35	.36	856	598.8	61.8	44.7	705
94.5	2.73	-1.16	1.6	.35	.36	855	598.4	62.6	44.7	705
95.0	2.82	-1.16	1.7	.33	.34	862	597.9	63.4	44.5	711
95.5	2.72	-1.15	1.6	.35	.37	854	597.5	64.2	44.3	704
38095.6	2.59	-1.15	1.4	-16.39	-16.41	842	597.4	64.3	44.2	694
95.8	2.69	-1.15	1.5	.36	.38	851	597.2	64.6	44.1	702
96.0	3.10	-1.15	1.9	.25	.27	883	597.0	64.9	44.0	728
96.2	3.83	-1.14	2.7	.10	.13	928	596.8	65.2	43.8	765
96.4	3.95	-1.14	2.8	.08	.11	934	596.6	65.6	43.7	770
96.6	3.81	-1.14	2.7	.11	.13	926	596.4	65.9	43.5	764
96.8	3.62	-1.14	2.5	.14	.16	915	596.2	66.2	43.3	755
97.0	3.54	-1.13	2.4	.15	.18	910	596.0	66.4	43.1	751
97.2	3.59	-1.13	2.5	.14	.17	913	595.7	66.7	42.9	754
97.4	3.53	-1.13	2.4	.15	.18	910	595.6	67.0	42.7	751
97.6	3.48	-1.12	2.4	.16	.19	907	595.4	67.3	42.4	748
97.8	3.42	-1.12	2.3	.17	.20	903	595.2	67.6	42.2	745
98.0	3.45	-1.12	2.3	.16	.20	905	595.0	67.8	41.9	747
98.2	3.51	-1.11	2.4	.15	.19	908	594.8	68.1	41.7	749
98.4	3.56	-1.11	2.4	.14	.18	911	594.6	68.4	41.4	751
98.6	3.57	-1.11	2.5	.14	.18	912	594.4	68.6	41.1	752

Table 3 (Continued)

MJD	$-10^6\dot{P}$	$10^6\dot{P}_R$	$-10^6\dot{P}_A$	$\log \rho_\pi$ (g/cm^3)	$\log \rho_s$ (g/cm^3)	T_π (°K)	z (km)	$\alpha_\pi - \alpha_\odot$ (deg.)	$\delta_\pi - \delta_\odot$ (deg.)	T_N
38098.8	3.60	-1.10	2.5	-16.13	-16.17	913	594.2	68.9	40.8	753
99.0	3.79	-1.10	2.7	.10	.14	923	594.0	69.1	40.5	761
99.2	3.59	-1.09	2.5	.13	.18	912	593.8	69.3	40.1	751
99.4	3.37	-1.09	2.3	.17	.22	899	593.6	69.5	39.8	741
99.6	3.31	-1.09	2.2	.18	.23	896	593.4	69.8	39.4	738
99.8	3.20	-1.08	2.1	.21	.25	888	593.2	70.0	39.1	732
38100.0	3.13	-1.08	2.0	.22	.27	883	592.9	70.2	38.7	727
00.2	3.08	-1.07	2.0	.23	.28	880	592.7	70.4	38.3	724
00.4	3.04	-1.07	2.0	.24	.29	877	592.5	70.5	37.9	722
38100.5	3.02	-1.06	2.0	-16.24	-16.29	876	592.4	70.6	37.7	721
01.0	2.94	-1.05	1.9	.26	.31	870	591.8	71.0	36.7	715
01.5	2.91	-1.04	1.9	.26	.32	868	591.3	71.4	35.6	713
02.0	2.84	-1.02	1.8	.27	.33	864	590.7	71.7	34.4	708
02.5	2.83	-1.01	1.8	.27	.34	863	590.1	71.9	33.2	707
03.0	2.82	-1.00	1.8	.27	.34	862	589.5	72.1	32.0	705
03.5	2.81	-0.98	1.8	.27	.34	862	588.9	72.3	30.7	704
04.0	2.81	-0.97	1.8	.26	.34	862	588.3	72.4	29.3	703
04.5	2.82	-0.96	1.9	.26	.34	862	587.7	72.4	27.9	703
05.0	2.86	-0.94	1.9	.24	.33	865	587.1	72.4	26.5	704
05.5	2.92	-0.93	2.0	.23	.32	869	586.5	72.3	25.0	707
06.0	3.08	-0.92	2.2	.19	.28	880	585.9	72.2	23.5	715
06.5	3.19	-0.91	2.3	.16	.26	887	585.4	72.1	22.0	719
07.0	3.34	-0.90	2.4	.13	.23	895	584.8	71.9	20.5	725
07.5	3.40	-0.90	2.5	.12	.22	898	584.3	71.7	18.9	726
08.0	3.32	-0.89	2.4	.13	.24	893	583.8	71.5	17.3	721
08.5	3.22	-0.89	2.3	.15	.26	887	583.3	71.2	15.7	715
09.0	3.12	-0.89	2.2	.17	.28	880	582.9	70.9	14.0	709
09.5	3.07	-0.89	2.2	.18	.29	876	582.5	70.6	12.4	705
10.0	2.92	-0.89	2.0	.21	.33	866	582.1	70.3	10.7	696
10.5	2.82	-0.90	1.9	.23	.35	858	581.7	69.9	9.0	689
11.0	3.01	-0.90	2.1	.19	.31	870	581.4	69.5	7.3	698
11.5	3.25	-0.91	2.3	.14	.27	884	581.1	69.1	5.6	708
12.0	3.36	-0.92	2.4	.12	.25	889	580.9	68.7	3.9	712
12.5	3.32	-0.92	2.4	.13	.26	887	580.6	68.3	2.2	709
13.0	3.30	-0.93	2.4	.14	.26	884	580.4	67.9	0.4	707
13.5	3.29	-0.95	2.3	.14	.27	883	580.2	67.5	-1.3	706
14.0	3.26	-0.96	2.3	.15	.28	880	580.1	67.1	-3.0	703
14.5	3.22	-0.97	2.2	.16	.29	876	580.0	66.6	-4.7.	700
15.0	3.17	-0.98	2.2	.17	.30	872	579.9	66.2	-6.5	697
15.5	3.11	-0.99	2.1	.19	.32	868	579.8	65.8	-8.2	693
16.0	3.10	-1.00	2.1	.19	.33	866	579.7	65.4	-9.9	691
16.5	3.14	-1.02	2.1	.19	.32	867	579.7	65.0	-11.6	693
17.0	3.16	-1.03	2.1	.19	.32	868	579.7	64.7	-13.3	694
17.5	3.20	-1.04	2.1	.18	.32	869	579.6	64.3	-15.0	695
18.0	3.22	-1.05	2.2	.18	.15	869	579.6	64.0	-16.6	695
18.5	3.23	-1.07	2.2	.18	.15	868	579.6	63.7	-18.3	695
19.0	3.25	-1.08	2.2	.18	.15	868	579.6	63.4	-19.9	696
19.5	3.27	-1.09	2.2	.18	.15	869	579.6	63.2	-21.5	697
20.0	3.33	-1.11	2.2	.17	.14	871	579.7	63.0	-23.1	700
20.5	3.38	-1.12	2.3	.17	.13	873	579.7	62.8	-24.7	702
21.0	3.41	-1.13	2.3	.16	.13	874	579.7	62.7	-26.2	704
21.5	3.30	-1.15	2.1	.19	.16	866	579.8	62.6	-27.8	698
22.0	3.12	-1.16	2.0	.23	.20	853	579.9	62.5	-29.2	689
22.5	3.05	-1.17	1.9	.25	.22	848	579.9	62.5	-30.7	686
23.0	3.10	-1.18	1.9	.24	.21	851	580.0	62.6	-32.1	690
38123.2	3.11	-1.18	1.9	-16.24	-16.21	851	580.0	62.6	-32.7	690
23.4	3.28	-1.18	2.1	.21	.17	862	580.0	62.6	-33.2	699
23.6	3.31	-1.19	2.1	.20	.16	864	580.0	62.7	-33.7	702

Table 3 (Continued)

MJD	$-10^6\dot{P}$	$10^6\dot{P}_R$	$-10^6\dot{P}_A$	$\log \rho_\pi$ (g/cm^3)	$\log \rho_s$ (g/cm^3)	T_π (°K)	z (km)	$\alpha_\pi - \alpha_\odot$ (deg.)	$\delta_\pi - \delta_\odot$ (deg.)	T_N
38123.8	3.58	-1.19	2.4	-16.15	-16.11	880	580.0	62.7	-34.3	715
24.0	4.02	-1.19	2.8	.07	.04	903	580.1	62.8	-34.8	734
24.2	4.22	-1.20	3.0	.04	.01	912	580.1	62.9	-35.3	742
24.4	4.11	-1.20	2.9	.06	.02	907	580.1	62.9	-35.8	739
24.6	3.93	-1.20	2.7	.09	.05	898	580.1	63.0	-36.3	732
24.8	3.83	-1.21	2.6	.11	.07	892	580.1	63.1	-36.8	728
25.0	3.75	-1.21	2.5	.12	.08	888	580.1	63.2	-37.3	725
25.2	3.76	-1.21	2.5	.12	.08	888	580.1	63.4	-37.8	725
25.4	3.76	-1.22	2.5	.12	.09	888	580.1	63.5	-38.2	726
25.6	3.75	-1.22	2.5	.12	.09	887	580.1	63.6	-38.7	726
25.8	3.67	-1.22	2.4	.14	.10	882	580.1	63.8	-39.2	722
26.0	3.57	-1.22	2.3	.16	.12	877	580.1	63.9	-39.6	718
26.2	3.54	-1.23	2.3	.16	.13	875	580.1	64.1	-40.0	717
26.4	3.50	-1.23	2.3	.17	.14	872	580.1	64.2	-40.5	715
38126.5	3.49	-1.23	2.3	-16.17	-16.14	871	580.1	64.3	-40.7	715
27.0	3.44	-1.23	2.2	.19	.15	867	580.0	64.8	-41.7	713
27.5	3.32	-1.24	2.1	.21	.18	859	579.9	65.3	-42.6	708
28.0	3.28	-1.24	2.0	.22	.19	856	579.8	65.9	-43.5	707
28.5	3.29	-1.24	2.0	.22	.19	857	579.6	66.5	-44.3	708
29.0	3.30	-1.24	2.1	.22	.19	857	579.4	67.2	-45.0	710
29.5	3.24	-1.24	2.0	.23	.20	852	579.2	67.9	-45.6	707
30.0	3.20	-1.24	2.0	.24	.22	849	578.9	68.6	-46.2	706
30.5	3.20	-1.24	1.9	.24	.22	848	578.6	69.4	-46.7	706
31.0	3.33	-1.24	2.1	.21	.19	856	578.3	70.2	-47.1	714
31.5	3.51	-1.24	2.3	.17	.15	867	577.9	71.0	-47.4	723
32.0	3.69	-1.24	2.5	.14	.12	877	577.5	71.8	-47.6	733
32.5	3.89	-1.23	2.7	.10	.09	887	577.1	72.6	-47.7	742
38132.6	3.93	-1.23	2.7	-16.09	-16.08	889	577.0	72.8	-47.8	744
32.8	4.06	-1.23	2.8	.07	.06	896	576.8	73.1	-47.8	749
33.0	4.12	-1.22	2.9	.06	.05	898	576.6	73.4	-47.8	752
33.2	4.47	-1.22	3.2	.01	.00	914	576.4	73.7	-47.8	765
33.4	4.31	-1.22	3.1	.03	.03	906	576.2	74.0	-47.8	759
33.6	4.21	-1.21	3.0	.05	.04	902	576.0	74.4	-47.8	756
33.8	4.07	-1.21	2.9	.07	.06	895	575.7	74.7	-47.7	750
34.0	4.07	-1.20	2.9	.07	.06	895	575.5	75.0	-47.7	750
34.2	4.16	-1.20	3.0	.05	.05	899	575.3	75.3	-47.6	754
34.4	4.64	-1.20	3.4	-15.98	-15.98	920	575.1	75.6	-47.5	772
34.6	4.35	-1.19	3.2	-16.02	-16.02	907	574.8	75.8	-47.4	761
34.8	3.69	-1.19	2.5	.13	.13	874	574.6	76.1	-47.3	734
38135.0	3.42	-1.18	2.2	-16.18	-16.18	859	574.3	76.4	-47.2	721
35.5	3.43	-1.17	2.3	.17	.18	859	573.7	77.1	-46.9	721
36.0	3.35	-1.16	2.2	.19	.20	854	573.0	77.7	-46.5	717
36.5	3.31	-1.14	2.2	.19	.21	851	572.3	78.3	-46.0	715
37.0	3.34	-1.13	2.2	.18	.20	853	571.6	78.8	-45.4	716
37.5	3.38	-1.11	2.3	.17	.01	856	570.8	79.3	-44.8	718
38.0	3.54	-1.09	2.4	.13	-15.98	864	570.0	79.7	-44.1	725
38.5	3.65	-1.07	2.6	.11	.96	870	569.3	80.0	-43.4	730
39.0	3.59	-1.05	2.5	.11	.98	867	568.5	80.3	-42.6	726
39.5	3.39	-1.02	2.4	.14	-16.01	856	567.7	80.6	-41.7	717
40.0	3.19	-1.00	2.2	.18	.05	844	566.9	80.8	-40.8	706
38140.2	3.11	-0.99	2.1	-16.19	-16.07	840	566.5	80.8	-40.4	703
40.4	3.13	-0.98	2.1	.18	.06	841	566.2	80.9	-40.0	703
40.6	3.10	-0.96	2.1	.19	.07	839	565.9	80.9	-39.6	701
40.8	3.03	-0.95	2.1	.20	.08	835	565.6	80.9	-39.2	698
41.0	3.01	-0.94	2.1	.20	.09	834	565.2	81.0	-38.8	697
41.2	2.97	-0.93	2.0	.21	.10	832	564.9	81.0	-38.4	694

Table 3 (Continued)

MJD	$-10^6\dot{P}$	$10^6\dot{P}_R$	$-10^6\dot{P}_A$	$\log \rho_\pi$ (g/cm^3)	$\log \rho_s$ (g/cm^3)	T_π (°K)	z (km)	$\alpha_\pi - \alpha_\odot$ (deg.)	$\delta_\pi - \delta_\odot$ (deg.)	T_N
38141.4	2.89	-0.91	2.0	-16.22	-16.11	827	564.6	81.0	-38.0	690
41.6	2.96	-0.90	2.1	.20	.09	832	564.3	81.0	-37.6	694
41.8	2.95	-0.88	2.1	.20	.09	832	564.0	81.0	-37.1	693
42.0	2.95	-0.87	2.1	.19	.09	833	563.7	81.0	-36.7	694
42.2	3.17	-0.85	2.3	.14	.05	846	563.3	81.0	-36.3	704
42.4	3.23	-0.84	2.4	.13	.03	849	563.0	80.9	-35.8	707
42.6	3.32	-0.82	2.5	.11	.02	855	562.7	80.9	-35.4	711
38143.0	2.98	-0.79	2.2	-16.17	-16.08	836	562.1	80.8	-34.4	695
43.5	2.59	-0.74	1.8	.25	.16	813	561.3	80.7	-33.3	674
44.0	2.51	-0.69	1.8	.25	.17	810	560.6	80.5	-32.1	671
44.5	2.47	-0.63	1.8	.25	.17	810	559.8	80.2	-30.8	670
45.0	2.44	-0.56	1.9	.23	.17	812	559.1	80.0	-29.6	670
45.5	2.58	-0.49	2.1	.18	.12	824	558.3	79.7	-28.3	679
46.0	2.64	-0.42	2.2	.16	.10	831	557.6	79.4	-27.0	683
38146.2	2.67	-0.39	2.3	-16.14	-16.09	834	557.4	79.2	-26.5	685
46.4	2.89	-0.35	2.5	.09	.04	847	557.1	79.1	-26.0	696
46.6	3.04	-0.32	2.7	.06	.01	856	556.8	79.0	-25.4	703
46.8	3.21	-0.28	2.9	.03	-15.98	865	556.5	78.8	-24.9	710
47.0	3.06	-0.25	2.8	.05	-16.00	859	556.3	78.7	-24.4	704
47.2	2.81	-0.21	2.6	.08	.04	848	556.0	78.5	-23.8	695
38147.5	2.70	-0.15	2.5	-16.09	-16.05	845	555.6	78.3	-23.0	691
48.0	2.65	-0.06	2.6	.08	.04	847	555.0	77.9	-21.7	692
48.5	2.43	0.03	2.5	.11	.07	838	554.4	77.4	-20.3	684
49.0	2.51	0.03	2.5	.09	.06	841	553.8	77.0	-18.9	685
49.5	2.55	0.03	2.6	.08	.06	842	553.3	76.6	-17.6	685
38149.6	2.48	0.03	2.5	-16.09	-16.07	839	553.2	76.5	-17.3	682
49.8	4.02	0.03	4.0	-15.88	-15.86	903	553.0	76.3	-16.7	734
50.0	4.59	0.03	4.6	.82	.80	921	552.8	76.1	-16.2	748
50.2	4.76	0.03	4.8	.81	.79	926	552.6	76.0	-15.6	752
50.4	5.90	0.03	5.9	.72	.70	957	552.4	75.8	-15.1	776
50.6	5.00	0.00	5.0	.79	.77	931	552.2	75.6	-14.5	755
50.8	4.49	-0.05	4.4	.84	.83	914	552.0	75.4	-14.0	741
51.0	4.33	-0.09	4.2	.86	.85	907	551.8	75.2	-13.4	734
51.2	4.14	-0.13	4.0	.89	.87	899	551.6	75.1	-12.9	727
51.4	4.16	-0.17	4.0	.89	.88	898	551.5	74.9	-12.3	726
51.6	4.21	-0.20	4.0	.88	.88	898	551.3	74.7	-11.8	726
51.8	4.23	-0.24	4.0	.89	.88	897	551.1	74.5	-11.2	725
52.0	4.27	-0.27	4.0	.89	.88	897	551.0	74.4	-10.7	724
52.2	4.29	-0.31	4.0	.89	.88	896	550.8	74.2	-10.1	724
52.4	4.20	-0.34	3.9	.90	.90	891	550.7	74.0	-9.6	719
52.6	4.33	-0.37	3.9	.89	.89	894	550.5	73.8	-9.0	721
52.8	4.42	-0.40	4.0	.88	.88	896	550.4	73.7	-8.5	723
53.0	4.48	-0.43	4.0	.88	.88	897	550.2	73.5	-7.9	723
53.2	4.60	-0.45	4.1	.87	.87	900	550.1	73.3	-7.4	725
53.4	4.86	-0.47	4.4	.85	.85	908	550.0	73.2	-6.8	731
53.6	5.10	-0.52	4.6	.83	.83	913	549.8	73.0	-6.3	735
53.8	5.09	-0.53	4.6	.83	.83	913	549.7	72.9	-5.7	734
38154.0	4.94	-0.55	4.4	-15.85	-15.85	907	549.6	72.7	-5.2	729
54.5	4.96	-0.60	4.4	.85	.85	905	549.3	72.3	-3.9	727
55.0	4.86	-0.65	4.2	.86	.87	900	549.0	72.0	-2.5	723
55.5	4.86	-0.69	4.2	.87	.88	897	548.8	71.7	-1.2	720
56.0	4.94	-0.73	4.2	.87	.88	898	548.5	71.4	0.1	720
56.5	5.08	-0.77	4.3	.85	.87	901	548.3	71.1	1.4	722
57.0	5.24	-0.80	4.4	.84	.86	904	548.1	70.9	2.6	725
57.5	5.38	-0.83	4.5	.83	.85	907	547.9	70.7	3.8	727

Table 3 (Continued)

MJD	$-10^6\dot{P}$	$10^6\dot{P}_R$	$-10^6\dot{P}_A$	$\log \rho_\pi$ (g/cm^3)	$\log \rho_s$ (g/cm^3)	T_π (°K)	z (km)	$\alpha_\pi - \alpha_\odot$ (deg.)	$\delta_\pi - \delta_\odot$ (deg.)	T_N
38158.0	5.49	-0.86	4.6	-15.82	-15.84	909	547.8	70.5	5.0	729
58.5	5.95	-0.89	5.1	.79	.80	921	547.7	70.4	6.2	738
59.0	6.22	-0.92	5.3	.77	.78	928	547.6	70.3	7.4	743
59.5	6.27	-0.94	5.3	.77	.78	928	547.5	70.3	8.5	744
60.0	6.18	-0.97	5.2	.78	.79	924	547.3	70.3	9.5	741
60.5	6.12	-0.99	5.1	.78	.80	922	547.2	70.3	10.6	739
61.0	6.11	-1.01	5.1	.79	.81	920	547.1	70.5	11.6	738
38161.2	6.10	-1.00	5.1	-15.79	-15.81	920	547.1	70.5	11.9	738
61.4	6.12	-1.03	5.1	.79	.81	920	547.0	70.6	12.3	738
61.6	6.10	-1.04	5.1	.79	.81	919	547.0	70.7	12.7	737
61.8	6.10	-1.04	5.0	.79	.81	918	546.9	70.8	13.0	737
62.0	6.11	-1.05	5.1	.79	.81	918	546.9	70.9	13.4	737
62.2	6.14	-1.06	5.1	.79	.81	919	546.8	71.0	13.7	738
62.4	6.69	-1.07	5.6	.75	.77	933	546.8	71.1	14.1	750
62.6	6.71	-1.07	5.6	.74	.77	934	546.7	71.2	14.4	750
62.8	6.25	-1.08	5.2	.78	.81	921	546.6	71.3	14.7	740
63.0	6.01	-1.09	4.9	.80	.83	913	546.6	71.5	15.0	734
38163.5	5.88	-1.10	4.8	-15.82	-15.84	909	546.4	71.9	15.8	731
64.0	5.70	-1.12	4.6	.84	.86	902	546.2	72.3	16.4	726
64.5	5.18	-1.13	4.0	.89	.92	884	546.0	72.8	17.0	712
65.0	4.90	-1.15	3.8	.92	.95	874	545.8	73.3	17.6	704
65.5	4.83	-1.16	3.7	.93	.97	870	545.5	73.9	18.0	702
66.0	4.82	-1.17	3.6	.94	.97	868	545.2	74.5	18.4	701
66.5	4.70	-1.18	3.5	.95	.99	862	544.9	75.2	18.7	697
67.0	4.69	-1.19	3.5	.96	-16.00	861	544.6	75.9	19.0	696
67.5	4.75	-1.20	3.5	.95	-15.99	862	544.3	76.6	19.1	698
68.0	4.36	-1.21	3.1	-16.00	-16.05	846	543.9	77.4	19.2	685
68.5	4.59	-1.22	3.4	-15.97	.02	854	543.5	78.1	19.2	693
38168.8	5.27	-1.23	4.0	-15.89	-15.94	878	543.3	78.6	19.2	712
69.0	5.68	-1.23	4.4	.85	.90	891	543.1	78.9	19.1	723
69.2	5.53	-1.23	4.3	.86	.92	885	543.0	79.2	19.1	719
69.4	4.87	-1.24	3.6	.94	.99	862	542.8	79.5	19.0	700
69.6	4.80	-1.24	3.6	.95	-16.00	859	542.6	79.8	18.9	698
69.8	4.74	-1.24	3.5	.95	.01	857	542.4	80.1	18.8	696
70.0	4.70	-1.24	3.5	.96	.02	855	542.3	80.4	18.7	695
70.2	4.65	-1.25	3.4	.97	.02	852	542.1	80.7	18.6	693
70.4	4.61	-1.25	3.4	.97	.03	850	541.9	81.0	18.4	692
38170.5	4.39	-1.25	3.1	-16.00	-16.06	841	541.8	81.1	18.4	684
71.0	3.96	-1.26	2.7	.07	.13	821	541.3	81.8	18.0	669
71.5	3.89	-1.26	2.6	.08	.15	817	540.8	82.5	17.5	665
72.0	3.83	-1.26	2.6	.09	.16	813	540.3	83.2	16.9	662
72.5	3.74	-1.27	2.5	.11	.18	807	539.8	83.8	16.3	658
73.0	3.65	-1.27	2.4	.12	.20	801	539.2	84.3	15.5	654
73.5	3.64	-1.27	2.4	.13	.21	800	538.7	84.8	14.8	653
74.0	3.73	-1.28	2.5	.11	.20	804	538.2	85.3	13.9	656
74.5	3.97	-1.28	2.7	.07	.16	814	537.6	85.7	13.0	665
75.0	4.12	-1.28	2.8	.04	.14	820	537.0	86.0	12.0	670
75.5	4.15	-1.28	2.9	.04	.14	820	536.4	86.3	11.0	670
76.0	4.14	-1.28	2.9	.04	.14	819	535.7	86.5	9.9	669
76.5	4.13	-1.28	2.8	.04	.15	817	535.1	86.7	8.8	667
38176.8	4.06	-1.28	2.8	-16.05	-16.16	813	534.7	86.8	8.1	665
77.0	4.42	-1.28	3.1	-15.99	.11	828	534.4	86.8	7.6	677
77.2	4.80	-1.28	3.5	.94	.06	842	534.2	86.9	7.1	688
77.4	5.21	-1.28	3.9	.89	.01	856	533.9	86.9	6.6	700
77.6	4.96	-1.28	3.7	.92	.04	847	533.7	86.9	6.1	693

Table 3 (Continued)

MJD	$-10^6\dot{P}$	$10^6\dot{P}_R$	$-10^6\dot{P}_A$	$\log \rho_\pi$ (g/cm^3)	$\log \rho_s$ (g/cm^3)	T_π (°K)	z (km)	$\alpha_\pi - \alpha_\odot$ (deg.)	$\delta_\pi - \delta_\odot$ (deg.)	T_N
38177.8	5.23	-1.28	3.9	-15.89	-16.01	856	533.4	86.9	5.6	700
78.0	5.54	-1.28	4.3	.86	-15.98	866	533.1	86.9	5.1	708
78.2	6.08	-1.28	4.8	.80	.93	881	532.9	86.9	4.6	721
78.4	5.98	-1.28	4.7	.81	.94	878	532.6	86.9	4.1	718
78.6	5.23	-1.28	3.9	.89	-16.02	854	532.4	86.9	3.5	698
78.8	5.20	-1.28	3.9	.89	.02	853	532.1	86.8	3.0	697
38179.0	5.12	-1.28	3.8	-15.90	-16.03	850	531.9	86.8	2.5	695
79.5	5.02	-1.28	3.7	.91	.05	845	531.2	86.7	1.1	691
80.0	4.92	-1.28	3.6	.92	.07	840	530.6	86.5	-0.3	687
80.5	4.92	-1.28	3.6	.92	.07	839	530.1	86.3	-1.7	686
38181.0	4.95	-1.28	3.7	-15.92	-16.07	839	529.5	86.0	-3.2	686
81.2	5.22	-1.28	3.9	.89	.04	848	529.3	85.9	-3.8	694
81.4	6.02	-1.27	4.7	.80	-15.96	873	529.1	85.8	-4.4	714
81.6	6.30	-1.27	5.0	.78	.93	880	528.9	85.7	-5.0	719
81.8	5.88	-1.27	4.6	.82	.97	868	528.7	85.6	-5.6	710
82.0	5.57	-1.27	4.3	.85	-16.01	858	528.5	85.4	-6.2	702
82.2	5.52	-1.27	4.2	.85	.01	856	528.3	85.3	-6.8	700
38182.5	5.43	-1.27	4.2	-15.86	-16.02	853	528.0	85.1	-7.7	697
83.0	5.40	-1.27	4.1	.86	.03	851	527.5	84.7	-9.2	696
83.5	5.42	-1.27	4.1	.86	.03	851	527.1	84.3	-10.7	696
84.0	5.23	-1.27	4.0	.88	.05	844	526.6	83.9	-12.3	690
84.5	4.62	-1.27	3.3	.96	.13	821	526.2	83.4	-13.9	672
85.0	4.48	-1.27	3.2	.97	.15	815	525.9	83.0	-15.4	668
85.5	4.41	-1.27	3.1	.98	.17	812	525.5	82.5	-17.0	665
86.0	4.09	-1.27	2.8	-16.03	.22	798	525.2	82.0	-18.6	654
86.5	3.78	-1.27	2.5	.09	.27	783	524.9	81.6	-20.2	642
38187.0	7.05	-1.28	5.8	-15.72	-15.90	890	524.6	81.1	-21.8	730
87.2	9.15	-1.28	7.9	.59	.77	934	524.5	80.9	-22.5	767
87.4	8.90	-1.28	7.6	.60	.78	929	524.4	80.7	-23.1	763
87.6	8.00	-1.28	6.7	.65	.84	910	524.3	80.5	-23.7	748
87.8	7.00	-1.28	5.7	.72	.91	887	524.2	80.3	-24.4	729
88.0	7.27	-1.28	6.0	.70	.89	894	524.1	80.1	-25.0	734
88.2	7.35	-1.28	6.1	.70	.88	895	524.0	79.9	-25.7	736
88.4	6.83	-1.28	5.5	.74	.92	883	524.0	79.7	-26.3	726
88.6	6.61	-1.28	5.3	.75	.94	877	523.9	79.6	-26.9	721
88.8	6.61	-1.28	5.3	.75	.94	877	523.9	79.4	-27.6	721
89.0	6.45	-1.28	5.2	.77	.96	872	523.8	79.2	-28.2	718

Table 4. --Density at perigee ρ_π on MJD 37650.0 with various assumptions for the drag coefficient C_D

Model	Accommodation coefficient α	C_D at perigee	C_D along orbit	ρ_π (g/cm^3)	Deviation from model a
a	≈ 1	2.2	constant	1.210×10^{-17}	—
b	≈ 1	2.2	varying with molecular speed ratio s	1.197×10^{-17}	-1%
c	$\frac{3.6\,\mu}{(1+\mu)^2}$	2.65	constant	1.005×10^{-17}	-17%
d	$\frac{3.6\,\mu}{(1+\mu)^2}$	2.65	varying with s and α	0.976×10^{-17}	-19%

Table 5.--Atmospheric variations related to geomagnetic storms[3]

n	MJD	a_p	Δt (d)	lt (h)	ϕ (deg.)	z_p (km)
1	37364	111	0.4	8.2	-2	650
2	368	132	0.3	8.0	-13	655
3	373	48	0.1	7.9	-27	663
4	385	80	0.1	8.8	-38	676
5	390	39	0.4	9.1	-30	677
6	392	80	0.4	9.1	-26	676
7	398	94	0.3	9.0	-9	675
8	37400	48	0.1	8.9	-3	675
9	404	179	0.2	8.7	+9	677
10	439	32	0.2	9.2	0	695
11	444	67	0.4	9.0	-15	700
12	456	56	0.0	9.3	-38	713
13	457	48	0.0	9.3	-39	713
14	472	132	0.2	9.8	-14	713
15	479	94	0.0	9.4	+7	714
16	485	94	0.3	9.1	24	718
17	493	236	0.4	9.5	38	725
18	496	67	0.2	9.7	39	727
19	498	179	0.4	9.9	38	728
20	37501	67	0.2	10.1	34	728
21	507	236	0.2	10.2	31	727
22	541	80	0.2	10.7	-15	746
23	554	48	0.1	10.3	+6	743
24	566	80	0.2	10.3	35	749
25	573	300	0.2	11.0	38	752
26	584	48	0.3	11.3	17	752
27	599	56	0.1	10.7	-26	762
28	37600	300	0.2	10.7	-28	764
29	610	94	0.2	11.5	-38	769
30	621	94	0.3	11.8	-18	762
31	37634	179	0.0	11.1	+19	757
32	636	111	0.0	11.2	25	757
33	661	27	0.0	11.8	12	760
34	674	94	0.6	11.1	-25	771
35	699	48	0.6	12.0	-11	767
36	37712	56	0.2	11.5	+26	764
37	722	27	0.4	12.1	39	765

[3]Results for events 1 to 31 are taken from Jacchia and Slowey (1964a); delay times 31 to 81 are based on data given in Table 3; and results for the geomagnetic storms 82 to 101 are derived from drag data given by Jacchia and Slowey (1965).

Table 5 (Continued)

n	MJD	a_p	Δt (d)	lt (h)	ϕ (deg.)	z_p (km)
38	37734	22	0.0	12.6	18	762
39	736	27	*0.0	12.6	12	762
40	742	27	0.2	12.3	-5	764
41	761	67	0.2	12.9	-38	770
42	764	48	0.3	13.2	-35	768
43	776	48	0.2	13.1	-5	758
44	37815	48	0.2	13.4	+1	747
45	837	27	*0.8	13.8	-37	749
46	850	39	0.3	13.9	-8	737
47	870	39	*0.4	13.3	+39	735
48	871	94	0.0	13.8	39	735
49	872	56	*0.4	13.9	39	735
50	898	56	0.3	13.8	-23	725
51	37919	154	0.2	15.0	-24	713
52	926	80	0.0	14.8	-5	705
53	937	56	0.2	14.4	+27	700
54	946	67	0.2	15.0	39	696
55	954	22	*0.2	15.6	30	689
56	956	48	0.4	15.6	26	686
57	963	56	*0.2	15.4	6	682
58	975	48	0.0	14.9	-28	684
59	984	67	0.4	15.5	-39	683
60	990	48	*-0.2	16.0	-32	676
61	998	56	0.4	15.9	-12	663
62	38002	27	0.2	15.6	0	657
63	009	56	0.1	15.2	20	652
64	016	111	0.1	15.3	35	650
65	024	39	0.0	15.9	37	644
66	070	67	0.4	16.3	-19	618
67	089	27	0.3	15.7	+33	601
68	096	56	0.0	16.3	38	596
69	098	94	0.2	16.5	37	595
70	38124	67	0.1	16.2	-29	580
71	133	32	0.2	16.9	-39	576
72	134	39	0.4	17.0	-38	575
73	142	27	*0.4	17.4	-24	563
74	146	22	*0.0	17.3	-13	557
75	150	80	0.5	17.1	-1	552

*Weight 1/2 has been assigned to these values.

Table 5 (Continued)

n	MJD	a_p	Δt (d)	lt (h)	ϕ (deg.)	z_p (km)
76	38153	32	0.2	16.9	+8	550
77	162	48	0.2	16.7	32	547
78	169	27	*0.0	17.3	39	542
79	177	27	0.2	17.7	29	533
80	178	67	0.1	17.8	27	533
81	187	132	0.2	17.4	1	524
82	38259	94	0.1	18.1	+4	472
83	261	132	0.2	18.0	-2	471
84	286	132	0.2	19.0	-29	457
85	289	94	0.1	19.0	-22	452
86	294	236	0.2	18.8	-7	442
87	295	300	0.4	18.7	-4	441
88	38326	154	0.1	19.5	+18	418
89	332	207	0.1	19.2	-1	413
90	350	39	0.3	19.7	-39	412
91	358	48	*0.1	20.0	-25	398
92	363	67	0.2	19.8	-10	389
93	396	111	0.4	20.1	+11	364
94	38410	48	*0.1	19.7	-33	367
95	425	48	0.2	20.7	-21	350
96	431	56	0.4	20.4	0	344
97	434	67	0.2	20.3	10	341
98	451	67	0.4	21.3	34	327
99	477	67	0.2	22.1	-38	319
100	478	80	0.2	22.2	-37	315
101	487	154	0.2	22.3	-6	300

NOTICE

This series of Special Reports was instituted under the supervision of Dr. F. L. Whipple, Director of the Astrophysical Observatory of the Smithsonian Institution, shortly after the launching of the first artificial earth satellite on October 4, 1957. Contributions usually come from the Staff of the Observatory. First issued to ensure the immediate dissemination of data for satellite tracking, the Reports have continued to provide a rapid distribution of catalogs of satellite observations, orbital information, and preliminary results of data analyses prior to formal publication in the appropriate journals.

The Reports are also used extensively for the rapid publication of preliminary or special results in other fields of astrophysics.

The Reports are indexed by the Science and Technology Division of the Library of Congress, and are regularly distributed to all institutions participating in the U. S. space research program and to individual scientists who request them from the Administrative Officer, Technical Information, Smithsonian Astrophysical Observatory, Cambridge, Massachusetts 02138.